UNIVERSIDADE DE LISBOA

FACULDADE DE FARMÁCIA

PREDICTING TRANSPORTER EFFECTS ON THE PHARMACOKINETICS OF METABOLIZED DRUGS

Maria Margarida André Oliveira Estudante

Doutoramento em Farmácia

Especialidade de Biofarmácia e Farmacocinética

2011

UNIVERSIDADE DE LISBOA

FACULDADE DE FARMÁCIA

PREDICTING TRANSPORTER EFFECTS ON THE PHARMACOKINETICS OF METABOLIZED DRUGS

Maria Margarida André Oliveira Estudante

Supervisor: Prof. Dr. José Augusto Guimarães Morais

Co-supervisers: Prof. Dr. Leslie Z. Benet

Profª. Drª. Maria da Graça Soveral Rodrigues

Doutoramento em Farmácia

Especialidade de Biofarmácia e Farmacocinética

2011

Supervisor: Prof. Dr. José Augusto Guimarães Morais

Co-supervisor: Prof. Dr. Leslie Z. Benet

Profª. Drª. Maria da Graça Soveral Rodrigues

The studies presented in this thesis were performed at Laboratório de Farmacocinética e Biofarmácia, iMed.UL, Faculdade de Farmácia da Universidade de Lisboa, Portugal, under supervision of Prof. Dr. José Augusto Guimarães Morais and Profª Drª Graça Soveral, and at the Department of Bioengineering & Therapeutic Sciences, Schools of Pharmacy & Medicine, University of California San Francisco, under the supervision of Prof. Leslie Z. Benet.

This work was financially supported by Fundação para a Ciência e Tecnologia (FCT), Lisboa, Portugal (SFRH/BD/31025/2011).

De acordo com o disposto no ponto 1 do artigo nº41 do Regulamento de Estudos Pós-Graduados da Universidade de Lisboa, deliberação nº 93/2006, publicada em Diário da República – II série nº 153- 5 de Julho de 2003, a autora desta dissertação declara que participou na concepção e execução do trabalho experimental, interpretação dos resultados obtidos e redacção dos manuscritos.

Acknowledgements/ Agradecimentos

This thesis is the result of four years of enthusiastic work and learning. First of all I would like to acknowledge my supervisors Prof. José Morais, Prof. Graça Soveral and Prof. Leslie Benet. I am so thankful and honored for the opportunity you gave me and, above all, for your friendship.

I arrived to San Francisco in January 2007 and Prof. Leslie Benet and his group received me with "open arms" and a friendly smile! I don't have the words to express my gratitude, your tireless support and inspired guidance helped me to move on in my work and made my graduate studies a truly rewarding experience. From the U-66 lab I will always remember the fun and my colleagues and friends, Joseph, Maribel (thanks for the Caco-2), Sarah, Allen (thanks for the HPLC hints), Selma (thanks for everything), Howard, Mike, Adam, Caroline and, of course, Frances. Thanks so much Frances for all your support and for always "catching" Les!

Regressei a Lisboa em Dezembro de 2007 e deparei-me com novos desafios. Tinha de colocar em funcionamento a sala de culturas celulares e que desenvolver técnicas de doseamento de fármacos. Agradeço mais uma vez ao Prof. José Morais pela confiança que depositou em mim e no meu trabalho, sem a sua orientação e conselhos não teria conseguido. Agradeço aos meus colegas de departamento Nuno, Carmo, Prof. Manuela e Prof. Rosário pelo apoio e ensinamentos que me deram. Obrigada pela ajuda no desenvolvimento de técnicas de HPLC e por estarem a meu lado no dia a dia, sempre disponíveis para me ouvir e me ajudar!

Como não se faz ciência sozinho, os meus resultados não teriam sido possíveis sem a ajuda preciosa de elementos de outros departamentos, que, com o seu "know-how" e dedicação, contribuiram para o sucesso das minhas experiências. Obrigada Quirina por toda a ajuda com as técnicas e "truques" das culturas celulares, obrigada João e Profª. Rosário Bronze sem os quais não teria conseguido usar o LC-MS/MS, a vossa dedicação é inegualável! Obrigada Cláudia pelo trabalho exemplar no biotério. Obrigada Prof. Rui pelo doseamento das digoxinas.

Ao avançar nos meus trabalhos tive a oportunidade de receber a orientação da Profª. Graça Soveral, que "vestiu a camisola" e me acompanhou até à conclusão da tese. As câmaras de Ussing não seriam as mesmas sem a sua preciosa ajuda. Obrigada Graça pelo pragmatismo mas também por todo o entusiasmo e força!

E já no último ano da tese aconteceu algo maravilhoso! Fiquei grávida do Miguel, o que me deu novo alento e forças redobradas para alcançar a meta. Quero deixar um agradecimento especial ao André, actualmente a fazer o doutoramento na Suécia, pela sua amizade e pelo facto de ter doseado as minhas últimas amostras, numa altura em que a barriga já não me deixava trabalhar. Não tenho palavras para agradecer esse gesto mas estou certa que o futuro te recompensará.

Por fim agradeço aos meus pais e irmã, aos meus amigos e familiares, pelo incentivo e por, mesmo à distância, estarem sempre presentes. Agradeço ao Pedro por toda a compreensão e apoio, nas horas longas e fins de semana que passei a trabalhar.

Deixo um último voto para o meu querido filho Miguel, que nos seus curtos sete meses já deu tanta alegria. Espero que ao longo da tua vida tenhas a sorte de contar com pessoas tão maravilhosas como estas!

Table of contents

Abbreviations

A – Apical

ADME – Absorption, distribution, metabolism and elimination

B – Basolateral

BA – Bioavailability

BD – Biodisponibilidade

BCRP – Breast cancer resistance protein

BCS – Biopharmaceutics Classification System

BDDCS – Biopharmaceutics Drug Disposition Classification System

BE – Bioequivalence

Caco-2 – Human colon adenocarcinoma cell line

CYP – Cytochrome P450 monooxygenase enzymes

ER – Extraction ratio

GG918 – N-[4-[2-(3,4-Dihydro-6,7-dimethoxy-2(1H)-isoquinolinyl)ethyl]phenyl]-9,10-dihydro-5-methoxy-9-oxo-4-acridinecarboxamide

GI – Gastrointestinal tract

GSTs – Glutathione -S- transferases

Log P/ Log D – Lipophilicity

LOQ/LLOQ – Lower limit of quantification

MDCK – Madin-Darby canine kidney cells

MDR1-MDCK (MM) – Madin-Darby canine kidney cells transfected with the P-gp gene (MDR1)

MRP – Multidrug resistance - associated protein family

OAT – Organic anion transporter

OATP – Organic anion transporter polypeptide

OCT – Organic cation transporter

P – Permeability

PAMPA – Parallel artificial membrane permeability assay

Papp – Apparent permeability

PEPT – Oligopeptide transporters

P-gp – P-glycoprotein

QUI – Quinidine

RIF – Rifampicin

S – Solubility

sd – Standard deviation

SULTs – Sulfotransferases (SULTs)

TEA – Tetraethylammonium

TEER – Transepithelial electrical resistence

UGTs – UDP-Glucuronosyltransferases

VER, V – Verapamil

Summary

There is an ongoing debate among the scientific community regarding the role of uptake and efflux transporters in drug BA and BA predictions from *in vitro* systems. The studies presented in this thesis were planned to clarify whether a simple categorization of drugs (BDDCS) may allow prediction of the importance of intestinal transporters on the disposition of drugs.

The bidirectional transport of the highly S and highly P drugs verapamil and diltiazem (Class 1 drugs) and the highly P and low S drug saquinavir (Class 2 drug) was investigated across Caco-2 and MDR1-overexpressing MDCK (MM) cells. All drugs behaved as P-gp substrates in MM cells, but diltiazem and verapamil Papp was P-gp independent in Caco-2 cells. It was concluded that the superior TEER values of MM cell line leads to increased sensitivity in identifying P-gp substrates, although the Caco-2 cells are more representative of the human intestine.

We know of no consistent evidence that P-gp affects verapamil absorption in the intestine, although it proved to be a P-gp substrate in the brain and in certain cellular systems. Therefore we studied the role of P-gp on the absorption of verapamil in the rat intestine in comparison with the Class 2 drug atorvastatin. Both drugs showed to be P-gp substrates in the rat intestine. Transporter-Cyp3a4 interplay was evaluated for verapamil but there were no statistically significant differences between Extraction ratios in the absence and presence of GG918.

Incubation of verapamil and digoxin was studied in the presence and absence of several uptake transporters inhibitors: tetraethylammonium, quinidine, rifampicin and verapamil, in Caco-2 cells. Initial uptake rates exhibited a linear profile for verapamil and suggested saturation for digoxin. The present results support the BDDCS prediction that transporter effects can be relevant in intestinal absorption of Class 2 drugs but not of Class 1 drugs.

Keywords: membrane transporters, drug metabolism, Biopharmaceutics Classification System, intestinal absorption, intestinal permeability.

Sumário

Muitos fármacos encontram problemas no seu desenvolvimento devido a propriedades pouco favoráveis na absorção, distribuição, metabolismo e excreção (ADME), o que tem vindo a suscitar um interesse crescente a nível das previsões de ADME. A previsão da biodisponibilidade (BD) de um fármaco, ou seja, da fração da dose oral que é medida intacta na corrente sanguínea sistémica, é um dos aspectos mais desafiantes uma vez que a BD é uma função complexa de muitos factores biológicos e físico-químicos.

Idealmente, um composto candidato a fármaco deve apresentar boa solubilidade nos conteúdos gastrointestinais (GI) e boa penetração através das membranas biológicas. Amidon *et al.* desenvolveram um Sistema de Classificação Biogalénica (BCS) que categoriza os fármacos em quatro classes com base na sua solubilidade aquosa (S) e permeabilidade intestinal (P), parâmetros fundamentais que controlam a taxa e extensão de absorção de um fármaco a partir de formulações orais sólidas de libertação imediata (IR). O BCS classifica os fármacos como Classe 1: Elevada S & P; Classe 2: Baixa S – Elevada P; Classe 3: Elevada S – Baixa P; Classe 4: Baixa S & P. Considera-se que um composto apresenta "elevada permeabilidade" quando a extensão de absorção em humanos é ≥ 90% da dose administrada. Quando o BCS foi desenvolvido existia conhecimento limitado sobre a importância dos transportadores para a BD. Alguns fármacos podem preencher o critério BCS de 90% para a P devido à actividade de transportadores de captação no intestino e não necessariamente devido a uma elevada permeabilidade lipídica passiva. Desta forma, alguns fármacos classificados como muito permeáveis podem apresentar alterações significativas na BD quando os transportadores de captação intestinal estejam inibidos.

Como previamente sugerido e demonstrado, a interacção entre os transportadores e as enzimas metabólicas pode controlar o acesso das moléculas de fármaco às enzimas e alterações na função dos transportadores podem modular o metabolismo hepático e intestinal sem alterações da actividade enzimática. Em 2005, Wu e Benet reconheceram que a grande maioria de fármacos muito permeáveis das Classes 1 & 2 sofrem metabolismo extenso, enquanto a grande maioria dos fármacos das Classes 3 & 4 são eliminados predominantemente por via biliar e/ou renal do fármaco inalterado. A equipa sugeriu a alteração da componente P para uma componente "via de eliminação", através de um Sistema de Classificação Biogalénica para a Distribuição e Eliminação de Fármacos (BDDCS), que possa ser útil na previsão da distribuição e

eliminação globais dos fármacos, incluindo vias de eliminação, potencial para interacções fármaco-fármaco e efeitos dos transportadores de efluxo e de captação na absorção oral de fármacos.

O papel dos transportadores de captação e de efluxo na BD e nas previsões da BD a partir de sistemas *in vitro* encontra-se em discussão na comunidade científica. Os estudos apresentados nesta tese foram planeados para clarificar se esta categorização de fármacos (BDDCS) poderá ajudar a prever a importância dos transportadores na distribuição e eliminação de fármacos. Um número de novas questões foram surgindo ao longo deste trabalho de pesquisa e, deste modo, os estudos apresentados na presente tese representam um avanço na área com especial relevo para a importância dos transportadores na absorção de uma série de fármacos de Classe 1 (verapamil, diltiazem), Classe 2 (saquinavir, atorvastatina) e Classe 3 (digoxina).

A primeira parte desta tese consiste numa introdução genérica ao trabalho experimental. Esta inclui os objectivos da presente tese (capítulo 1) e uma revisão da literatura (capítulo 2) focando o estado da arte relativamente às enzimas metabólicas e transportadores de fármacos como intervenientes chave na absorção e BD de fármacos. O capítulo 2 inclui ainda uma revisão da metodologia experimental actualmente usada para o estudo da permeabilidade intestinal e dos transportadores intestinais, realçando as suas vantagens e limitações. Finalmente, esta revisão da literatura apresenta as bases do BCS e do proposto BDDCS.

O BDDCS prevê que, para os compostos de Classe 1 (elevada P e elevada S) o papel dos transportadores não será importante clinicamente, enquanto que para os compostos de Classe 2 (elevada P e reduzida S) os transportadores de efluxo irão afectar a extensão da biodisponibilidade oral e a velocidade de absorção. Adicionalmente, para os fármacos de Classe 2, será pouco provável que ocorra saturação dos enzimas intestinais tais como CYP3A4 e UDP-glucuronosiltransferases (UGTs) devido à sua baixa solubilidade. Deste modo, a inibição ou indução dos transportadores de efluxo causará alterações no metabolismo intestinal dos fármacos que sejam substratos das enzimas intestinais. Muitos fármacos de Classe 2 são substratos da enzima CYP3A e simultaneamente substratos ou inibidores do transportador de efluxo glicoproteína P (P-gp). Para os fármacos de Classe 3 (reduzida P e elevada S) o BDDCS prevê que os efeitos dos transportadores de captação predominem e para os fármacos de Classe 4 (reduzida P e reduzida S) que ambos os efeitos dos transportadores de captação e dos transportadores de efluxo possam ser importantes.

O transporte bidirecional dos fármacos de elevada S e elevada P verapamil e diltiazem (Classe 1) e de elevada P e baixa S saquinavir (Classe 2) foi investigado em células Caco-2 e células MDCK com sobreexpressão de MDR1 (células MDR1-MDCK) (capítulo 3). As células foram incubadas com as soluções de fármacos, na ausência e na presença do inibidor selectivo da P-gp GG918 (0.5 μM). Concluiu-se que os três fármacos investigados são substratos da P-gp, com base nos resultados obtidos com as células MDR1-MDCK. No entanto, os resultados obtidos com as células Caco-2 demonstram que o verapamil e o diltiazem não são substratos da P-gp, uma vez que o transporte bidirecional da parte apical (A) para a parte basolateral (B) e da parte B para a parte A originou perfis sobrepostos e razões de efluxo (P B-A/P A-B) aproximadas à unidade. Por outro lado, para o saquinavir foi visível um transporte da zona B para a zona A superior ao da zona A para a zona B, com uma razão de efluxo superior a 2. Quando as razões de efluxo são superiores a 2-3 considera-se estarmos em presença de um substrato de um transportador de efluxo. O transporte do saquinavir foi afectado pela adição do GG918, fazendo com que as razões de efluxo se aproximassem de 1, o que confirma o envolvimento da P-gp. As células MDR1-MDCK possuem uma resistência eléctrica transepitelial (TEER) muito elevada, bem como elevada expressão da P-gp, o que as torna mais sensíveis na identificação de substratos deste transportador. Deste modo, consideramos que as células Caco-2 são mais representativas do intestino humano.

Não existe evidência conclusiva relativamente ao facto da P-gp afectar a absorção do verapamil no intestino, apesar de se ter provado que interfere com o transporte deste fármaco no cérebro e em certos sistemas celulares (ex.: células MDR1-MDCK). No capítulo 4 estudámos o papel da P-gp na absorção do fármaco de Classe 1 verapamil em intestino de rato. Segmentos de jejuno de rato foram montados em câmaras de Ussing e os compartimentos dador e receptor preenchidos com Krebs. Nas experiências de inibição adicionou-se GG918 0.5 μM à solução de Krebs.

O verapamil apresentou razões de efluxo superiores a 3 em ambas as concentrações estudadas (1 μM e 10 μM) e a mesma razão aproximou-se de 1 nas experiências de inibição. O norverpamil (metabolito desmetilado do verapamil) formado *in situ*, apresentou valores consistentemente mais elevados no compartimento apical relativamente ao compartimento basolateral, sugerindo ser um substrato da P-gp. Este resultado levou-nos a realizar uma experiência independente, usando norverapamil como fármaco dador, o que resultou numa razão de efluxo de 13.5. Este

valor aproximou-se da unidade na presença de GG918. O fármaco de Classe 2 atorvastatina foi igualmente estudado e apresentou uma razão de efluxo superior a 3, a qual se aproxima da unidade com a adição de GG918.

Para além de ser um substrato da P-gp, o verapamil é também metabolizado no intestino pela enzima CYP3A4. A interacção transportador-enzima foi avaliada para o verapamil mas não se observaram diferenças estatisticamente significativas entre as razões de extracção na ausência e presença de GG918.

A metodologia analítica usada no capítulo 4 encontra-se descrita no anexo 1.

Investigámos ainda o papel dos transportadores de captação intestinais na absorção do verapamil (Classe 1) e da digoxina (Classe 3) (capítulo 5). As células Caco-2 cresceram em placas de 12 poços durante uma semana. Foi efectuada uma incubação de 2 minutos com os fármacos em estudo, verapamil e digoxina, numa gama de concentrações dos 10 nM a 2 mM. A incubação de 1 μM verapamil e 1 μM digoxina foi avaliada na ausência e na presença de vários inibidores dos transportadores de captação: tetraetilamónio (100 μM e 1 mM), quinidina (100 μM e 1 mM), rifampicina (100 μM e 1 mM) e verapamil (100 μM e 1 mM). A concentração do fármaco nas amostras dos capítulos 3 e 5 foi determinada através de um contador de cintilações. As velocidades de captação iniciais de verapamil pelas células Caco-2, em concentrações de 10 nM a 2 mM, exibiram um perfil linear. Pelo contrário, as velocidades de captação iniciais de digoxina pelas células Caco-2, em concentrações de 10 nM a 2 mM, exibiram saturação, com um Km e Vmax de 530.3 nM e 312.3 nM/ug prot/ min, respectivamente. Na presença de inibidores verifica-se um decréscimo aparente na captação da digoxina pelas células Caco-2, apesar de não ter atingido significância estatística para nenhum dos inibidores testados. Estes resultados suportam a previsão efectuada pela BDDCS de que o efeito dos transportadores de captação pode ser relevante para a absorção intestinal de fármacos de Classe 3, mas não são relevantes para a absorção de fármacos de Classe 1.

A parte final da tese inclui uma discussão global dos principais resultados obtidos e conclusões (capítulo 6). Contém uma análise das diferentes perspectivas estudadas e do impacto destes resultados em futuras direcções de pesquisa.

Palavras-chave: transportadores de membrana, metabolismo de fármacos, classificação biogalénica, absorção intestinal, permeabilidade intestinal.

Chapter 1

Aims and outline of the thesis

1. General aims

The effect of transporters on the extent of bioavailability is a significant concern during drug development. A drug-transporter interaction model would be beneficial in the early stages of drug development when preclinical predictions could be of particular use and service to the industry. Although various *in vitro* and *in vivo* models can be found, to date no standard system exists to predict the effect of transporters on drug absorption. In 2000, the Food and Drug Administration (FDA) implemented the Biopharmaceutics Classification System (BCS) system to allow waiver of *in vivo* bioequivalence testing of immediate release (IR) Class 1 (highly permeable (P) and highly soluble (S) drugs) solid dosage forms that exhibit rapid dissolution. Despite the importance of this measure in lowering development costs for generic products, only a limited number of drug substances have received regulatory acceptance. Based on transporter data gathered over the years, in 2005, Wu and Benet proposed a new classification system: they suggested that changing the permeability component to a route of elimination component in a Biopharmaceutics Drug Disposition Classification System (BDDCS) may be useful in predicting overall drug disposition, including routes of drug elimination, potential for drug-drug interactions and the effects of efflux and absorptive transporters on oral drug-absorption. BDDCS predicts transporter effects to be clinically irrelevant for Class 1 (highly P and highly S drugs), efflux transporter effects and efflux transporter-metabolizing enzyme interplay to be relevant for Class 2 drugs (highly P and low S), uptake transporter effects to be most relevant for Class 3 drugs (low P and high S) and both uptake and efflux transporters to be relevant to the absorption of Class 4 drugs (low P and low S).

Recent research focused on the role of transporters in the liver and kidney but much less is known about the effect of efflux and uptake transporters in the intestine. Investigation on the role of transporters in the intestine is therefore an area in need of further research, especially as we realize that the majority of drugs marketed worldwide are administered orally.

The present work aimed to investigate the intestinal transporter effects on Class 1 drug diltiazem and Class 2 drug saquinavir and the intestinal transporter effects and intestinal transporter-enzyme interplay on BDDCS Class 1 drug verapamil and Class 2 drug atorvastatin, experimentally testing the predictive relevance of the newly proposed classification system BDDCS regarding transporter effects.

2. Outline of the thesis

Chapter 1 and 2 introduce the general aims of this project and a comprehensive introduction to the field under study. The current knowledge on drug enzyme and drug transporters is summarized and the major studies related to intestinal drug permeability are reviewed and mostly focused on transporter and transporter-enzyme interplay in the gut. The topics mentioned in chapter 2 have relevance on the design of the following experimental chapters (3, 4 and 5).

In order to study our formulated hypothesis, several *in vitro* and *in situ* intestinal models were used in this work, bringing to light the potential different answers that may arrive from different experimental models and the relevance of each individual model to the study of intestinal transporters effects. Briefly, the *in vitro* models consisted of cellular bidirectional and uptake studies with Caco-2 cells (chapters 3 and 5, respectively) and cellular bidirectional studies with Mardin-Darby (MDCK) and MDCK over-expressing MDR1, the P-glycoprotein (P-gp) gene (MDR1-MDCK) cells (chapter 3). The rat jejunum was chosen as the *in situ* permeability model, where segments of rat proximal jejunum were mounted in Ussing chambers and drug permeability assessed from the apical (A) to the basolateral (B) side in comparison to the basolateral (B) to the apical (A) side, as in bidirectional cell monolayer's studies.

The effect of P-gp on the intestinal drug absorption of Class 1 drugs (verapamil and diltiazem) and Class 2 drug (saquinavir) across Caco-2, MDCK and MDR1-MDCK cells monolayer's is evaluated in chapter 3. Caco-2, MDCK and MDR1-MDCK cells are widely used to evaluate intestinal permeability of drugs. We used digoxin, a well-known P-gp substrate, as a positive control for P-gp in our Caco-2 cell line. Despite being used for the same purpose we decided to study the three cell systems as they present considerable differences in transepithelia electrical resistance (TEER) and pores size, which directly influences the measured permeability. Additionally, these cells present different levels and types of transporter expression. Caco-2 cell line is derived from human adenocarcinoma and therefore contains P-gp and other relevant intestinal human efflux and uptake transporters. MDCK are derived from kidney canine cells, so it is expected that they would present different types and levels of transporters. MDR1-MDCK cells are transfected with the MDR1 gene (P-gp gene) and, consequently, over-express P-gp. We questioned whether this latter cell line is more sensitive in identifying P-gp substrates and what is the relevance of transfected cell lines in predicting *in vivo* human intestinal P-gp transporter effects.

Due to structural similarities of intestinal membrane, drug absorption in rats may be used to predict drug absorption in humans. Therefore, we repeated a similar bidirectional study in rat intestinal segments (chapter 4). We questioned whether intestinal P-gp would have an effect on Class 1

(verapamil) and Class 2 (atorvastatin) drug absorption, using digoxin to validate our experimental conditions concerning P-gp function. The rat intestinal model has as an advantage over the Caco-2 cells the fact that intestinal CYP3A enzymes are present at physiological levels. Caco-2 cells are known to express hydrolase, esterase and brush border enzymes but they don't express sufficient levels of the principal CYP enzyme in enterocytes, the CYP3A4, responsible for the metabolism of 37% of the top 200 prescribed pharmaceuticals.

Verapamil is known to be a CYP3A4 substrate, so additionally to the P-gp effect we were able to study verapamil metabolism in the rat intestine and to evaluate transporter-enzyme interplay in this system. The quantification of verapamil oxidative metabolite, norverapamil, in both the apical and the basolateral sides of the intestine raised the question whether it constitutes a substrate of P-gp. Therefore, we repeated the experiment using norverapamil as the donor drug and were able to confirm norverapamil as a P-gp substrate in the rat intestine.

In all the inhibitory studies presented in chapter 4, GG918 [(N-[4-[2-(3,4-Dihydro-6,7-dimethoxy-2(1H)-isoquinolinyl)ethyl]phenyl]-9,10-dihydro-5-methoxy-9-oxo-4-acridinecarboxamide)] was used as a selective P-gp inhibitor. These studies were designed in order that all the permeability values (A to B and B to A) were measured in the absence and the presence of GG918. In the presence of the inhibitor B to A over A to B permeability should approach the unity.

The kinetics of Caco-2 uptake for the Class 1 drug verapamil and Class 3 drug digoxin was studied in chapter 5. We wanted to investigate the BDDCS hypothesis that drug uptake intestinal transporters are not relevant for Class 1 drugs (highly P and highly S) but have an effect on Class 3 (low P and highly S) drugs. The fact that we found digoxin uptake to be saturable, led us to delineate further studies using classical uptake inhibitors such as tetraethylammonium, quinidine, rifampicin and verapamil, in the attempt to identify the transporter responsible for digoxin uptake.

The work presented in annex 1 focuses the analytical methods optimized for the analysis of Ussing chamber samples of verapamil and norverapamil (HPLC with fluorescence detection) and atorvastatin (LC/MS-MS). Although these methods are secondary regarding the aim of this project, they were nevertheless essential for the quantification of studied drugs.

Chapter 2

General introduction

Table of contents

1. Drug metabolizing enzymes

Enzyme systems have evolved in humans to maintain cellular homeostasis and to facilitate the disposition of endogenous lipophilic compounds, such as steroids, and xenobiotics including drugs. Metabolism allows the utilization of nutrients and the subsequent detoxification and excretion of potentially harmful compounds and metabolites. Traditionally, drug metabolism has been classified in two groups based on the types of enzymatic reaction catalyzed by the enzyme family under investigation. Phase I drug metabolism typically involve the functionalization of endogenous and xenobiotics to generate more polar derivatives (alcohols, phenols, carboxylic acids). Phase I reactions can also involve reduction reactions, hydrolysis of compounds and cyclization/decyclization reactions. Phase I oxidative reactions are typically carried out in the liver by mixed function oxidases primarily involving hepatic cytochromes P450 (CYPs) that utilize NADPH and oxygen in their catalytic cycle. Other phase I enzymes include flavin-containing monooxygenases (FMO), monoamine oxidases (MAO), alcohol dehydrogenases (ADH), glutathione peroxidases (GPX), epoxide hydrolase, esterases, etc (1).

CYP enzymes are also expressed extrahepatically where they can participate in drug metabolism in target tissues. CYPs expressed in the intestinal tract are particularly important in the first-pass metabolism of many classes of drugs. In some cases, metabolites produced by phase I reactions are of sufficient polarity to undergo excretion, but many others require additional metabolism by phase II detoxification enzymes. These reactions occur in series or are said to be sequential reactions. Because they often occur first, oxidation, reduction and hydrolysis are commonly referred to as Phase I reactions, and conjugations as a Phase II reactions. Some drugs, however, undergo only Phase II reactions. Phase II reactions commonly involve conjugation of a substrate with an obligatory cosubstrate specific to each family of phase II enzymes. The most common phase II families include the glutathione -S- transferases (GSTs), UDP-glucuronosyltransferases (UGTs), sulfotransferases (SULTs), and N-acetyltransferases (NATs) (2).

1.1. Cytochrome P450

1.1.1. Structure, Classification and Function

The cytochromes P450 (CYPs) comprise a vast superfamily (> 6000 known members) of heme-containing mono-oxygenase enzymes found in virtually all life forms (3). Mammalian cytochrome P450s are

membrane bound and they are found in the mitochondrial inner membrane and in the endoplasmatic reticulum (ER) of cells in the liver, intestinal wall, lung, kidney, adrenal cortex and nasal epithelium. The name cytochrome P450 derives from the fact that these proteins have a heme group and an unusual spectrum with a very strong absorption band at 450 nm, thus P450 (P is for pigment). The reason why cytochrome P450 absorbs in this range is the original ligand to the heme iron. Four ligands are provided by nitrogens on the heme ring. Above and below the plane of the heme, there is room for two more ligands, the 5^{th} and 6^{th} ligands. In cytochrome P450s, the 5^{th} ligand is a thiolate anion, a sulfur with a negative charge. The sulfur comes from a conserved cysteine at the heme binding region of the active site (4).

The three-dimensional (3D) structure of a protein can provide valuable insight into its function, particularly in complex with ligand(s) of interest. Over the years, many homology models of the CYPs have appeared in the literature based on the X-ray crystal structures of distantly related bacterial CYP isoforms. In 2000 a major breakthrough was achieved with the determination of the first mammalian CYP, that of the rabbit enzyme CYP2C5 (5). Recently, the determination of X-ray crystal structures for several human isoforms (CYP1A2, CYP2A6, CYP2C8, CYP2C9, CYP2D6 and CYP3A4) has improved significantly the study of CYPs-ligand interactions (3).

The genes of the P450 superfamily have been categorized by Nelson *et al.* (6). The P450 proteins are categorized into families and subfamilies by their sequence similarities. Sequences that are greater than 40% identical at the amino acid level belong to the same family. Sequences that are greater than 55% identical are in the same subfamily . A specific gene (isoenzyme) is then designated by a number.

Humans have 18 families of cytochrome P450 genes and 44 subfamilies, with a total of 57 sequenced genes (Table 1) (6). Selective substrates, inducers and inhibitors of human CYP P450 isoenzymes are described in the literature (7).

Cytochrome P450s metabolize physiologically important compounds in many species of microorganisms, plants and animals. They are important in the oxidative, perioxidative and reductive metabolism of numerous and diverse endogenous compounds such as steroids, bile, fatty acids, prostaglandins, leukotrienes, retinoids and lipids. In mammals, xenobiotic metabolizing CYPs provide crucial protection from the effects of exposure to a wide variety of chemicals, including environmental toxins and therapeutic drugs. Cytochrome P450s are known to catalyse hydroxylations, epoxidation, N-, S- and O-

dealkylations, N-oxidations, sulfoxidations, dehalogenations and other reactions (8). Mutations in cytochrome P450 genes or deficiencies of the enzymes are responsible for several human diseases (4).

1.1.2. Importance in Drug Metabolism

The number of enzymes involved in drug metabolism is large and the number of possibilities with a new drug candidate can be a challenge. Of the enzymes participating in drug metabolism, the dominant players (~75%) are the P450s enzymes, followed by UDP-glucuronosyltransferases (UGT) and esterases- Figure 1(a). A further breakdown of the P450 enzymes is presented in Figure 1(b), with five of the P450s (1A2, 2C9, 2C19, 2D6 and 3A4) accounting for 90% of the reactions. A single enzyme, P450 3A, is involved in about half of these reactions (1).

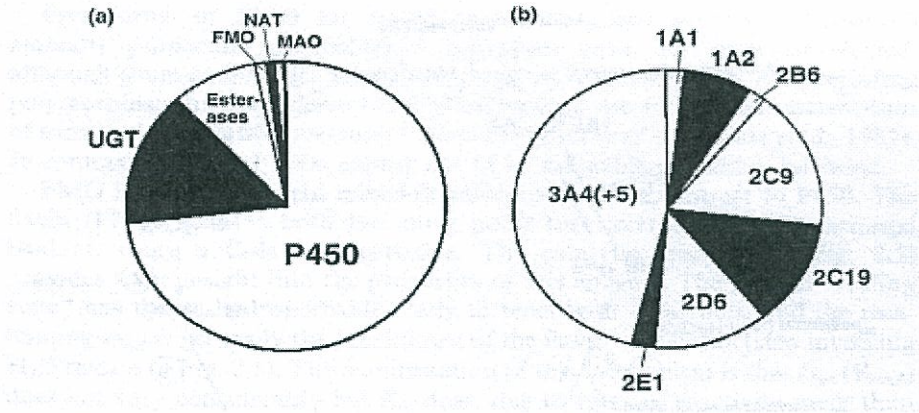

Figure 1- (a) Fractions of drugs metabolized by various enzyme systems. (b) Fractions of drugs that are P450 substrates metabolized by individual P450s. UGT-UDP-glucuronosyltransferases; FMO-Flavin-Containing Monooxygenase; NAT- N-acetyltransferases; MAO- Monoanine oxidasee. *In* Guengerich. Oxidative, Reductive, and Hydrolytic Metabolism of Drugs (1).

Of the top 200 prescribed pharmaceuticals, CYP3A4 metabolizes 37% of them (9).

One of the characteristics of these drug metabolizing CYPs is their capacity to interact with a wide range of chemically diverse substrates, and some CYPs have overlapping substrate specificities. This lack of specificity is useful in terms of defence of the organism against potentially harmful xenobiotics, but in

some instances can lead to a rapid drug clearance/inactivation (specially for lipophilic compounds), production of toxic compounds and/or adverse drug-drug interactions (3).

There are common drugs that inhibit P450 enzymes. Clinically important CYP3A4 inhibitors include antibacterials (e.g. clarithromycin, erythromycin and isoniazid), anticancer agents (e.g. tamoxifen and irinotecan), anti-HIV agents (e.g. ritonavir and delavirdine), antihypertensives (e.g. dihydralazine, verapamil and diltiazem), sex steroids and their receptor modulators (e.g. gestodene and raloxifene) and several herbal constituents (e.g. bergamottin in grapefruit juice and glabridin) (10). If these drugs are given with other drugs that are normally metabolized by CYP3A4 the half-life of the second ones will be prolonged and plasma levels will be increased with extension of the effect. The resultant drug interactions may lead to more or less serious adverse reactions, including fatal events. When CYP3A4 inhibitors are coadministrated with terfenadine, cisapride or astemizole (all CYP3A4 substrates), *torsades de poins*, a life-threatening ventricular arrhythmia associated with QT prolongation, may occur.

P450 enzymes have a variety of gene regulatory mechanisms. Many of these genes can be turned on or induced by a chemical signal, like cigarette smoke, polycyclic aromatic hydrocarbons, phenobarbital, rifampin, etc. Under an induction scenario P450 enzyme substrates will be submitted to an increase in metabolism and eventual impairment of effect due to sub therapeutic concentrations (8).

There are significant differences in P450s among species (11). Data indicate that rat and human show similar drug intestinal absorption profiles due to similar transporters expression patterns in the small intestine, while the two species exhibit distinct expression levels and patterns for metabolizing enzymes in the intestine. Therefore, a rat model can be used to predict oral drug absorption in the small intestine of human, but not to predict drug metabolism or oral bioavailability in human.

Another level of complexity results from the fact that these enzymes exhibit different tissue distribution (section 1.1.3) and polymorphisms between individuals and ethnic populations. Of the drug metabolizing isoforms, CYP2D6 and CYP2C9, present polymorphisms that can result in the poor metabolism of drugs (3). CYP2C19 has a polymorphism that changes the enzyme's ability to metabolize mephenytoin. In Caucasians, the polymorphism for the poor metabolizer phenotype is only seen in 3% of the population. However, it is seen in 20% of the asian population. Because of this difference it is important to be aware of a person's race when drugs are given that are metabolized differently by different populations. CYP2D6 is responsible for more than 70 different drug oxidations and to date

there are 72 alleles identified in this isoform. Since there may be no other way to clear these drugs from the system, poor metabolizers may be at severe risk for adverse drug reactions (8).

1.1.3. Tissue Distribution of CYP450 Isoforms

The liver contains the greatest amount of P450 enzymes, although they have been found in virtually all organs in the body including kidney, small intestine, skin, nasal mucosa, eyes, lungs, adrenals, pancreas, heart, brain, erythrocytes and platelets. On the basis of the concentrations of individual P450 enzymes in human liver microsomes, CYP3A represents 30% of total hepatic P450 content; CYP2C represents 18%; CYP1A2, 13%; CYP2E1, 7%; CYP2A6, 4%; CYP2D6, 1.5% and CYP2B6, 0,2%. However, the relative contribution of individual P450s to the metabolism of drugs may not mimic the relative abundance of P450 in the liver. For example, CYP2D6 metabolizes approximately 19% of all drugs metabolized by P450, although represents only 1,5% of P450 liver content (7).

Drug metabolism in the gastrointestinal tract is mainly mediated by enzymes located in the enterocyte and by enzymes produced by intestinal bacteria. In the esophagus and stomach there is minimal CYP expression. The small intestine is the first site of significant metabolism of orally compounds, and intestinal P450 enzymes can significantly affect the bioavailability of drugs. For example, small intestinal metabolism of midazolam (CYP3A4/5 substrate) has been shown in humans and the extent of metabolism was comparable to that found in the liver (12). CYP3A4 is the predominant isoenzyme found in the small intestine, and accounts for approximately 70% of enterocyte P450 content. CYP2C9 and CYP2C19 are expressed in the small intestine at low levels, as is CYP1A1. CYP3A5 is the main isoenzyme in the colon. In general, microsomal enzyme content is the highest in the duodenum and decreases markedly toward the ileum (7). Despite the much lower concentration of enzymes present in the small intestine compared to the liver, their role is significant because of the large surface area of the intestine and their obligatory interaction with drugs that are transcellularly absorbed.

1.2. Phase II Metabolic Enzymes

1.2.1. UDP-Glucuronosyltransferases (UGTs)

Glucuronidation is the addition (conjugation) of glucuronic acid to various functional groups. Compounds may be glucuronidated directly or after oxidative metabolism. Reactions can occur on alcohols, phenols, amines, tertiary and heterocyclic amines, amides, tiols and acidic carbon atoms. Addition of glucuronic acid results in conjugates that are more polar, ionized at physiologic pH (pKa =4) and with increased molecular weight (+176). These features facilitate excretion of glucuronides via the kidney either by glomerular filtration or by active secretion or both. In addition, glucuronides are commonly excreted by the liver via the bile into the small intestine. Glucuronides are too polar to diffuse through cell membranes and therefore specific transporters are necessary for their movement across membranes. Monoglucuronides are generally considered to be final metabolites, although there is some recent evidence with some of the nonsteroidal anti-inflammatory agents, that glucuronides may be substrates for CYP2C9 oxidation. The active site of the UGTs face the lumen of the endoplasmatic reticulum, whereas the active site of P450, also microsomal enzymes, faces the cytosolic side (13).

1.2.2. Sulfotransferases (SULTs)

Hepatic sulfation of xenobiotics is a common phase II metabolic mechanism for increasing molecular hydrophilicity in preparation for biliary excretion or efflux across the hepatic basolateral membrane for subsequent renal clearance. Sulfation of chemicals involves the conjugation of the substrate with a sulfonyl ($SO3^-$) group (13). Xenobiotic detoxification may occur by direct sulfation of the parent compound or may follow phase I oxidation. However, hepatic xenobiotic sulfation also can lead to activation of hepatotoxins. Sulfation is a high affinity and low capacity phase II reaction, which works in concert with glucuronidation on overlapping subtrates; sulfation predominates at low substrate concentrations and glucuronidation at high substrate concentrations, when sulfation has been saturated (14).

Cytosolic SULTs exists as homodimers or heterodimers in solution. Cytosolic SULTs are responsible for the conjugation of endogenous substrates such as steroids, bile acids, and neurotransmitters, as well as several xenobiotics. Membrane-bound SULTs are present in the Golgi apparatus of cells, and catalyze

sulfation and posttranslational modification of peptides, proteins, lipids and glycosaminoglycans. Sulfation activity is found to be the highest in the liver and small intestine, although other organs also express the SULTs (13).

The class of cytosolic SULTs enzymes is subdivided into three families: SULT1 (phenol sulfotransferase family), SULT2 (hydroxysteroid sulfotransferase family), and brain-specific SULT4 (15).

1.2.3. Glutathione-S-Transferases (GSTs)

Glutathione conjugation is of particular importance because substrates of this reaction are often potent electrophiles. Conjugation with intracellular glutathione results in the detoxification of these species, which could otherwise covalently bind intracellular macromolecules. A broad spectrum of diverse electrophiles can undergo glutathione conjugation. Molecular moieties suitable to glutathione conjugation include electrophilic carbon atoms as well as electrophilic nitrogen, oxygen and sulfur atoms (14). Substrates of glutathione conjugation can be parent compound electrophiles, as well as electrophilic phase I metabolites, and even certain phase II conjugates. A number of anticancer agents (nitrogen mustards, busulfan) and inhalation anesthetics (halothane, enflurane, sevoflurane) are metabolized by GST enzymes. Glutathione conjugates are excreted via transporters into the bile or are converted to their mercapturic acid derivates and excreted into the urine (13).

There are six major classes of human cytosolic GST enzymes, namely, alpha, mu, omega, pi, theta and the newly discovered zeta class (16). Alpha, mu and pi expression is increased when cells are exposed to electrophiles (e.g., diethymaleate, paraquat) that generate reactive oxygen species (hydrogen peroxide, OH radicals) (13).

Given the high intracellular concentrations (~10 mM) of glutathione in the liver, glutathione conjugation may occur spontaneously, but is much more efficient when catalized by GSTs. GST-mediated metabolism predominantly occurs in the cytosol, but some GST activity also resides in the endoplasmatic reticulum. Soluble GSTs are found in most cells in the body (13). Since hepatic concentrations of glutathione are by far the highest of the co-factors utilized in the three discussed reactions, intracellular glutathione is difficult to deplete. When intracellular glutathione is depleted, severe hepatotoxicity may follow (14).

Table 1 – The families of human P450s (*Adapted* from (6)).

CYP Family	**Function**	**Number of subfamilies**	**Number of genes**
CYP1	Drug metabolism	3	3
CYP2	Drug and steroid metabolism	13	16
CYP3	Drug metabolism	1	4
CYP4	Arachidonic acid or fatty acid metabolism	6	12
CYP5	Tromboxane A_2 synthase	1	1
CYP7A	Bile acid biosynthesis (7-alpha hydroxylase of steroid nucleous)	1	-
CYP7B	Brain specific form of 7-alpha hydroxylase	1	-
CYP8A	Prostacyclin synthase	1	-
CYP8B	Bile acid biosynthesis	1	-
CYP11	Steroid biosynthesis	2	3
CYP17	Steroid biosynthesis (17-alpha hydroxylase)	1	1
CYP19	Steroid biosynthesis (aromatase)	1	1
CYP20	Unknown function	1	1
CYP21	Steroid biosynthesis	1	1
CYP24	Vitamin D degradation	1	1
CYP26A	Retinoic acid hydroxylase important in development	1	-

CYP26B	Retinoic acid hydroxylase	1	-
CYP26C	Retinoic acid hydroxylase important in development	1	-
CYP27A	Bile acid biosynthesis	1	-
CYP27B	Vitamin D3 1 –alpha hydroxylase activates vitamin D3	1	-
CYP27C	Unknown function	1	-
CYP39	7-alpha hydroxylation of 24-hydroxy cholesterol	1	-
CYP46	Cholesterol 24-hydroxylase	1	-
CYP51	Cholesterol biosynthesis	1	1

2. Drug transporters

Membrane transporters can be major determinants of the pharmacokinetics, safety and efficacy profiles of drugs (17). Transporters are the gatekeepers for all cells and organelles, controlling uptake and efflux of crucial compounds such as sugars, amino acids, nucleotides, inorganic ions and drugs (18). Specific membrane transporters are expressed in the luminal and/or basolateral membranes of enterocytes, hepatocytes, renal tubular epithelial cells and other important barrier tissues, including the blood-brain barrier, blood-testis barrier and the placental barrier (19) (Figure 2) (Table 2) (page 30).

Traditionally transporters can be divided into passive and active transporters. Passive transporters, also known as facilitaded transporters, allow passage of solutes (e.g., glucose, amino acids, urea) across membranes down their electrochemical gradients. Active transporters create ion/solute gradients across membranes, utilizing diverse energy-coupling mechanisms. These active transporters are classified as primary or secondary active transporters according to the directness of coupling to cellular energy (e.g. ATP hydrolysis).

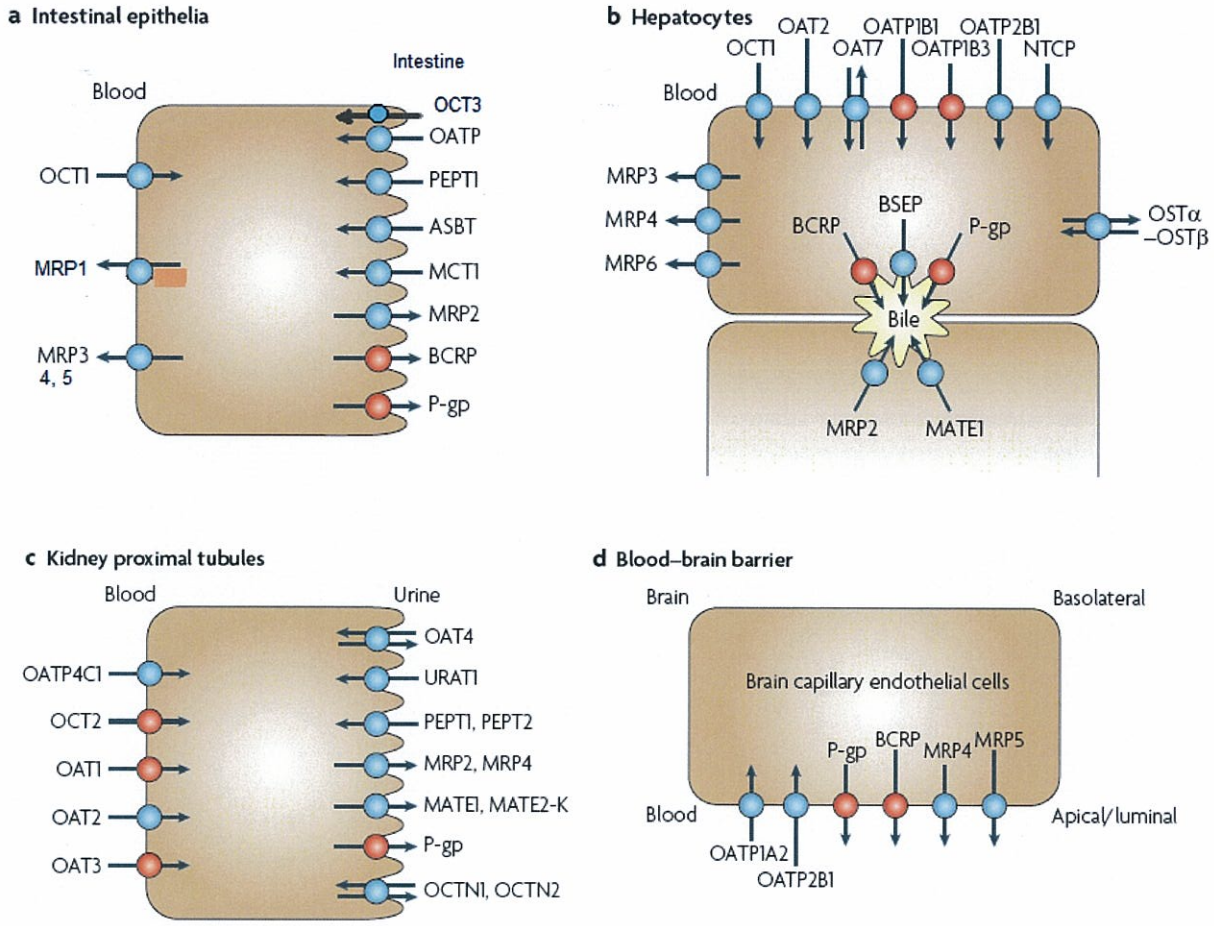

Figure 2- Diagram of major transporters proteins expressed at a) intestinal epithelia, b) hepatocytes, c) kidney proximal tubules and the d) blood-brain barrier. OCT- organic cation transporter; OATP-organic anion transporter polypeptide; PEPT-peptide transporter; ASBT-apical sodium/bile acid co-transporter; MCT-monocarboxylic acid transporter; MRP-multidrug resistance protein; BCRP-breast cancer resistance protein; P-gp-P-glycoprotein; NTCP-sodium/taurocholate co-transporting peptide; OAT-organic anion transporter; BSEP-bile-salt export pump; MATE-multidrug and toxin extrusion protein; URAT- urat transporter; OCTN-organic cation transporter. *Adapted* from (17) and (20).

Primary active, ATP-dependent transporters include members of the ATP-binding cassette (ABC) transporter family and ion pumps (ATPases). Ion pumps hydrolyze ATP to pump ions such as Na^+, K^+, H^+, Ca^{2+} and Cu^{2+} out of cells or into organelles. These pumps also generate and maintain electrochemical ion gradients across membranes, and thus are called active transporters. Such ion gradients are used in

turn by secondary-active, ion-coupled transporters to drive uphill transport of nutrients across biological membranes. Similar to transporters, channels allow movement of solutes down their electrochemical gradients.

Following the development of the expression cloning approach for transporters 12 years ago the transporter field has undergone a renaissance (18). Extensive studies on functional expression of transporters have been performed by many scientists using heterologous gene expression systems, including Xenopus oocytes and transfected mammalian cell lines such as 293, CHO, HeLA and COS cells. Those studies have revelead that, in general, the substrate specificities of transporters are lower than those of physiological receptors. Transporters recognize many structurally related and unrelated compounds with Km and Ki values at submicromolar to milimolar levels (19).

According to the guidelines of the HUGO Gene Nomenclature Committee, membrane transporters have been classified into the solute carrier (SLC) and the ATP-binding cassette (ABC) transporter superfamilies (18). In particular, more than 400 membrane transporters in the two major superfamilies have been annotated in the human genome (17). Drug transporters are integral membrane proteins typically having 12 transmembrane domains (TMDs), although there are some exceptions. Many SLC family transporters consist of 300-800 amino acid residues with a molecular mass in the range of 40-90 kDa, while the corresponding values for ABC family transporters are 1200-1500 residues and 140-180 kDa, respectively (19).

2.1. ATP Binding Cassette Transporters (ABC)

The most investigated transporters are the ABC family efflux transporters P-glycoprotein (P-gp), multidrug resistance–associated protein 2 (MRP 2) and breast cancer resistance protein (BCRP), expressed in organs of excretion including gut, liver and kidney. Members of this superfamily use ATP as an energy source, allowing them to pump substrates against a concentration gradient. Many clinically important and frequently prescribed drugs such as statins, antibiotics, HIV protease inhibitors, immunosuppressants, anticancer and cardiac drugs were shown to be substrates of such efflux carriers. ABC transporters P-gp, MRP2 and BCRP are highly abundant at the apical (luminal) membrane of

enterocytes thereby limiting the intestinal absorption of numerous drugs such as talinolol, fexofenadine, digoxin and HIV protease inhibitors.

ABC transporter superfamily isoforms constitute a broad array of substrate specificities from endogenous fatty acid metabolites to synthetic therapeutics. A common characteristic shared by ABC transporters is the presence of nucleotide binding domain(s) (NBDs), which enable these integral membrane proteins to hydrolyze ATP to drive efflux (Figure 3) (21).

The cloning of the human genome, coupled with various genomic and functional studies, has revealed 49 human ABC transporter isoforms that are separated into seven distinct subfamilies based on their sequence homology. Among these subfamilies, the ABCB and ABCC subfamily contain the most widely investigated transporters influencing human intestinal absorption. Specifically, P-glycoprotein (ABCB1, P-gp) and multidrug resistance-associated proteins (ABCC, MRPX) have not only been shown to be expressed along the GI tract, but due to their cellular apical localizations and broad substrate specificities, appear to be the primary efflux pumps determining xenobiotic absorption. The ABCG2 isoform, also known as the breast cancer resistance protein (BCRP), has also been demonstrated to affect intestinal absorption of various therapeutic agents (22). In the liver, efflux transporters are expressed on the apical canalicular membrane under normal conditions (Figure 2). Active and unidirectional efflux of organic anions and bile salts into the bile occur via MRP2 and bile salt export pump (BSEP), respectively. P-gp efflux several physiological molecules and xenobiotics from the hepatocyte into the bile (23).

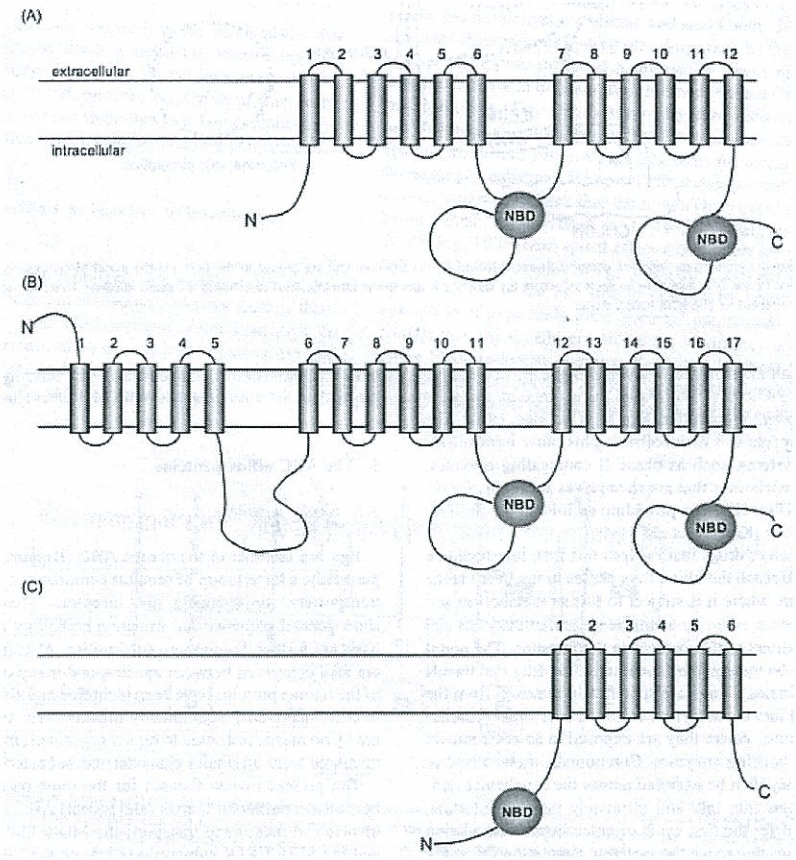

Figure 3- Transmembrane arrangement of ABC efflux proteins. (A) P-gp (MDR1), MDR3, BSEP, MRP4, MRP5, and MRP8, have 12 TM (transmembrane) regions and two NBDs (nucleotide binding domains). (B) Typical MRP transporters (MRP1-3 and 6-7) have five extra TM regions towards the N terminus (C) BCRP have just six TM regions and one NBD. (N – amino terminus ; C – carboxyl terminus). In Eur J Pharm Sci. (21).

2.1.1. MDR1 drug-transporting P-glycoprotein (P-gp, ABCB1)

The gene responsible for encoding P-gp belongs to the ABCB family of ABC transporters, and is known as the Multidrug Resistance 1 (MDR1) gene. The two commonly considered MDR gene families in humans are MDR1 (ABCB1) and MDR2/3 (ABCB4). In rodents, the gene responsible for the primary MDR isoforms' expression is depicted by lower case letters as mdr1 (a and b) and mdr2 (22).

Numerous studies have demonstrated that P-gp possesses broad subtrate specificity, with a preference for hydrophobic, amphipathic molecules containing a planar ring system ranging in size from 200 to 1.900 Da. P-gp is also involved in the transport of neutral compounds such as digoxin and cyclosporine A, negatively charged carboxyl groups such as those found on atorvastatin and fexofenadine, and hydrophilic drugs such as methotrexate. The degree of hydrogen bonding and partitioning into the lipid membrane has been determined to be a rate-limiting step for substrate interactions with P-gp (22).

Naturally occuring substrates for P-gp include biologically active compounds found in normal diet, such as plant chemicals, and endogenous compounds like steroid hormones, bile salts, glycocholate, tauroursodeoxycholate, etc. The polarised, apical membrane localisation (Figure 2) of P-gp within the intestine, liver, kidney and blood-brain barrier suggests a normal excretory or barrier role for P-gp in mediating the efflux of xenobiotics and toxins into the intestinal lumen, bile, urine, and blood (21). Intestinal P-gp is localised to the villus tip enterocytes, i.e. the main site of absorption for orally administered compounds and in close proximity to the lumen. P-gp is therefore ideally positioned to limit the absorption of compounds by driving efflux back into the lumen. The first evidence indicating that P-gp acts as a secretory detoxifying system to limit drug absorption came from studies in human intestinal epithelial cell lines Caco-2, HT29 and T84. Polarised, apical P-gp expression in these cells was accompanied by secretory (basolateral-to-apical; blood-to-lumen) transport of the cytotoxic anticancer drug, vinblastine, which was reduced in the presence of MRK16, an inhibitory monoclonal antibody directed against P-gp, and the P-gp inhibitors/ substrates verapamil and nifedipine (24). It was demonstrated the role of P-gp in the specific and saturable binding of vinblastine in membrane vesicles from highly multidrug-resistant human KB carcinoma cell lines. The binding of vinblastine to P-gp is competitively inhibited by vincrastine and daunorubicin, suggesting these compounds share the same binding site. Competitive binding studies using colchicine and actinomycin D revealed a lack of competition for the vinblastin-binding site, further supporting the findings that P-gp has multiple drug binding domains (22). Shapiro *et al.* (25) demonstrated that progesterone was not effluxed by P-gp, although it was shown to bind P-gp and block the efflux of other substrates. Recently, a high-resolution structure of the mouse P-gp has been described, which revealed distinct binding sites for drugs. Mutiple binding sites for substrates and inhibitors on P-gp have been identified using site-directed mutagenesis (17).

The P-gp inhibitors include several calcium channel blockers, immunosuppressive agents and other well-characterized compounds such as SDZ, PSC 833, LY335979 and GF120918 (GG918) (22). Additionally, common pharmaceutical excipients such as hydrophilic cyclodextrin, cosolvents (PEG 400) and surfactants (Tween 80, Cremophor EL) have also shown to inhibit P-gp activity. Surfactants or cosolvents have also been shown to indirectly influence P-gp by inducing changes in cellular membrane fluidity. Such changes can alter the microenvironment of the apically oriented TM domain, and subsequently alter substrate recognition, binding, and efflux by P-gp. The flavonoids and other ingredients present in fruits, vegetables and herbs have been found to modulate the activity of P-gp function and may cause detrimental effects on drug pharmacokinetics (22). One of the most recognized interactions is the ingestion of grapefruit juice and/or St John's Wort which results in the change of the pharmacokinetic profiles of cyclosporine A and digoxin due to inhibition or induction of P-gp mediated transcellular intestinal epithelial absorption (26). In a representative case, the oral coadministration of grapefruit juice with talinolol (10 mg/Kg) resulted in an increase of talinolol Cmax, AUC and a reduced Tmax without significantly affect the terminal talinolol half-life (27). This study indicated that grapefruit juice acted to inhibit intestinal P-gp mediated efflux and resulted in enhanced talinolol bioavailability. Therefore concomitant intake of herbal extracts or fruits/ foods and nutraceuticals may modulate the pharmacokinetic profile of the therapeutic index of drugs, in particular for those agents with a narrow therapeutic index, resulting in an altered clinical response. Recently, Custodio et al. (28) demonstrated in MDCK/ MDR1-MDCK cell lines the inhibitory effect of monoglycerides on the P-gp efflux of vinblastine. These results suggest a potentially important effect of monoglycerides, breakdown products from a high fat meal, on increasing drug bioavailability.

P-gp expression can be induced by various factors, such as xenobiotics, environmental stress, differentiating agents, and hormones under cell culture conditions. In the rat liver, P-gp expression was increased after acute treatment by chemical carcinogens including 2-acetylaminofluorene and aflatoxin B1, suggesting xenobiotic-mediated transcriptional induction. Concomitant rifampin therapy (600 mg/day for 10 days, p.o.) has also resulted in significant reduction in the area under the plasma concentration time curve (AUC) of oral digoxin (single-dose, 1 mg oral and 1 mg intravenous), a known P-gp substrate. These results were confirmed by measuring intestinal P-gp levels, which revealed a threefold increase in this efflux transporter expression (22).

It is important to note that substrate specificity of P-gp may also vary across populations due to genetic polymorphisms. Kurata et al. (29) demonstrated a significant difference in oral digoxin bioavailability between two allelically diverged MDR1 populations, which resulted in population specific absorption and/or distribution outcomes. Nevertheless, findings from many studies on the effect of ABCB1 polymorphisms on P-gp substrates have not been consistently reproduced; therefore, routine applications of ABCB1 polymorphism analysis to clinical studies is not warranted at this time. Studies with larger number of samples may be needed to clarify the role of ABCB1 polymorphisms in pharmacokinetics and pharmacodynamics (17).

2.1.2. Multidrug Resistance -Associated Protein Family (MRP, ABCC)

The human MRP gene encodes an MRP polypeptide with an apparent mass of 170 kD, which is posttranslationally converted to a 190 kDa form by the addition of N-linked complex oligosaccharides. To date, nine members within the MRP family have been identified, although only MRPs 1 to 5 have been demonstrated to have a well-defined role in the transport of clinical relevant drugs (30).

2.1.2.1. MRP1 (ABCC1)

MRP1 was first cloned by Cole et al (31) from a multidrug-resistant human lung cancer cell line. MRP1 is highly expressed in the intestine, where it is localized in the basolateral membrane of enterocytes and is involved in the absorptive efflux of its substrates into blood (32). MRP1 expression has also been demonstrated in brain, liver, lung, kidney and testis (33). Substrate anticancer drugs include substances like Vinca alkaloids, anthracyclines, etoposide, teniposide, mitoxantrone and methotrexate. Unlike P-gp, MRP1 does not confer high levels of resistance to paclitaxel or bisantrene in cells. It can transport hydrophobic drugs or other compounds that are conjugated or complexed to the anionic tripeptide glutathione (GSH), to glucuronic acid, or to sulfate. Knockout mice lacking Mrp1 are viable and fertile, but they do show deficiencies in LTC_4-metiated inflammatory reactions, suggesting that secretion of LTC_4 is an important phisiological role function of MRP1 (30). Other studies demonstrated that a combined deficiency of Mdr1a and Mdr1b P-gps and Mrp1 in knockout mice resulted in a dramatically increased sensitivity to intraperitoneally administered vincristine (up to 128-fold), but also to etoposide (3.5 fold), whereas a P-gp deficiency alone resulted in a 16- and 1.75- increased sensitivity to these drugs, respectively (34).

So far, it has been much more difficult to find good small molecule inhibitors for MRP1 than for P-gp, especially ones that work in intact cells. This probably has to do with the preference of MRP1 for anionic compounds as substrates and inhibitors: most anionic compouns enter cells poorly, so it may be difficult to obtain sufficient intracellular concentrations of the inhibitor for efficacious inhibition. A variety of inhibitors of MRP1 has been described. Some examples are the LTC_4 analogue MK571, LTC_4 itself, sulfinprazone, benzbromarone and probenecid. Nevertheless, for specific in vivo inhibition of MRP1 these compounds are also not very appropriate as they affect extensively organic anion uptake systems as well. For the specific aim of in vivo MRP1 inhibition, inhibitors will have to be developed, with reasonable specificity and cellular penetration properties (30).

2.1.2.2. MRP2 (ABCC2)

MRP2 transports leukotrienes C_4, D_4 and E_4 and various glutathione conjugates, including oxidized glutathione, 2,4-dinitrophenyl-S-glutathione, bromosulfophthalein glutathione, as well as those conjugates of heavy metals including arsenic and cadmium. Additionally, MRP2 also transports glucuronide and sulfate conjugates of several bile salts, a range of unconjugated organic anions such as methotrexate, reduced folates, irinotecan and its metabolite SN-38, pravastatin, ceftriaxone and ampicillin (22).

Unlike MRP1, but similar to MDR1 P-gp, the overlapping substrate specificity of MRP2 with P-gp, coupled with their intestinal and cellular colocalization to the apical membrane, suggests a concerted function between these two transporters that would comprise a significant barrier to the intestinal absorption of many xenobiotics. As example we have grepafloxacin, which uptake was observed to be directly influenced by the combined effect of P-gp and MRP2 (35). As with MRP1, small molecule inhibitors of MRP2 than can be used in intact cells is quite limited. Obviously, many of the anionic transported substrates of MRP2 will readily serve as competitive inhibitors when applied in in vitro systems where MRP2 is present in an inside-out (vesicle) orientation. Some examples are LTC_4, MK571, phenolphtalein glucuronide and fluorescein methotrexate. Although such compounds do not penetrate cells to a sufficient extent to obtain useful levels of inhibition, it should be noted that normal

hepatocytes have a multitude of carrier uptake systems for organic anions, so that in vivo drug interactions mediated by MRP2 inhibitors in the liver could be highly relevant (30).

MRP2 has clinically relevant genetic polymorphisms (17) and the gene is fully deficient in two mutant rat strains (TR$^-$/GY and EHBR), and in patients suffering from Dubin-Johnson syndrome (30). These individuals suffer from a recessively inherited conjugated hyperbilirubinemia, which can result in jaundice.

2.1.3. Breast cancer resistance protein (BCRP, ABCG2)

BCRP was first cloned based on its overexpression in a highly doxorubicin-resistant MCF7 breast cancer cell line (MCF-7/AdrVp). Transfection of BCRP cDNA demonstrated that BCRP itself could confer resistance to mitoxantrone, doxorubicin and daunorubicin, and that it acted by energy-dependent (most likely through ATP hydrolysis) extrusion of its drug substrates. Because the gene was isolated from a breast cancer cell line, it was called the breast cancer resistance protein (BCRP) gene. BCRP sequences were also cloned by Miyake et al (36) and Allikmets et al. (37), who called the gene MXR (for mitoxantrone resistance) and ABCP (for placental ABC protein), respectively. Since structural and sequence homology revealed that BCRP belongs to the ABCG gene subfamily, the Human Genome Nomenclature Committee conferred the oficial designation as ABCG2 (22).

BCRP is a "half ABC transporter" consisting of 655 aminoacids and six transmembrane domains (TMDs) involved in drug binding and efflux, as well as a single amino-terminal cytosolic NBD that functions as an ABC involved in ATP hydrolysis (17, 38). BCRP is expressed in the gastrointestinal tract, liver, kidney, brain endothelium, mammary tissue, testis and placenta. It has a role in limiting oral bioavailability and transport across the blood-brain barrier, blood-testis barrier and the maternal-fetal barrier of some selected substrates. The physiological functions of BCRP include the extrusion of porphyrins from haematopoietic cells and hepatocytes, as well as the secretion of vitamin B_2 (riboflavin) and possibly other vitamins (such as biotin and vitamin K) into breast milk. BCRP substrates include mitoxantrone, methotrexate, topotecan, irinotecan, imatinib, statins, sulphate conjugates and porphyrins(39). Intestinal BCRP acts as a barrier for the oral bioavailability of drugs such as topotecan and sulphasalazine, which had a 10-fold to 110-fold increase in relative AUCs when administered to Bcrp$^{-/-}$

knockout mice. BCRP presents clinically relevant genetic polymorphisms (17). Recent studies have demonstrated that individuals with reduced BCRP expression levels (Q141K variant) are at increased risk for gefitinib-induced diarrhoea and alterede pharmacokinetics of 9-aminocamptothecin, diflomotecan, irinotecan, rosuvastatin, sulphasalazine and topotecan (17). Known inhibitors of BCRP consist of oestrone, 17-β-oestradiol, flavonoids, tamoxifen, novobiocin and HIV protease inhibitors. Fumitremorgin C, an extract of Aspergillus fumigatus, selectively inhibits BCRP with no overlapping affinity for P-gp (40).

2.2. Solute Carrier Transporters (SLC; SLCO)

The major uptake transporters responsible for xenobiotic transport belong to the two solute carriers (SLC and SLCO) superfamilies (20). The members of these superfamilies are involved in the transport of a wide range of substrates including amino acids, peptides, sugars, vitamins, bile acids, neurotransmitters, and xenobiotics. The SLC superfamily includes many pharmacokinetically important transporters such as proton dependent oligopeptide transporters (PepT1, PepT2, PHT1, etc; SLC15A family), organic anion transporters (OAT; SLC22A), organic cation transporters (OCT; SLC22A family), nucleoside transporters (CNT and ENT; SLC28A and 29A family) and the monocarboxylate transporters (MCT; SLC16A family) (22). The SLCO family is made up of the organic anion transporting polypeptides (OATP; SLC21A). These uptake transporters use a variety of porter mechanisms (i.e. uniporter, antiporter, symporter), not all of which have been fully elucidated for each specific transporter and use chemiosmotic gradient created by translocations of ions across the membrane (20).

2.2.1. Oligopeptide Transporters (PEPT; SLC15A)

The currently known peptide transporters include the Peptide transporters 1 and 2, PEPT1 and PEPT2 and the Peptide/Histidine Transporters 1 and 2, PHT1 and PHT2 (22). The cloned human PEPT1 cDNA sequence encodes a 708 amino acid protein with an estimated molecular weight of 79 kDa and an isoelectric point of 8.6 (41). PEPT1 protein expression has been demonstrated in the human small intestine and was localized on the apical plasma membrane of enterocytes in rats, exhibiting high homology between species (42). Peptidomimetic drugs are increasingly utilized as therapeutic agents for

the treatment of numerous disorders including AIDS, hypertension and cancer. Among PEPT1 substrates are cephalosporins, penicillins, ACE inhibitors and antivirals, which present different degrees of affinity and capacity, depending on the chemical structure. Generally PEPT1 has a high transport capacity, which makes it highly attractive as a drug target (22).

2.2.2. Organic Anion Transporters (OAT; SLC22A)

To date, five structurally related isoforms of organic anion transporters (OAT1-5) have been identified. OAT family members share some common topology characteristics including twelve α-helix transmembrane domain (TMD), one large hydrophilic extracellular loop between TMD 1 and 2 carrying several potential glycosylation sites and a large intracellular loop containing multiple potential phosphorylation sites between TMD 6 and 7 (43). OAT1 and OAT3 are mainly expressed in the kidney and localized on the basolateral membrane of the proximal tubules. Their substrates include relatively small and hydrophilic organic anions, such as p-aminohippurate (PAH), methotrexate, β-lactam antibiotics, nonsteroidal anti-inflammatory drugs (NSAIDs) and antiviral nucleoside analogs which are excreted into the urine (44). Most OAT isoforms have important functions in renal clearance of relevant substrates. The reported toxicity of some drugs is occasionally caused by concentrative tissue distribution due to transporters. The OAT1-mediated transport of adenovir, cephalosporin antibiotics and β -lactam antibiotics cause extensive accumulation in the proximal tubules, which may result in drug induced toxicity (44). OAT2 transports relatively small and hydrophilic organic anions, such as indomethacin and salicylate and may be involved in the hepatic uptake of these drugs (45).

In contrast to the liver and kidney, OATs are expressed to a lesser extent in brain, muscle, eye and placenta. While OAT isoforms have broad substrate specificity, members of the OAT family have not been identified in the human intestine. The intestinal expression of OAT members is limited, with only one report suggesting the presence of oat2 mRNA in mouse fetal intestine. Therefore, the role of the OAT family in the intestinal absorption of drugs is considered negligible (22).

2.2.3. Organic Cation Transporter (OCT, OCTN; SLC22A)

The SLC22 family is a member of the major facilitador superfamily that comprises transporters from bacteria, plants, animals and humans in 18 transporter families. This group of transporters consists of the electrogenic cation transporters OCT1-3, the carnitine and organic cation transporters (OCTN1, OCTN2) and OCT6, and the multidrug and toxin extrusion H^+/cation antiporters MATE1, MATE2-K and MATE2-B. Like most members of the SLC22 family, the organic cation and carnitine transporters have a predicted membrane topology that comprises 12 α-helical transmembrane domains (TMDs), an intracellular N-terminus, a large glycosylated extracellular loop between TMDs 1 and 2, a large intracellular loop with phosphorylation sites between TMDs 6 and 7, and an intracellular C-terminus (46).

Organic cation transporter 1 (OCT1) was the first member of the OCT family identified and was cloned from rat kidney (47).

This family of transporters is involved in the uptake of organic cations such as dopamine, choline, N-methylnicotinamide, TEA, cimetidine, antihistamines, muscle relaxants, antiarrhymics and β-adreno receptor blocking agents (44), into the liver or kidney from blood. OCT1 and OCT2 are expressed in epithelial cells of the kidney, liver and intestine and appear to the localized to the basolateral membranes of the cells. Rat Oct1 is expressed in both the liver and kidney, although its human counterpart is expressed predominantly in the liver, while human and rat Oct2 are present mainly in kidney and brain. The pharmacological and physiologic role of Oct1 has been investigated using Oct1 knockout ($Oct1^{-/-}$) mice. In $Oct1^{-/-}$ mice, accumulation of TEA in the liver was 4- to 6-fold lower than in wild-type mice, indicating that for TEA, Oct1 is the main uptake system in the liver. In addition, direct intestinal excretion of TEA was reduced about 2-fold, showing that Oct1 also mediates basolateral uptake of TEA into enterocytes. Rat Oct3 mRNA has been found to be most abundant in the placenta, with a moderate presence in the intestine, heart and brain (44). Most of the literature dealing with the function of OC transporters have been conducted in the liver and kidney, while few discuss the role of OC transporters in the gastrointestinal tract (22, 48).

Recent studies suggest that genetic variation in OCT1 may be a significant determinant in inter-individual variability in the disposition and response to cationic drug substrates, particularly metformin.

In Chinese and Korean populations, a common OCT2 variant (A270S) has been associated with a significant reduction in renal clearance of metformin (17).

2.2.4. Organic Anion Transporter Polypeptide (OATP; SLCO)

The SLCO family is made up of the organic anion transporting polypeptides (OATPs) (20). These transporters mediate the sodium-independent transport of a diverse range of amphiphilic organic compounds with a relatively high molecular weight, including bile acids, steroid conjugates, thyroid hormones, anionic peptides, numerous drugs and other xenobiotic. OATP substrates are eliminated from the liver by metabolism and/or biliary excretion, while small and hydrophilic organic anions, such as OAT substrates, are excreted into the urine (44). The general predicted OATP structure consists of proteins with 12 transmembrane domains and a large 5th extracellular loop. The mechanism of transport appears to consist of anion exchange by coupling the cellular uptake of substrates with the efflux of endogenous intracellular substances such as bicarbonate in a process that seems to be electroneutral. Interestingly, OATP family members are poorly conserved evolutionarily and orthologues for human OATPs may not exist in rodents (17). In rats, main Oatps are Oatp1a1 (formerly known as oatp1) expressed in the liver and kidney, the widely expressed Oatp2a1 (formerly known as rPGT), Oatp1a4 (formerly known as oatp2) expressed in the retina, liver and brain and Oatp1a5 (formerly known as oatp3) expressed in retina, brain, liver, kidney and the intestine (49).

OATP1A2 (formerly termed OATP-A) was described in 1995 and followed by the discovery of the second member OATP1B1 (formerly termed OATP2 or OATP-C). Today the OATP family consists of 11 members, including 10 OATPs and the prostaglandin transporter OATP2A1 (formerly known as PGT). While most of the OATP proteins are expressed in multiple tissues, OATP1B1 and OATP1B3 are predominantely if not exclusively expressed in the liver. OATP1A2 shows highest expression in brain and testis, whereas OATP2B1 and OATP4A1 are ubiquitously expressed in all tissues investigated so far. Almost all OATP family members are localised to the basolateral membrane of polarized cells. OATP1B1, OATP1B3 and OATP2B1 have been localised to the basolateral membrane of human hepatocytes, whereas OATP1A2 has been localised to the basolateral membrane of brain endothelial cells. Interestingly, in addition to its basolateral localisation in liver and placenta, OATP2B1 and OATP1A2 have been detected in the apical membrane of enterocytes (50). Since expression and substrates for all human OATP family members have not been completely characterized, additional functional studies and investigations of protein

localisations are required to determine the specific role of each OATP family member in drug disposition (50).

A series of functional polymorphisms of OATP1B1 have been characterized that have different activities and also occur at different frequencies in various ethnic groups. Pharmacokinetic studies indicate that individuals with the SLO1B1*5 or SLO1B1*15 haplotypes have increased exposure to statin drugs such as pravastatin, pitavastatin, simvastatin, atorvastatin and rosuvastatin. They also have increased exposure to other drugs such as repaglinide, atrasentan, irinotecan and ezetimibe. Compeling clinical evidence supporting an important role for SLCO1B1 polymorphisms has come from a genome wide association study of simvastatin-induced myopathy (17).

In rodents, the transporters have the same name than in humans, but are written with lower caps. E.g.:

OATP in humans, Oatp in rodents; OAT in humans, Oat in rodents; OCT in humans, Oct in rodents.

3. Intestinal permeability assessment

Within the gastrointestinal tract (GI), the upper small intestine (i.e. duodenum, proximal jejunum) represents the main site for absorption of nutrients and drugs offering an appropriately large absorption area of nearly 200 m^2 (51). Approximately 90% of all absorption in the GI occurs in the small intestine region. The intestinal surface of the small intestine has surface projections that increase the potential surface area for digestion and absorption. Macroscopic valve like folds, called circular folds, encircling the inside of the intestinal lumen is estimated to increase the surface area of the small intestine threefold. Vili increase the area 30-fold and the microvilli increase by a factor of 600. Thus, such unique structures lead to a tremendous increase in surface area available for absorption in the small intestine (Table 3) (52).

The epithelial cells in the intestinal region are a heterogenous population of cells which include enterocytes or absorptive cells, goblet cells which secret mucin, endocrine cells, paneth cells, M cells, tuft and cup cells. The most common epithelial cells are the enterocytes or absorptive cells. These cells are polarized with distinct apical and basolateral membrane that are separated by tight junctions (53).

Table 2- Drug transporters involved in the absorption and disposition of drugs. *Adapted from (17) and (20).*

Gene/ Transporter	**Localisation**	**Substrates**	**Inhibitors**
SLC16A1 (MCT1)	Intestine (A, B)	Lactate, pyruvate, benzoic acid	AR-C117977
SLC15A1 (PEPT1)	Intestine (A)	Ampicillin, captopril, valacyclovir	4-aminomethylbenzoic acid
SLC15A2 (PEPT2)	Intestine (A)	Ampicillin, captopril, valacyclovir	Cefadroxil, captopril
SLCO2B1 (OATP2B1)	Intestine (A), Hepatic (B)	Estrone-3-sulfate, atorvastatin	Rifampin, bromosulfophthalein
SLCO1A2 (OATP1A2)	Intestine (A), Hepatic (B)	Estrone-3-sulfate, fexofenadine	Rifampin, bromosulfophthalein
SLC22A3(OCT3)	Intestine (A)	Cimetidine	Corticosterone, decynium22 S-8921, SC-435
SLC10A2(ASBT)	Intestine (A)	Bile salts (taurocholate)	Adenosine
SLC28A1 (CNT1)	Intestine (A)	Thymidine, zidovudine	Thymidine
SLC28A2(CNT2)′	Intestine (A)	Guanosine, ribavirin	Cimetidine, pyrilimine, verapamil
SLC22A4 (OCTN1)	Intestine (A)	Quinidine, verapamil	Pyrilimine, TEA
SLC22A5 (OCTN2)	Intestine (A)	Quinidine, verapamil	GG918, verapamil
ABCB1 (P-gp)	Intestine (A), Hepatic (A)	Digoxin, fexofenadine, indinavir, vincristine, colchicine, topotecan, paclitaxel	MK-571, cyclosporine
ABCC2 (MRP2)	Intestine (A), Hepatic (A)	Indinavir, cisplatin, glutathione-, glucuronide-, sulfate conjugates	FTC, Ko-143
ABCG2 (BCRP)	Intestine (A), Hepatic (A)	Rosuvastatin, doxorubicin, sulfasalazine, topotecan	MK-571
ABCC4 (MRP4)	Intestine (A, B) Hepatic (B)	Topotecan, ceftizoxime, cefazolin	
SLCO3A1 (OATP3A1)	Intestine (B)	PGE1, PGE2, BQ-123, vasopressin	Montelukast, prazosin, verapamil
SLCO4A1 (OATP4A1)	Intestine (B)	Deesterified unoprostone carboxylate	Bromosulfophthalein

SLC22A 1 (OCT1)	Intestine (B), Hepatic (B)	Acyclovir, amantadine, desipramine, ganciclovir, metformin	MK-571, probenecid MK-571, indomethacin
SLC22A2 (OCT2)	Intestine (B)	Amantadine, cimetidine,	MK-571, sildenafil
ABCC1 (MRP1)	Intestine (B)	memantine	
ABCC3 (MRP3)	Intestine (B)	Adefovir, indinavir	Nitrobenzylmercaptopurine riboside, dipyridamole
ABCC5 (MRP5)	Intestine (B), Hepatic (B)	Etoposide, methotrexate, tenoposide	Nitrobenzylmercaptopurine riboside, dipyridamole
SLC29A1 (ENT1)	Intestine (B)	cGMP, methotrexate, mercaptopurine	Cyclosporine, vinblastine, verapamil
SLC29A2 (ENT2)	Intestine (B)	Adenosine	Cyclosporine, troglitazone Rifampin
ABCB4 (MDR3)	Hepatic (A)	ddC, AZT, ddI	Rifampin
ABCB11(BSEP)	Hepatic (A)	Digoxin, paclitaxel, vinblastine	Bosentan, propranolol,
SLCO1B1(OATP1B1)	Hepatic (B)		cyclosporine
SLCO1B3	Hepatic (B)	Vinblastine	Pravastatin, probenecid,
(OATP1B3)	Hepatic (B)		taurocholate
SLC10A1 (NTCP)	Hepatic (B)	Rifampin, rosuvastatin, methotrexate, pravastatin	MK-571, indomethacin
SLC22A7 (OAT2)	Hepatic (B)	Digoxin, rifampin, methotrexate Rosuvastatin	Verapamil, indomethacin, benzbromarone
ABCC3 (MRP3)	Hepatic (B)	Zidovudine, etoposide, methotrexate, tenoposide	
ABCC6 (MRP6)	Hepatic (B)	Cisplatin, daunorubicin	

During enterocyte differentiation, the cells adopt a columnar appearance and develop microvilli on their apical surfaces. Before the compound is able to diffuse across the absorptive cells, it has to diffuse across a mucus layer adjacent to enterocytes composed of large glycoproteins with net negative charge.

Table 3- Biological and physical parameters of human intestinal tract *in* (52).

Gastrointestinal segment	**Surface area**	**Segment length (cm)**	**Residence time**	**pH of the segment**
Oral cavity	100 cm^2		sec. to minutes	6.5
Esophagos	200 cm^2	23-25	seconds	
Stomach	3.5 m^2	25	1.5 h	1-2
Duodenum	1.9 m^2	35	0.5-0.75 h	4.0-5.5
Jejunum	184 m^2	280	1.5-2.0 h	5.5-7.0
Ileum	276 m^2	420	5-7 h	7.0-7.5
Colon and rectum	1.3 m^2	150	1-60 h (average = 30)	7.0-7.5

Together with water, lipids and cellular proteins, luminal and cellular debris, the enterocyte apical membrane is preceeded by an unstirred water layer (UWL) with pH between 5.2 and 6.2 which is regulated independently of the variable luminal pH (Figure 4)(54).

The jejunum is further characterized by a high expression of several physiologically relevant uptake carriers for nutrients including carbohydrates (e.g GLUTs), fatty acids (MCTs, FATs), peptides (PEPTs) and drugs like the organic cation transporter (OCT3) and the organic anion transporters (OATP1A2, OATP2B1). ABC transporters P-gp, MRP2 and BCRP are also highly abundant at the apical (luminal) membrane of enterocytes thereby limiting the intestinal absorption of numerous xenobiotics (20) (Figure 5C). Several studies have indicated that enterocytes have a high expression of phase I and II metabolizing enzymes (e.g. CYP3A4, UGTs, SULTs) being responsible for the high first-pass metabolism of many compounds (51) (Figure 5E). Therefore, the intestinal epithelium acts not only as a phisycal barrier but also as a complex biochemical barrier to drug absorption.

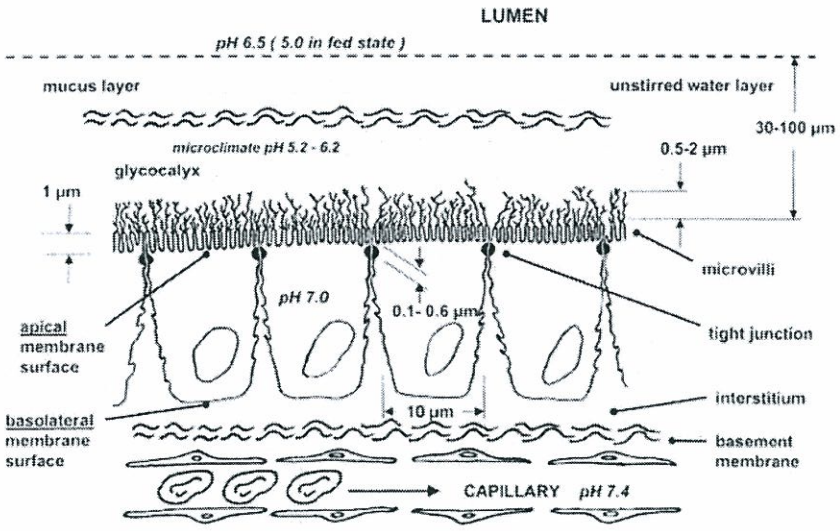

Figure 4 – Schematic structure of intestinal epithelial cells. *In* Curr Top Med Chem (55).

Solutes that can penetrate this epithelial barrier must possess either the optimal physicochemcial characteristics that allow them to passively diffuse via the transcellular route or the structural features necessary to serve as a substrate for one of the uptake transporters. Another feature of this epithelia is that it possess a low level of transcytotic activity, limiting the entrace of macromolecules (e.g. proteins) (56). Thus, the bulk of absorption takes place in the small intestine by various mechanisms such as passive diffusion (paracellular and transcellular) and carrier-mediated process (facilitated and active). A number of small hydrophilic, ionised drugs are absorbed via the paracellular pathway (Figure 5A). However, absorption via this route is generally low since intracellular tight junctions restrict free transepithelial movement between epithelial cells. Transcellular absorption from lumen (apical side) to blood (basolateral side) requires uptake across the apical membrane, followed by transport across the cytosol, then exit across the basolateral membrane into blood (Figure 5B).

The extent of drug absorption and bioavailability (BA) are the central questions for pharmaceutical scientists during the course of drug discovery and development (57). A system that allows for the assessment of the interplay occuring following administration of an oral dose would greatly benefit the early stages of drug development (28). Amidon et al. (58) recognized that one of the fundamental parameters controlling BA was the drug's gastrointestinal permeability.

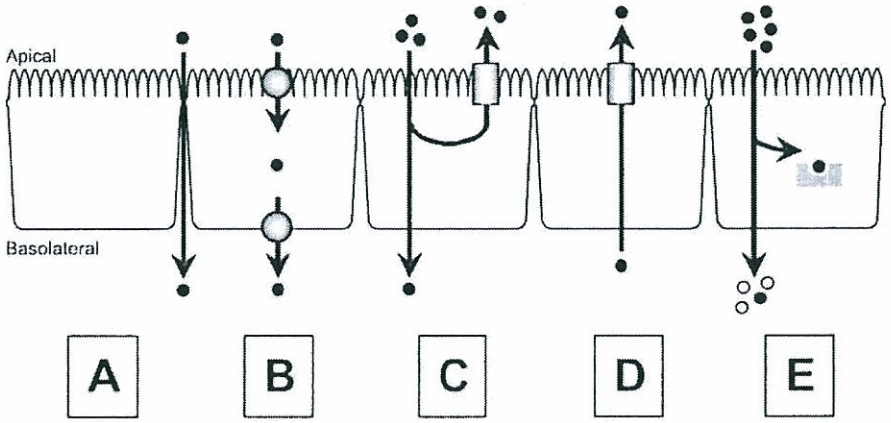

Figure 5- The intestinal epithelium forms a selective barrier against the entry of compounds. A) Absorption of compounds via the paracellular route. B) Transcellular absorption of compounds, either passively, or with the involvement of carrier-mediated transport. C) Efflux transporters at the apical membrane limit the absorption of compounds. D) Apical efflux transporters may also facilitate the clearance of compounds from blood. E) Intracellular metabolising enzymes may modify compounds before they enter the blood.

Because of the multivariated process involved in the intestinal absorption of drugs it is often difficult to accurately predict the *in vivo* permeability characteristics of a compound. Several physicochemical, *in vitro* and *in vivo* models can be used to estimate intestinal permeability. Important physicochemical characeristics are size, charge, lipophilicity and hidrogen-bonding potential. *In vitro* methods include artificial lipid membranes such as parallel artificial membrane permeability assay (PAMPA), cell based systems such as Caco-2 cells, Mardin-Darby canine kidney cells and tissue based Ussing chamber. *In situ* methods consist of intestinal single pass perfusion and *in vivo* methods use whole animal absorption studies (53, 59).

Because *in vivo* studies performed with humans and laboratory animals are expensive, time consuming and often even unethical, *in vitro* methods, as accurate as possible, are needed in screening new drug candidates (54) (Figure 6). Computational or virtual screening has received much attention in the last few years and *in silico* predictive models would minimize extremely time consuming steps of synthesis as well as experimental studies (59).

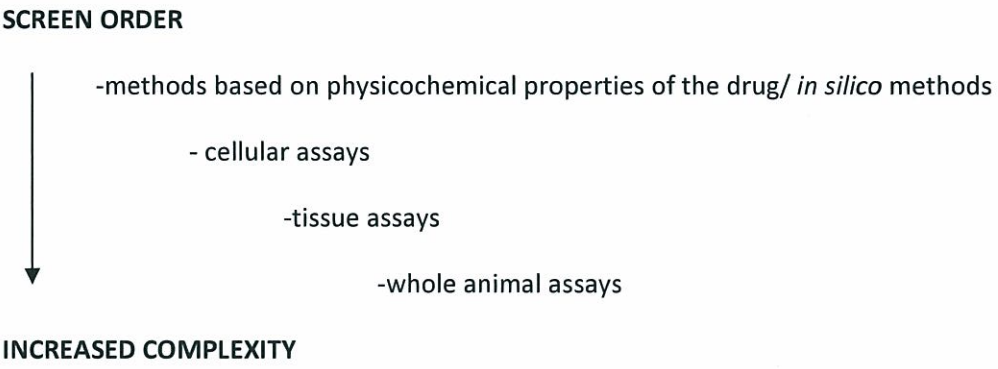

Figure 6 - Methods for assessment of oral drug absorption.

3.1. Physicochemical Methods

3.1.1. Lipophilicity (Log P/Log D)

As a measure of drug-membrane interaction, lipophilicity is one of the most important physicochemical parameters in predicting and interpreting membrane permeability. Historically, the octanol-water partition ratio (*Log P*) was accepted as a surrogate to biological systems for predicting absorption. Nowadays is widely recognized that use of *Log P* alone for predicting absorption is an over simplification of a complex process. *Log P* values provide indirect information of the extent of passive transcellular transport possible for various drugs in which transport is largely mediated by a passive mechanism. However, several other factors may contribute to overall passive permeability such as polar surface area, molecular volume/flexibility, hydrogen bonding, ionization, etc (59) (60). For compounds with parallel transport processes, the correlation with lipophilicity is normally lacking (61).

3.1.2. Lipinski's rule-of-five analysis

Christopher Lipinski's rule-of-five analysis helped to raise awareness about properties and structural features that make molecules more or less drug-like. The guidelines were quickly adopted by the pharmaceutical industry as it helped apply ADME considerations early in preclinical development and could help avoid costly late-stage preclinical and clinical failures. The guidelines predict that poor

absorption or permeation of an orally administered compound is more likely if the compound meets the following criteria:

- Molecular mass greater than 500 Da
- High lipophilicity (expressed as *LogP* greater than 5)
- More than 5 hydrogen bond donors
- More than 10 hydrogen bond acceptors

Since its publication in 1997, the "Lipinski rule of five" has been a critical filter for drug development programs. A simple algorithm that helps identify successful drug candidates, the principles filter out molecules likely to have poor intestinal permeability or poor aqueous solubility, and hence poor oral absorption. This landmark contribution to drug development has influenced the way that the pharmaceutical industry approaches the development of orally active drugs. Drug discovery programs worldwide use the Rule as a filter in high-throughput screening libraries (62). As well as *Log P,* this rule does not preview the role of transporters on drug absorption and is better applied to drugs that are absorbed by passive diffusion.

3.2. *In vitro* Methods

In vitro techniques for assessment of permeability are less labor and cost intensive compared to *in vivo* animal studies. One universal issue with all the *in vitro* systems is that the effect of physiological factors such as gastric empting rate and GI transit rate cannot be incorporated in the data interpretation. Based on the specific role, one or more of these methods can be used as a screening tool for the assessment of GI permeability (59).

3.2.1. Cell-Based Methods

Normal intestinal epithelial cell lines are not available. Despite of the efforts to maintain them in culture, the major problems i.e., low viability and short life-time, are still not overcome (54). Therefore, the use of immortalized (tumor) cell lines that grow rapidly into confluent monolayers have been developed and currently enjoy widespread popularity. These cells exhibit several characteristics of

Table 3 – Cell culture models commonly used for drug permeability assessment (53) and (60).

Cell line	**Species of origin**	**Special characteristics**
Caco-2	Human colon adenocarciona	Most well-established cell model. Differentiates and expresses some relevant efflux transporters. Expression of uptake transporters is variable.
MDCK	Mardin-Darby canine kidney cells	Polarized cells with low intrinsic expression of ABCtransporters. Ideal for transfections. (E.g. MDR1-MDCK).
LLC-PK1	Pig kidney epithelial cells. Lewis lung carcinoma-porcine kidney	Polarized cells with low intrinsic transporter expression. Ideal for transfections.
2/4/A1	Rat fetal intestinal epithelial cells	Temperature-sensitive. Ideal for paracellularly absorbed compounds because of leakier pores with 9.0±0.2 Angstroms, similar to human small intestine pores. TEER of 50 ohms.cm^2. Contains brush-border enzymes as well as transporter proteins.
TC-7	Caco-2 subclone	Similar to Caco-2.
HT-29	Human colon	Contains mucus-production goblet cells.
IEC-18	Rat small intestinal cell line	Provides a size-selective barrier for paracellularly transported compounds.

differentiated epithelial cells and cell culture models provide an ideal system for the rapid assessment of the intestinal permeability of drugs (53). Examples of cell models that are used routinely for permeability screenig are described in Table 3.

3.2.1.1 Caco-2 cells

The Caco-2 cell line is a continuous line of heterogeneous human epithelial colorectal adenocarcinoma cells. This cell line is now routinely cultivated as monolayers on permeable filters for studies of the transepithelial transport of drugs (60). The first study attempting to correlate passive drug permeability in Caco-2 monolayers with drug absorption in humans after oral administration suggested that the cell monolayers might be used to identify drugs with potential absorption problems. Completely absorbed drugs were found to have high permeability coefficients (Papp $>1x10^{-6}$ cm/s) whereas incompletely absorbed drugs had low permeability coefficients (Papp $<1x10^{-7}$ cm/s) in the Caco-2 monolayers (63).

Another studies (64) in Caco-2 cells have shown that drugs with Papp values less than $1x10^{-6}$ cm/s are poorly (0-20%) absorbed; drugs with Papp values between 1 and $10x10^{-6}$ cm/s are moderately (20-70%) absorbed; and drugs with Papp values greater than $10x10^{-6}$ are well (70-100%) absorbed. These correlation studies were mainly performed with passively transported drugs which indicates that Caco-2 cells are an excellent model of the passive transcellular pathway, the most common drug permeation route in the intestine. The correlation of the permeabilities of the slowly and incompletely absorbed drugs in the Caco-2 monolayers and human jejunum was qualitative rather than quantitative. These drugs were transported at a 30- to 80-fold slower rate in the Caco-2 monolayers than in the human jejunum (65) The two most likely explanations for this discrepancy are related to possible differences in the permeability of the paracellular pathway and in the absorptive surface areas. Electrophysiological and permeability data indicate that the permeability of the tight junctions in Caco-2 monolayers is lower than the average permeability observed in the human intestine *in vivo*. On the other hand, drugs having a lower permeability will remain longer in the intestinal lumen before they are absorbed. These drugs may therefore diffuse further down the length of the villi, with increase in the absorptive surface area by comparison with Caco-2, that area presented as a flat monolayer (60). The relationship between the permeability and the fraction absorbed is very steep for incompletely absorbed drugs. When the

permeability coefficient increases from $1x10^{-7}$ to $1x10^{-6}$ cm/s the predicted absorbed fraction of a drug increases from 0 to 100% *in vivo* (63).

After 2-3 weeks in cell culture, the Caco-2 monolayers have well developed junctional complexes (63). Transepithelial electrical resistance (TEER) of the monolayer can be measured by the Millicell electrical resistance system utilizing "chopstick" electrodes and are expressed in units of resistance and surface area. For a semi-porous membrane with a pore size of 0.4 μm and surface area of 4.2 cm^2 the ohm resistance measured is then multiplied by 4.2 cm^2. In this membrane, the Caco-2 cell line possesses TEER values of approximately 800-1000 ohm.cm^2 (28), while the reported small intestinal TEER is in the range of 25-45 ohm.cm^2. Additionally, the paracellular pore radius of Caco-2 cells is approximately 3.7±0.1 Angstroms *vs.* 9.0±0.2 Angstroms in the human small intestine (53).

The limitations of many of the early studies was the use of drugs which are mainly transported passively by the transcellular and paracellular routes without consideration of drugs transported by a carrier-mediated mechanism. Recent attempts to include transported compounds in these studies have given variable results. When correlation analysis was performed between *in vitro* drug permeability in Caco-2 cells and *in vivo* drug permeability in humans, the permeability correlation coefficient increased from 0.7276 to 0.8492 when drugs absorbed through a carrier-mediated process were excluded (66). A >100 fold decrease in the permeability of L-dopa, L-leucine and D-glucose (all have an uptake-carrier in the human jejunum) was found in Caco-2 cells in comparison to the human jejunum. This decrease may be related to the lower expression of uptake carriers for these drugs in the Caco-2 monolayer than *in vivo* (60). On the other hand, in another study including drugs absorbed by an uptake-carrier mechanism the drug permeabilities in Caco-2 correlated with those in the perfused rat intestine (67). Caco-2 cells are known to express intrinsically the physiological relevant transporters [e.g. P-gp (24, 68), BCRP, MRP2 (68), peptide transporters, organic cation transporter, organic anion transporter, large neutral amino acids transporter, bile acids transporter, cobalamin and dipeptides transport systems (63)] but the gene expression profiles of the cells and the human intestine can be significantly different (68-70) and in Caco-2 these transporters are quantitatively underexpressed when compared with levels of production *in vivo* (53, 70). Thus we conclude that the strength of the Caco-2 monolayers *vs. in vivo* correlations may vary according with the group of drugs. Other sources of variability are related to the experimental conditions and the cell line itself. Caco-2 cells are a heterogenous cell population which is exposed to different selection pressures in different laboratories (71). The characteristics of Caco-2 cells, including

TEER and transporter expression, may vary from one laboratory to another and even within the same laboratory its properties can change with seeeding density, feeding frequency, monolayers washing steps, passage number, the time in culture, the filter support and the cell culture medium, which can produce dramatic differences in the permeability value (28, 60, 72). Terefore it is useful to repeat investigation of the transport of reference compounds at regular time intervals. Methods for validation of a Caco-2 cell culture have been described by several authors which includes the use of low, medium and high permeability markers (73, 74) as well as known P-gp substrates and inhibitors (74-76). The TEER and the transepithelial permeability of a paracellular flux marker such as mannitol are commonly used to monitor monolayer integrity or cell damage (77). The Caco-2 cell model can only serve as a one-way screen such that compounds with high permeability in this model are typically well absorbed in vivo; however, compounds with low permeability cannot be ruled out as poorly absorbed compounds *in vivo* (53).

Cytochrome P450 CYP3A4 is the most prominent oxidative CYP enzyme present in the intestine and plays a significant role in first-pass metabolism (78). Although Caco-2 cell based models are known to express adequate amounts of hydrolase, esterase and brush border enzymes (53), they fail to simulate complete *in vivo* intestinal environment because they do not express adequate quantities of CYP3A4, the principle CYP present in human epithelial cells. Efforts have been made to develop Caco-2 cells expressing high levels of cDNA-derived CYP3A4, either by modification of the growth media or using the transfection technique (53). Cummins and colleagues (79) used CYP3A4-transfected Caco-2 cells as an *in vitro* system to predict the importance of drug metabolism and transport on overall drug absorption of sirolimus and midazolam.

Caco-2 cells are often used in combination with Parallel Artifical Membrane Permeability Assays (PAMPA) (80) to evaluate the permeability properties of a large number of compounds at the early drug discovery phase . PAMPA model has been demonstrated in recent years to be an efficient, economical and high-throughput model. PAMPA captures the transcelullar passive permeability across lipoidal membrane barrier without the contribution from pores or drug transporters. Caco-2 cell model is capable of incorporating not only the transcellular passive permeability but also the transporter mediated (efflux and influx) and the paracellular components of transport (59).

Another current use of Caco-2 cells is the bidirectional permeability assay, where the basolateral to apical (secretory direction, B to A) permeability is compared to the apical to basolateral (absorptive direction, A to B) permeability. This assay allows calculation of apparent permeability (Papp) values as well as net efflux ratios (B-A Papp/A-B Papp) and is regarded as the gold standard in identifying P-gp substrates because it is functionally the most direct method of measuring efflux characteristics of drugs candidates. Compounds with an efflux ratio greater than 2-3 are typically considered as P-gp substrates (28). However, it is well known that efflux transporters other than P-gp (e.g., MRP2, BCRP) are also functionally expressed in the Caco-2 cells (59, 68). As a confirmatory study, a paralel assay using GF120918 (GG918; N-[4-[2-(3,4-Dihydro-6,7-dimethoxy-2(1H)-isoquinolinyl)ethyl]phenyl]-9,10-dihydro-5-methoxy-9-oxo-4-acridinecarboxamide), a selective inhibitor of P-gp, is usually run to confirm P-gp efflux inhibition. Nevertheless, some recent publications have reported that GG918 interacts not only with P-gp but also with BCRP (81). Similarly, MK-571 and fumitremorgin C (FTC) are used to selectively inhibit the MRP2 and BCRP activity, respectively (82). Comparison of efflux ratio in the absence and presence of these specific inhibitors can delineate the potential role of the individual efflux transporter. Because it is a cell-based assay with a physical barrier (lipid bilayer), the test compounds must have adequate cell permeability for the bidirectional P-gp assay. One major drawback of the bidirectional permeability assay is that the P-gp subtrates with insufficient transcellular permeability cannot be identified. Drugs such as famotidine and ranitidine are substrates for secretory transporters proteins (83) but often they fail to be detected as P-gp substrates due to their low passive permeability (59).

3.2.1.2. MDCK cells

Apart from Caco-2, Mardin-Darby canine kidney cells (MDCK cells) are other model most frequently used for permeability assessment (84, 85). These cells differentiate into columnar epithelial cells and form tight junctions when cultured on semi-permeable membranes. A good correlation between permeation of passively absorbed drugs was reported between Caco-2 and MDCK cells. MDCK cells are derived from dog kidney cells, and thus there is a high probability that the expression levels of some transporters would be different in these two cell lines. More studies are required in MDCK cell line to confirm that the correlation of permeability to human absorption values would be conserved for transporter-mediated uptake and/or efflux compounds. One of the major advantages of MDCK cells over Caco-2 cells is the shorter cultivation period (three days *vs.* three weeks) (53) and lower TEER values (200-300

ohm.cm^2). MDCK cells are frequently transfected with the P-gp gene (MDR1-MDCK cells) for the screening of P-gp substrates. Compared to alternative cell monolayers, the MDR1-MDCK cell system possesses very tight junctions as reflected by the high TEER values of 5000 to 6000 ohm. cm^2 (28). As for Caco-2 cells, bidirectional transport, apical to basolateral (A to B) and basolateral to apical (B to A) across the monolayer allows for the calculation of apparent permeability (Papp) values as well as net efflux ratios (B-A Papp/A-B Papp). P-gp substrates display a net efflux ratio of 2 or higher (28).

3.2.2. Animal tissue based protocols

Due to the structural similarities of intestinal membrane, drug absorption in animal models may be used to predict drug absorption in humans. Cao *et al* (11) showed that drug permeability in the rat is generally five to ten-fold lower than the permeability in the human, although there is a reasonable correlation (r^2=0.7). A previous study reported that effective permeability estimates of passively absorbed solutes correlate highly in rat and human jejunum while carrier-mediated transport requires scaling between the models because the substrate specificity and/or transport maximum may differ (86). Excised animal tissue models have been used since the 1950s to explore the mechanism of absorption of nutrients from the intestine. However, the viability of the excised tissue is difficult to maintain since the tissues are devoided of direct blood supply and need constant oxygenation (59). Excised tissue preparations share two important advantages, preservation of the architectural integrity and ability to determine absorption across different gastrointestinal segments (77). Another advantage, compared to cell culture models, is that transporters and enzymes are expressed at physiologically relevant levels, so the rat intestine model can be used to study transporter-enzyme interplay in the intestine. Some of the more widely used methods for absorption and permeability studies are described below.

3.2.2.1. Everted Gut Technique

The everted sac was one of the first *in vitro* techniques used to study intestinal drug absorption. It was used as early as the 1950s in the transport study of sugars and amino acids from the mucosal (apical) to serosal (basolateral) side (52). It is prepared by inverting a piece of intestine using a glass rod. The two

ends of the intestinal segment are tied and the inside of the resulting sac is filled with an oxygenated buffer. The sac is then placed in a container that has the test compound. Drug absorption is measured by sampling the solution inside and outside the sac. It includes the mucosa plus underlying muscle layers. The presence of this muscle layer could accumulate drugs, and thus lead to poor recovery (77). In addition, everting the intestinal sac can lead to morphological damage causing misleading results. The everted gut model has an additional analytical advantage over other *in vitro* models because the sample volume on the basolateral side is relatively small and drugs accumulate faster (52).

3.2.2.2 Ussing Chamber

Transport studies across intestinal sheets from animals are also a widely used *in vitro* method to study drug absorption (87). This method involves the isolation of the intestinal tissues, cutting it into strips of appropriate size, clamping it on a suitable device and then the rate of drug transport of across this tissue is measured. In this method, the permeability is assessed based on the appearance of drug in the basolateral side rather than the disappearance of drug in the apical side. The unique feature of this approach is that electric resistance of the membrane can be measured during the course of the experiment. The short-circuit current across the membrane, as well as the resistance across the membrane, can be monitored. These parameters are routinely used as an indicator of the viability of the intestinal tissue during the transport studies with Ussing chamber (52). The integrity of the intestinal membrane can be also monitored by addition of a paracellular marker, such as mannitol, fluorescein or phenolred (88). Although mucosal sheets are used with or without the underlying muscle layer, *in vivo*, the muscle layer is not a barrier to absorption. The removal of this muscle layer, a process known as stripping, is advantageous because it removes an artificial permeability barrier and stripped tissues can be oxygenated more efficiently (77). On the other hand, the removal of the muscle layer is a very sensitive operation that can lead to intestinal epithelium damage.

The Ussing chamber technique is an ideal method to study regional differences on the absorption of drugs by mounting intestinal tissues from various intestinal regions. It is also possible to perform studies with human intestinal tissues (87, 89) thus providing a methodology to compare the permeability values across species. Nevertheless it is extremely difficult to obtain viable human tissues for permeability studies on a regular basis (52). A comparison between the Ussing chamber technique and human jejunal permeability found a good correlation for a discrete small series of 12 compounds (90).

3.2.2.3. Isolated membrane vesicles

Cell membrane preparations include brush-border membrane vesicles and basolateral membrane vesicles. Membrane vesicles can be prepared from either intestinal scrapings or isolated enterocytes. The membrane vesicles are suspended in a physiologic buffer that contains the test compound. Uptake into these vesicles is supposed to mimic transport across cell membranes. These preparations constitute simplified models to study mucosal absorption (77). They have been proved useful to study specific membrane processes such as, binding of organic cations and uptake of PEPT1 substrates by small intestine (91, 92).

Membrane vesicle studies allow a complete manipulation of solute environment both inside and outside of the vesicle and facilitate isolation and identification of transporter proteins that are specifically expressed either on the brush border or the basolateral side of the membranes (52). Advantages of this preparation include the small amount of material needed as well as the short duration of transport experiments (77). Additionaly, multiple experiments can be performed with vesicles prepared from a single laboratory animal, as vesicles can be cryopreserved and used for a long duration (52). However, the lack of cellular metabolism makes it difficult to study important aspects of ATP-dependent transport and uptake into membrane vesicles does not provide any insight into paracellular transport (77).

3.3. *In situ* studies

3.3.1. Perfused Rat Intestine

In situ perfusion of intestinal segments of rodents (rats or rabbits) is commonly used to study the permeability and absorption kinetics of drugs. The major advantage of the *in situ* system compared to the *in vitro* techniques discussed earlier is the presence of an intact blood and nerve supply in the experimental animals. Various modifications of the perfusion technique have been studied by different investigators: single pass perfusion, recirculating perfusion, oscillating perfusion and the closed loop method (52). The single pass perfusion model can be used to determine regional disposition of drugs (93). This methodology is found to be highly accurate for predicting the permeability of passively transported compounds, however the use of a scaling factor has been recommended for predicting permeability of carrier-mediated compounds.

As it is commonly used, this technique only allows sampling from the mucosal side; drug disappearance is assumed to be equal to drug absorption. This assumption is valid when apical uptake is the rate-limiting step in drug absorption. However, considering that drug absorption is not the only factor responsible for luminal drug disappearance, this assumption could be misleading. For example, luminal and mucosal metabolism and mucosal accumulation could lead to an overestimation of true drug absorption (77). Indeed, an earlier study found that, for several β-lactam antibiotics, absorption based on luminal disappearance was approximately twice the true amount transported across the tissue (94).

The method is also limited because of its cost factor as it requires a large number of animals to get statistically significant absorption data (52). It was also demonstrated that the surgical manipulation of intestine combined with anesthesia caused a significant change in the blood flow to intestine and had a significant effect on absorption rate (95).

3.3.2. Perfused Human Intestinal segments

3.3.2.1. Lock I Gut

Lennernas (96) has extended the perfusion studies to humans, allowing direct measurements of intestinal absorption, secretion, and metabolism of drugs. In general, four different clinical tools have been employed in the small intestine (97):

- triple-lumen tube including a mixing segment,
- multilumen tube with a proximal occluding balloon,
- multilumen tube (Loc-I-Gut) with two ballons occluding a 10-cm-long intestinal segment,
- two 20-cm adjacent jejuna segments were isolated with the multilumen perfusion catheter.

Loc-I-Gut is a perfusion technique for the proximal region of the human jejunum. The multichannel tube is 175 cm long and is made of polyvinyl chloride with an external diameter of 5.3 mm. It contains six channels and is provided distally with two 40-mm-long elongated latex balloons, placed 10 cm apart, and each separately connected to one of the smaller channels. The two wider channels in the center of

the tube are for infusion and aspiration of perfusate. The two remaining peripheral smaller channels are used for administration of marker substances and/or for drainage (97). The direct measurement of human intestinal permeability as major advantages as it is possible to measure regardless of the transport mechanism, predicts the fraction absorbed (f_a) and can be used to assess *in vitro-in vivo* correlations which validates the use of different intestinal absorption models commonly applied in drug discovery and preclinical development (96).

4. Synergistic action of CYP3A4 and P-glycoprotein

CYP3A4 is the most prominent oxidative cytochrome P450 enzyme present in human enterocytes. Despite the lower CYP3A4 content in the intestine relative to the liver, first-pass metabolism in the intestine by CYP3A has conclusively been shown to be important in the disposition of midazolam and cyclosporine (CsA) from studies with anhepatic patients. Drug interaction studies performed with grapefruit juice (inhibitor of intestinal CYP3A) have also shown significant increases in the oral bioavailability of many CYP3A4 substrates including felodipine. As discussed in above sections, drug absorption can also be impaired by efflux transporters in the intestine (98).

The synergistic action of CYP3A and P-glycoprotein in limiting oral drug delivery is suggested by their joint presence in small intestine enterocytes, the significant overlap in their substrate specificities and the poor oral bioavailability of joint substrates for CYP3A and P-glycoprotein. These proteins are induced or inhibited by many of the same compounds (99). In the enterocyte, the spatial separation of P-gp, located on the apical plasma membrane, and that of CYP3A4, located in the endoplasmatic reticulum, supports the idea that P-gp may control the access of drugs to intracellular metabolism by CYP3A4. Drugs absorbed into the intestinal epithelium can interact with P-gp and be actively extruded back into the intestinal lumen. If this process of diffusion and active transport occurred repeatedly, the circulation of the drug from the lumen to the intracellular compartment would potentially prolong the intracellular residence time of the drug, decrease the rate of absorption, and result in increased drug metabolism by CYP3A4 relative to the parent drug crossing the intestine. Support for this hypothesis was obtained from a simulation model (100) as well as experimental studies examining the metabolism and transport of indinavir in vitamin D3-induced Caco-2 cells (101). Further studies from Cummins *et al.* (98) were designed to identify the contribution of P-gp in determinating the extent of CYP3A4 drug metabolism

using selective CYP3A4/P-gp substrates and inhibitors in CYP3A4-transfected Caco-2 monolayers. Two compounds were tested: one a dual P-gp and CYP3A4 substrate (K77: N-methyl piperazine-Phe-homoPhe-vinylsulfone phenyl) and the other only a CYP3A4 substrate (felodipine). The substrates were administered with the inhibitors CsA (dual inhibitor of P-gp and CYP3A4) or GG918 (inhibitor of P-gp and not CYP3A4). When P-gp alone was inhibited, the extent of metabolism of the dual CYP3A4 and P-gp substrate was decreased, but there was no change in the extent of metabolism for the exclusive CYP3A4 subtrate. These data indicate that P-gp, when active, can work in concert with CYP3A4 to increase metabolism. Studies using the *in vivo* rat single pass intestinal perfusion model were performed to determine whether a similar drug metabolism-efflux alliance existed *in vivo* (102). The results obtained were the first to show the specific interaction of P-gp with CYP3A in this isolated organ and support the proposed interplay between P-gp and CYP3A in the intestine.

Figure 7 shows the topographical relationship between the enzyme CYP3A4 and the efflux transporter P-glycoprotein in both the intestine and the liver. In the intestine, during the absorption process, part of the drug encounters the efflux transporter, P-glycoprotein, before coming in contact with the enzyme CYP3A4.

As stated above, in the intestine, inhibition of the efflux transporter P-gp with no effect on the enzyme, will decrease metabolism. Thus, when both the enzyme and the efflux transporter are inhibited, a significant decrease in metabolism will be observed with the achievement of higher AUCs (Figure 8). In contrast, in the liver, the enzyme topographically precedes the efflux transporter and the opposite effect is observed with respect to inhibition of P-gp. In this organ, inhibition of P-gp will increase metabolism as the drug will be more available within the hepatocyte to interact with the enzymes before it is excreted in the bile. However, inhibition of CYP3A4 in the liver decreases metabolism so that a potential confounding result occurs when both the enzyme and the transporter are inhibited since the two processes result in counteractive effects (Figure 8) (78).

Until recently, *in vitro* predictions of drug interactions were most frequently carried out using hepatic microsomal systems to evaluate the potential for metabolic interactions. However, those systems will not allow predictions that occur through the interplay of enzymes and transporters. The isolated perfused rat liver is a useful intact organ system for examination the hepatobiliary disposition of drugs.

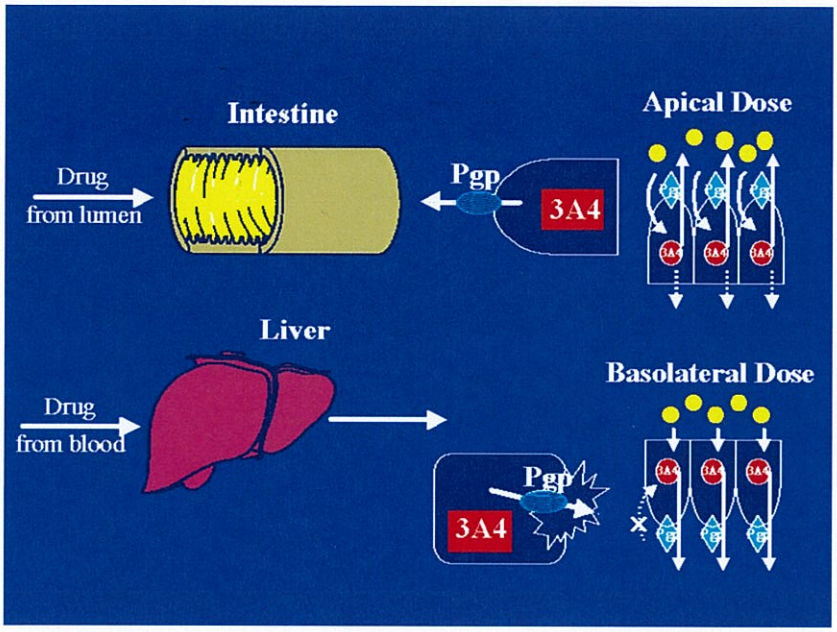

Figure 7 – The spatial relationship between the enzyme and transporter in the intestine and the liver as mimicked by the cellular system of Cummins. *In* Curr Drug Metab (78).

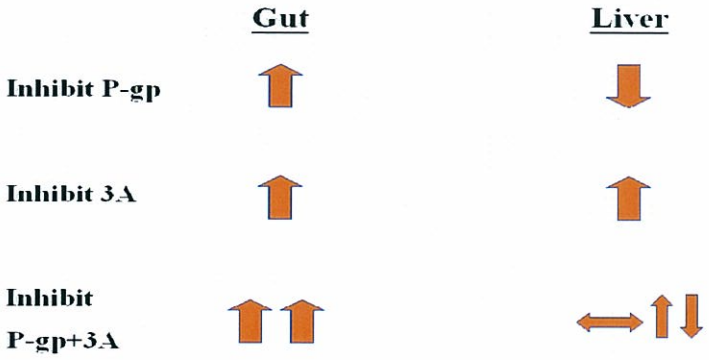

Figure 8 - Predicted AUC Changes for *In Vivo - In Situ* Studies for dual CYP3A4 and P-gp substrates when Co-incubated with Inhibitors. *Adapted from* Curr Drug Metab (78).

In contrast to *in vitro* models like microsomes, hepatocytes and liver slices, the perfused liver preserves the hepatic architecture, cell polarity and bile flow (78). The role of P-gp and CYP3A in modulating hepatobiliary drug disposition was examined *ex situ* using the isolated perfused rat system by Wu and

Benet (103). The transport and metabolism of tacrolimus, an immunosuppressive agent that is a substrate for both P-gp and CYP3A, was examined alone and in the presence of transporter and enzyme inhibitors. Troleandomycin, a specific CYP3A inhibitor, GG918, a specific P-gp inhibitor, and cyclosporine, a dual CYP3A and P-gp inhibitor were added 5 min before the addition of tacrolimus. In the presence of troleandomycin, relative AUC significantly increased to 2.30 as would be expected. In the presence of GG918 the relative AUC for tacrolimus significantly decreased to 0.77, again as predicted in Figure 8. That is, when the efflux transporter is inhibited, more drug is available to be metabolized by the enzyme and AUC will decrease. In the presence of cyclosporine the relative AUC was 1.94, intermediate between the effects of the CYP3A inhibitor and the P-gp inhibitor (Figure 8). More recently, Lau and Benet (104) investigated the interaction between an uptake transporter, Oatp2, P-gp and cyp3a4, on digoxin elimination in the isolated perfused rat liver. The AUC of digoxin was increased by one previous dose of rifampin (100 μM), an inhibitor of Oatp2, which decreased hepatic uptake of digoxin, resulting in less metabolism. As predicted, the AUC of digoxin was decreased by quinidine (10 μM), an inhibitor of P-gp. When digoxin metabolism was investigated in rat hepatic microsomes no changes were observed when rifampicin or quinidine were added (105). These results all together revealed that metabolism can be altered by changes that occur only in drug transport. Incorporating efflux, as well as uptake, processes affecting drug distribution should lead to better predictions of drug clearances from *in vitro* systems (78).

5. BCS and BDDCS: prediction of oral absorption

5.1. Biopharmaceutics Classification System (BCS)

The oral absorption of a drug is fundamentally dependent on that drug's aqueous solubility, dissolution and gastrointestinal permeability. Extensive research into these fundamental parameters by Amidon et al. (58) led to the Biopharmaceutics Classification System (BCS) that categorizes drugs into four groups, Class 1–Class 4 (Figure 9). The BCS classifies immediate release (IR) compounds based on the critical components related to oral absorption.

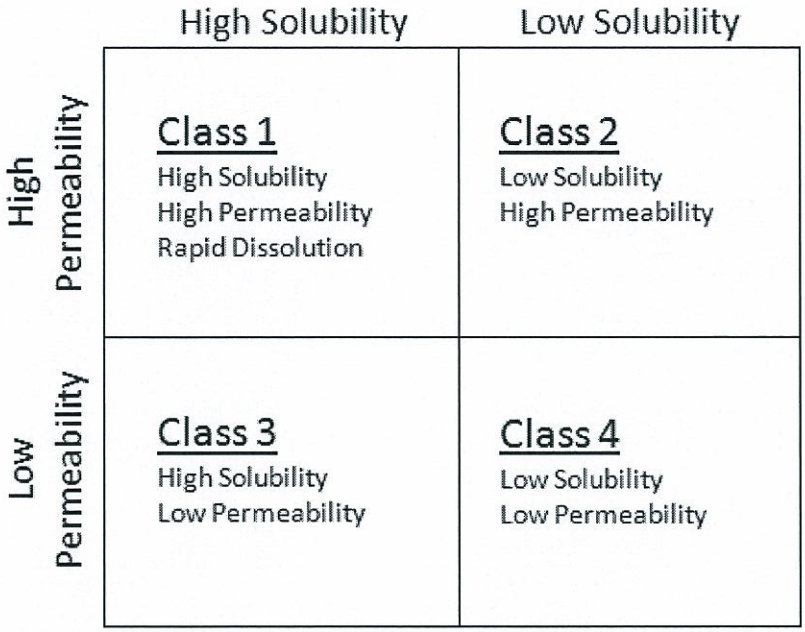

Figure 9 - The Biopharmaceutics Classification System (BCS) after Amidon *et al.* (58)

According to the BCS approach, the rate of drug absorption is determined by the dissolution rate (Kd) and the permeability rate (Kp) (Figure 10). The rate of dissolution is a function of drug solubility (intrinsic solubility) and formulation characteristics (disintegration), while the permeability rate is largely a function of a drug compound's chemical structure (polarity, functional groups, salt form, etc). Four distinct scenarios are defined by the BCS absorption model. In the simplest case both Kd and Kp are large. This results in the drug being rapidly solubilized and well absorbed (Class 1 drugs). When Kp is much greater than Kd, drug dissolution is the rate limiting step to drug absorption (Class 2 drugs). If Kd is higher than Kp, the drug is rapidly released and solubilized from the formulation and the permeation of the drug controls drug absorption (Class 3 drugs). Lastly, when Kd and Kp are both small (Class 4 drugs), drug absorption will be slow and controlled by the smallest of the constants (106).

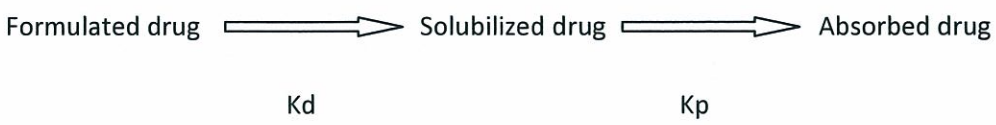

Figure 10 - A typical BCS-based drug absorption process.

Centrally embracing permeability and solubility, the objective of the BCS is to allow prediction of *in vivo* pharmacokinetic performance of drug products from *in vitro* measurements of permeability and solubility.

A drug substance is considered "highly soluble" when the highest marketed dose strength is soluble in 250 ml of aqueous media over a pH range of 1–7.5 at 37 °C. A drug is considered rapidly dissolving if no less than 85% of label claims is released within 30 minutes across the before mentioned pH range in either United States Pharmacopeia (USP) dissolution apparatus I (baskets) at 100 rpm or USP dissolution apparatus II (paddles) at 50 rpm. A drug substance is considered to be "highly permeable" when the extent of absorption in humans is determined to be greater or equal to 90% of an administered dose based on a mass balance determination or in comparison to an intravenous reference dose (106). This is based on extensive research that revealed a significant correlation between the human jejunal permeability measured using intestinal perfusion approaches and the fraction of drug absorbed obtained from pharmacokinetic studies in humans (57). Recommended methods not involving human subjects include *in vivo* or *in situ* intestinal perfusion in an animal model (e.g., rats), and/or *in vitro* permeability methods using excised intestinal tissues or monolayers of suitable epithelial cells (107). Accordingly, Class 1 compounds possess high properties of both solubility and permeability, while Class 4 compound possess low properties; Class 2 are highly permeable and poorly soluble, while Class 3 possess the opposite characteristics of poor permeability and high solubility.

The classification framework of the BCS is believed to be useful in the earliest stages of drug discovery research to predict the oral absorption and disposition of new molecular entities and, as a result, has been incorporated into a number of regulatory guidances worldwide. The BCS was proposed by FDA as a bioavailability-bioequivalence (BA/BE) regulatory guideline (107). If a molecule is classified has highly soluble and highly permeable (Class 1) and does not have a narrow therapeutic index, it may qualify for a waiver of the very expensive BA/BE clinical testing, as long as the drug product also exhibit rapid dissolution (55, 108).

5.2. Biopharmaceutics Drug Disposition Classification System (BDDCS)

In 2005, Wu and Benet (109) constructed a table of 130 compounds in the four BCS classes. These compounds were predominantly gathered from available literature but judiciously edited. Extensive research into the assembled list of compounds in the four categories has demonstrated that the BCS provides further predictive utility (28). Critical evaluation of drug substances listed in the four BCS classes on Table 5 allows for prominent trends to become apparent specifically with respect to major routes of elimination. Class 1 and Class 2 compounds are eliminated primarily via metabolism, whereas Class 3 and Class 4 compounds are primarily eliminated unchanged into the urine and the bile (Figure 11). This is consistent with the generally held belief that more permeable lipophilic compounds make good substrates for Cytochrome *P450* (CYP) enzymes (110). While the theory that metabolism increases as lipid solubility (log *P*) increases was noted, it had not been previously recognized in terms of the Biopharmaceutics Classification System (109). It is important to note that the differential permeability characteristics defined in the BCS do not necessarily reflect differences in permeability into hepatocytes. This is evident by the fact that a high number of Class 3 and Class 4 compounds are eliminated into the bile. The differential permeability characteristics denoted by the high versus low designation reflects the differential access of the compound to the metabolizing enzymes within the hepatocytes.

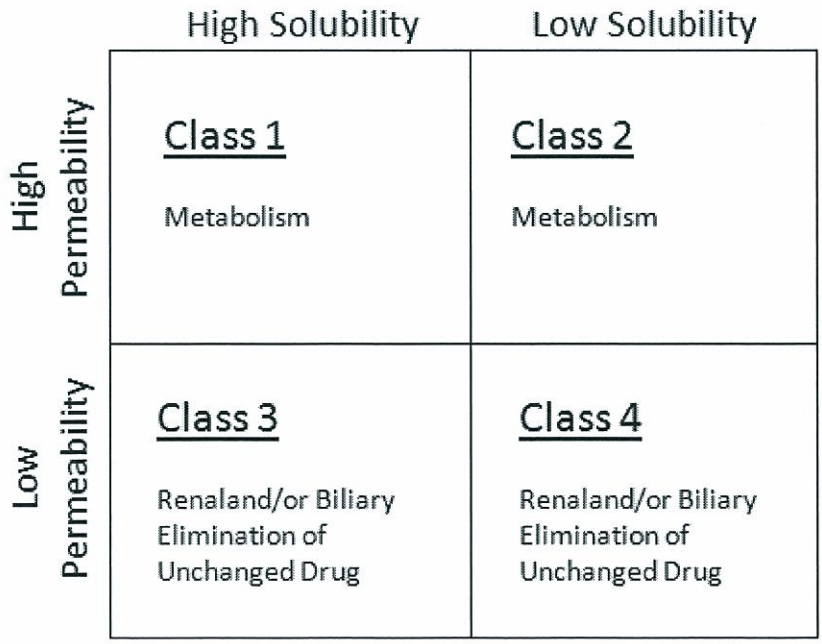

Figure 11 - Predominant routes of elimination by BCS class. *In* Pharm Res. (109).

Recognition of the elimination pathway differences for Class 1 and Class 2 drugs versus Class 3 and Class 4 drugs, combined with the inherent difficulty in quantifying the percent of drug absorbed in humans at a level of 90%, prompted Wu and Benet (109) to suggest a revised category scheme entitled the Biopharmaceutics Drug Disposition Classification System (BDDCS) (Figure 12).

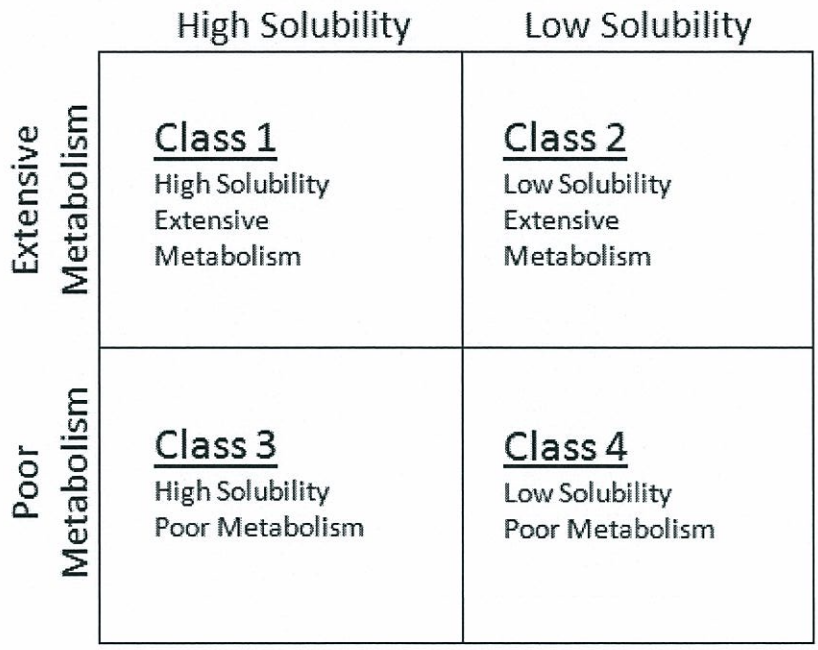

Figure 12 - The Biopharmaceutics Drug Disposition Classification System (BDDCS) after Wu and Benet. *In* Pharm Res. (109).

The BDDCS replaces the permeability criteria with the major route of elimination because of the belief that it is easier and less ambiguous to determine the assignment of BDDCS for marketed drugs based on the extent of metabolism than using permeability (i.e. extent of absorption) in BCS assignments thereby eliminating many instances of uncertainly in human permeability leading to differences in class designation by different authors. There is also a good correlation between the extent of drug metabolism and measure of permeability defined under BCS (57).

"Extensive metabolism" was defined as ≥ 70% metabolism of an oral dose *in vivo* in humans while the "poor metabolism" was defined as ≥ 50% of the dose be excreted unchanged.

Chen and Yu (57) studied 51 drugs that had high intestinal permeability with no reported instability in the gastrointestinal tract to examine the use of drug metabolism for predicting permeability. To facilitate comparison between BCS and BDDCS, information on the degree of drug metabolism was obtained from standard references and the classification of "extensive metabolism" was given when 50% or more of the oral dose was metabolized in humans. In addition, the estimated *n*-octanol/water partition coefficient for the unchanged form of a drug molecule (C LogP), where available from the literature, was recorded to assess compound lipophilicity. All compounds were classified as high permeability based on BCS but only 73% of the compounds were found to exhibit extensive metabolism. Indeed, many of the highly permeable compounds possess a fair degree of lipophilicity (as reflected by their high C LogP values), and thus are readily transported by passive transcellular diffusion across the intestinal membrane. However, there are exceptions to this general principle where a group of compounds that appear to be hydrophilic (C LogP<0) are classified as "high permeability" based on the BCS criteria. Some of these compounds, including D-glucose, levodopa, L-leucine and phenylalanine, are known to be absorbed via the endogenous carrier mediated mechanism (111). Another possibility for transport of hydrophilic drugs is through intestinal paracellular route, which may be important for small molecules with molecular weight less than 250-300 (97).

Besides the routes of elimination, BDDCS also allows for predictions related to the effects of transporters on oral absorption, direction of food effects, and significance of transporter-enzyme interplay in drug-drug interactions (109).

When the BCS was first developed there was little understanding of the importance of drug transporters to BA. Both uptake and efflux transporters in the intestine (78, 98, 102) and liver (103-105, 112) are important in determining oral drug disposition by controlling absorption and BA. As described above, some drugs may fulfill the BCS 90% P criteria because of the activity of uptake transporters in the intestine, rather than just due to high passive P. Thus some drugs listed as highly P according to BCS may show marked changes in BA when intestinal uptake transporters are inhibited. Moreover, it was demonstrated that interplay between transporters and intestinal metabolic enzymes may control the access of drug molecules to the enzymes and changes in transporter function can modulate intestinal metabolism without changes of enzyme activity (78, 113). There is an ongoing debate among the scientific community regarding the role of transporters in drug intestinal BA and intestinal BA predictions from *in vitro* systems (20, 28, 57, 109, 114, 115).

5.2.1. Predicting the effects of transporters on oral dosing

The body of data evaluating the role of transporters and transporter-enzyme interplay (Point 4) led Wu and Benet (109) to the generalizations regarding transporter effects following oral dosing depicted in Figure 13.

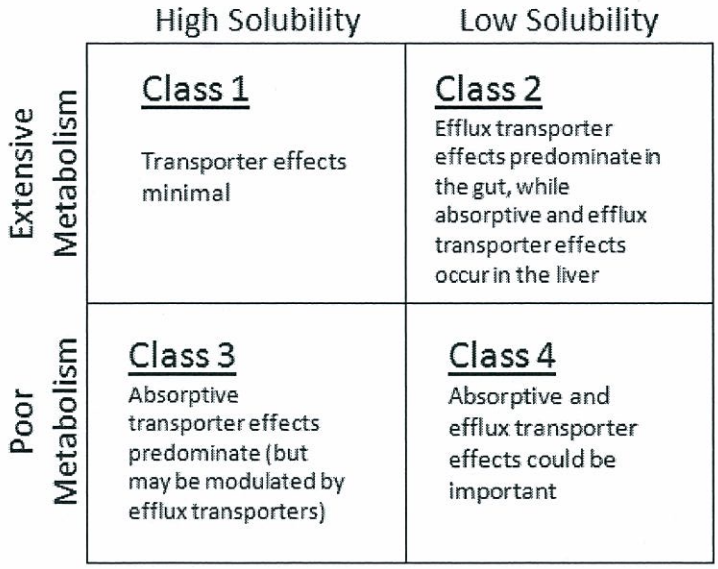

Figure 13 - Transporter effects, following oral dosing, by BDDCS class. *In* Pharm Res. (109).

5.2.1.1. Class 1 compounds

The gut lumen of the gastrointestinal tract is sufficiently leaky so that small molecular weight, soluble, non-polar compounds (i.e. Class 1 compounds) readily pass through the membrane. Alternatively, the high permeability/ high solubility of Class 1 drugs allows high concentrations in the gut to saturate any transporter, both efflux and absorptive. That is, Class 1 compounds may be substrates for both uptake and efflux transporters *in vitro* in cellular systems under the right conditions (for example, midazolam (116) and verapamil (107) are substrates for P-glycoprotein), but transporter effects will not be important clinically.

5.2.1.2. Class 2 compounds

Similarly, for Class 2 drugs, the high permeability will allow ready access into the gut membranes making intestinal uptake transporters generally unimportant due to the rapid permeation of the drug molecule

into the enterocytes. That is, absorption of Class 2 compounds is primarily passive and a function of lipophilicity. However, the low solubility of these compounds will limit the concentrations coming into the enterocytes, thereby preventing saturation of the efflux transporters. Consequently, efflux transporters will affect the extent of oral bioavailability and the rate of absorption of Class 2 drugs. Moreover, there will be little opportunity to saturate intestinal enzymes such as CYP3A4 and UDP-glucuronosyltransferases (UGTs) due to the low solubility. Thus, changes in transporter expression, and inhibition or induction of efflux transporters will cause changes in intestinal metabolism of drugs that are substrates for the intestinal enzymes. Many Class 2 compounds are primarily substrates for CYP3A as well as substrates or inhibitors of the efflux transporter P-glycoprotein. However, as noted in Figure 13, Class 2 compounds may be affected by both uptake and efflux transporters in the liver (117).

5.2.1.3. Class 3 and Class 4 compounds

For Class 3 compounds, sufficient drug will be available in the gut lumen due to good solubility, but an absorptive transporter will be necessary to overcome the poor permeability characteristics of these compounds. However, intestinal apical efflux transporters may also be important for the absorption of such compounds when sufficient enterocyte penetration is achieved via an uptake transporter. That is, since influx of Class 3 compounds will generally be rate limited by an absorptive transporter, the counter effects of efflux transporters will not be saturated and can also be important. In general, these principles also hold for Class 4 compounds, although Class 4 drugs may achieve sufficient solubility in the natural surfactant containing gut contents so that they act like Class 3 compounds (Figure 13).

5.2.1.4. Predicting food effect

Food-drug interactions have been widely associated with alterations of pharmacokinetics and pharmacodynamic parameters and proven to have significant clinical implications (118, 119). The effect of food on the extent of availability is a significant concern during drug development. Ideally, it is most advantageous if a recommendation of oral drug administration can be provided independent of meal considerations. A food drug interaction model would be beneficial in the early stages of development when preclinical predictions can be of particular use and service to the industry (28). In general, high fat meals have no effect on the extent of oral drug availability for BCS Class 1 compounds, generally showed increased availability for Class 2 compounds, and generally showed decreased availability for Class 3

compounds (120). These observations are in line with what could be predicted, in terms of BDDCS, if high fat meal ingestion results in an inhibitory effect on intestinal transporter function. BDDCS predicts that high fat meals will have no significant effect on Class 1 drugs, despite the fact that many Class 1 drugs are transporter substrates, because the high gut permeability and intestinal fluid high solubility possessed by this class of drugs dictate that transporter effects should be minimal. For Class 2 compounds, which are highly metabolized and therefore are often dual substrates of enzymes and transporters, we predict an increase in bioavailability due in part to transporter inhibition resulting in decreased extraction of the drug. This increased bioavailabilty with a concomitant high fat meal could be due to inhibition of efflux transporters, such as P-gp, in the intestine. For Class 3 compounds, which are poorly metabolized and poorly permeable and therefore are often reliant on uptake transporters, we predict a decrease in bioavailability due in part to transporter inhibition resulting in the reduction of AUC. For Class 4 compounds, it is difficult to predict what will occur, as all of the interacting effects mentioned for Class 2 and Class 3 compounds can be seen there. Nevertheless, if high fat meal effects are to occur, an increase in the extent of bioavailability is more likely, resulting from the combination of increased solubilization of drugs in the intestine and inhibition of efflux transporters (28).

REFERENCES

1. Guengerich. Oxidative, Reductive, and Hydrolytic Metabolism of Drugs., Drug Metabolism in Drug Design and Development, Wiley-Interscience, 2008.

2. S.K.a.F.F. Kadlubar. Enzymatic Basis of Phase I and Phase II Drug Metabolism. In K.S.P.A.D.R. ·and R.M. Peter (eds.), Enzyme- and Transporter-Based Drug–Drug Interactions Progress and Future Challenges, Springer AAPS Press, 2010.

3. Maréchal. Insights into drug metabolism by cytochromes P450 from modeling studies of CYP2D6-drug interactions. . Brit J Pharmacol 153:S82-S89 (2008).

4. Nelson. Cytochrome P450s in humans. http://drnelson.utmem.edu/cytochromeP450.html.

5. P.A. Williams, J. Cosme, V. Sridhar, E.F. Johnson, and D.E. McRee. Mammalian microsomal cytochrome P450 monooxygenase: structural adaptations for membrane binding and functional diversity. Mol Cell. 5:121-131 (2000).

6. Nelson. P450 superfamily: update on new sequences, gene mapping, accession numbers and nomenclature. Pharmacogenetics. 6:1-42 (1996).

7. Kashuba. Drug Metabolism, Transport and the Influence of Hepatic Disease. Applied Pharmacokinetics and Pharmacodynamics, Lippincott Williams & Wilkins, 2006.

8. P.A. Williams. US Patent 7148046 - Crystal Structure of Cytochrome P450 in http://www.patentstorm.us/patents/7148046/fulltext.html. (2003).

9. U.M. Zanger, M. Turpeinen, K. Klein, and M. Schwab. Functional pharmacogenetics/genomics of human cytochromes P450 involved in drug biotransformation. Anal Bioanal Chem. 392:1093-1108 (2008).

10. S. Zhou, S. Yung Chan, B. Cher Goh, E. Chan, W. Duan, M. Huang, and H.L. McLeod. Mechanism-based inhibition of cytochrome P450 3A4 by therapeutic drugs. Clin Pharmacokinet. 44:279-304 (2005).

11. X. Cao, S.T. Gibbs, L. Fang, H.A. Miller, C.P. Landowski, H.C. Shin, H. Lennernas, Y. Zhong, G.L. Amidon, L.X. Yu, and D. Sun. Why is it challenging to predict intestinal drug absorption and oral bioavailability in human using rat model. Pharm Res. 23:1675-1686 (2006).

12. M.F. Paine, D.D. Shen, K.L. Kunze, J.D. Perkins, C.L. Marsh, J.P. McVicar, D.M. Barr, B.S. Gillies, and K.E. Thummel. First-pass metabolism of midazolam by the human intestine. Clin Pharmacol Ther. 60:14-24 (1996).

13. S.N.a.U.A. Rory Remmel. Conjugative metabolism of drugs. In M.Z. Donglu Zhang, W. Griffith Humphreys (ed.), Drug Metabolism in Drug Design and Development, Wiley-Interscience, 2007.

14. M.J. Zamek-Gliszczynski, K.A. Hoffmaster, K. Nezasa, M.N. Tallman, and K.L. Brouwer. Integration of hepatic drug transporters and phase II metabolizing enzymes: mechanisms of hepatic excretion of sulfate, glucuronide, and glutathione metabolites. Eur J Pharm Sci. 27:447-486 (2006).

15. C.N. Falany, X. Xie, J. Wang, J. Ferrer, and J.L. Falany. Molecular cloning and expression of novel sulphotransferase-like cDNAs from human and rat brain. Biochem J. 346 Pt 3:857-864 (2000).

16. B. Mannervik, P.G. Board, J.D. Hayes, I. Listowsky, and W.R. Pearson. Nomenclature for mammalian soluble glutathione transferases. Methods Enzymol. 401:1-8 (2005).

17. K.M. Giacomini, S.M. Huang, D.J. Tweedie, L.Z. Benet, K.L. Brouwer, X. Chu, A. Dahlin, R. Evers, V. Fischer, K.M. Hillgren, K.A. Hoffmaster, T. Ishikawa, D. Keppler, R.B. Kim, C.A. Lee, M. Niemi, J.W. Polli, Y. Sugiyama, P.W. Swaan, J.A. Ware, S.H. Wright, S.W. Yee, M.J. Zamek-Gliszczynski, and L. Zhang. Membrane transporters in drug development. Nat Rev Drug Discov. 9:215-236.

18. M.A. Hediger, M.F. Romero, J.B. Peng, A. Rolfs, H. Takanaga, and E.A. Bruford. The ABCs of solute carriers: physiological, pathological and therapeutic implications of human membrane transport proteins. Introduction. Pflugers Arch. 447:465-468 (2004).

19. Y. Sai. Biochemical and molecular pharmacological aspects of transporters as determinants of drug disposition. Drug Metab Pharmacokinet. 20:91-99 (2005).

20. S. Shugartsand L.Z. Benet. The role of transporters in the pharmacokinetics of orally administered drugs. Pharm Res. 26:2039-2054 (2009).

21. L.M. Chan, S. Lowes, and B.H. Hirst. The ABCs of drug transport in intestine and liver: efflux proteins limiting drug absorption and bioavailability. Eur J Pharm Sci. 21:25-51 (2004).

22. Rajinder. Intestinal Transporters in Drug Absorption. In R.K.a.L. Yu (ed.), Biopharmaceutics Applications in Drug Development, Springer, 2008.

23. K. Ito, H. Suzuki, T. Horie, and Y. Sugiyama. Apical/basolateral surface expression of drug transporters and its role in vectorial drug transport. Pharm Res. 22:1559-1577 (2005).

24. J. Hunter, M.A. Jepson, T. Tsuruo, N.L. Simmons, and B.H. Hirst. Functional expression of P-glycoprotein in apical membranes of human intestinal Caco-2 cells. Kinetics of vinblastine secretion and interaction with modulators. J Biol Chem. 268:14991-14997 (1993).

25. A.B. Shapiro, K. Fox, P. Lam, and V. Ling. Stimulation of P-glycoprotein-mediated drug transport by prazosin and progesterone. Evidence for a third drug-binding site. Eur J Biochem. 259:841-850 (1999).

26. D.G. Bailey, J. Malcolm, O. Arnold, and J.D. Spence. Grapefruit juice-drug interactions. Br J Clin Pharmacol. 46:101-110 (1998).

27. H. Spahn-Langguthand P. Langguth. Grapefruit juice enhances intestinal absorption of the P-glycoprotein substrate talinolol. Eur J Pharm Sci. 12:361-367 (2001).

28. J.M. Custodio, C.Y. Wu, and L.Z. Benet. Predicting drug disposition, absorption/elimination/transporter interplay and the role of food on drug absorption. Adv Drug Deliv Rev. 60:717-733 (2008).

29. Y. Kurata, I. Ieiri, M. Kimura, T. Morita, S. Irie, A. Urae, S. Ohdo, H. Ohtani, Y. Sawada, S. Higuchi, and K. Otsubo. Role of human MDR1 gene polymorphism in bioavailability and interaction of digoxin, a substrate of P-glycoprotein. Clin Pharmacol Ther. 72:209-219 (2002).

30. A.H. Schinkeland J.W. Jonker. Mammalian drug efflux transporters of the ATP binding cassette (ABC) family: an overview. Adv Drug Deliv Rev. 55:3-29 (2003).

31. S.P. Cole, G. Bhardwaj, J.H. Gerlach, J.E. Mackie, C.E. Grant, K.C. Almquist, A.J. Stewart, E.U. Kurz, A.M. Duncan, and R.G. Deeley. Overexpression of a transporter gene in a multidrug-resistant human lung cancer cell line. Science. 258:1650-1654 (1992).

32. K.C. Peng, F. Cluzeaud, M. Bens, J.P. Duong Van Huyen, M.A. Wioland, R. Lacave, and A. Vandewalle. Tissue and cell distribution of the multidrug resistance-associated protein (MRP) in mouse intestine and kidney. J Histochem Cytochem. 47:757-768 (1999).

33. M.J. Flens, G.J. Zaman, P. van der Valk, M.A. Izquierdo, A.B. Schroeijers, G.L. Scheffer, P. van der Groep, M. de Haas, C.J. Meijer, and R.J. Scheper. Tissue distribution of the multidrug resistance protein. Am J Pathol. 148:1237-1247 (1996).

34. D.R. Johnson, R.A. Finch, Z.P. Lin, C.J. Zeiss, and A.C. Sartorelli. The pharmacological phenotype of combined multidrug-resistance mdr1a/1b- and mrp1-deficient mice. Cancer Res. 61:1469-1476 (2001).

35. K. Naruhashi, I. Tamai, N. Inoue, H. Muraoka, Y. Sai, N. Suzuki, and A. Tsuji. Involvement of multidrug resistance-associated protein 2 in intestinal secretion of grepafloxacin in rats. Antimicrob Agents Chemother. 46:344-349 (2002).

36. K. Miyake, L. Mickley, T. Litman, Z. Zhan, R. Robey, B. Cristensen, M. Brangi, L. Greenberger, M. Dean, T. Fojo, and S.E. Bates. Molecular cloning of cDNAs which are highly overexpressed in

mitoxantrone-resistant cells: demonstration of homology to ABC transport genes. Cancer Res. 59:8-13 (1999).

37. R. Allikmets, L.M. Schriml, A. Hutchinson, V. Romano-Spica, and M. Dean. A human placenta-specific ATP-binding cassette gene (ABCP) on chromosome 4q22 that is involved in multidrug resistance. Cancer Res. 58:5337-5339 (1998).

38. J. Xu, Y. Liu, Y. Yang, S. Bates, and J.T. Zhang. Characterization of oligomeric human half-ABC transporter ATP-binding cassette G2. J Biol Chem. 279:19781-19789 (2004).

39. M.L. Vlaming, J.S. Lagas, and A.H. Schinkel. Physiological and pharmacological roles of ABCG2 (BCRP): recent findings in Abcg2 knockout mice. Adv Drug Deliv Rev. 61:14-25 (2009).

40. S.K. Rabindran, H. He, M. Singh, E. Brown, K.I. Collins, T. Annable, and L.M. Greenberger. Reversal of a novel multidrug resistance mechanism in human colon carcinoma cells by fumitremorgin C. Cancer Res. 58:5850-5858 (1998).

41. R. Liang, Y.J. Fei, P.D. Prasad, S. Ramamoorthy, H. Han, T.L. Yang-Feng, M.A. Hediger, V. Ganapathy, and F.H. Leibach. Human intestinal H+/peptide cotransporter. Cloning, functional expression, and chromosomal localization. J Biol Chem. 270:6456-6463 (1995).

42. H. Ogihara, T. Suzuki, Y. Nagamachi, K. Inui, and K. Takata. Peptide transporter in the rat small intestine: ultrastructural localization and the effect of starvation and administration of amino acids. Histochem J. 31:169-174 (1999).

43. G. You. The role of organic ion transporters in drug disposition: an update. Curr Drug Metab. 5:55-62 (2004).

44. N. Mizuno, T. Niwa, Y. Yotsumoto, and Y. Sugiyama. Impact of drug transporter studies on drug discovery and development. Pharmacol Rev. 55:425-461 (2003).

45. N. Morita, H. Kusuhara, T. Sekine, H. Endou, and Y. Sugiyama. Functional characterization of rat organic anion transporter 2 in LLC-PK1 cells. J Pharmacol Exp Ther. 298:1179-1184 (2001).

46. H. Koepsell, K. Lips, and C. Volk. Polyspecific organic cation transporters: structure, function, physiological roles, and biopharmaceutical implications. Pharm Res. 24:1227-1251 (2007).

47. D. Grundemann, V. Gorboulev, S. Gambaryan, M. Veyhl, and H. Koepsell. Drug excretion mediated by a new prototype of polyspecific transporter. Nature. 372:549-552 (1994).

48. B. Steffansen, C.U. Nielsen, B. Brodin, A.H. Eriksson, R. Andersen, and S. Frokjaer. Intestinal solute carriers: an overview of trends and strategies for improving oral drug absorption. Eur J Pharm Sci. 21:3-16 (2004).

49. T. Mikkaichi, T. Suzuki, M. Tanemoto, S. Ito, and T. Abe. The organic anion transporter (OATP) family. Drug Metab Pharmacokinet. 19:171-179 (2004).

50. J. Konig, A. Seithel, U. Gradhand, and M.F. Fromm. Pharmacogenomics of human OATP transporters. Naunyn Schmiedebergs Arch Pharmacol. 372:432-443 (2006).

51. S. Oswald, M. Grube, W. Siegmund, and H.K. Kroemer. Transporter-mediated uptake into cellular compartments. Xenobiotica. 37:1171-1195 (2007).

52. P.V. Balimane, S. Chong, and R.A. Morrison. Current methodologies used for evaluation of intestinal permeability and absorption. J Pharmacol Toxicol Methods. 44:301-312 (2000).

53. P.V. Balimaneand S. Chong. Cell culture-based models for intestinal permeability: a critique. Drug Discov Today. 10:335-343 (2005).

54. L. Laitinem. Caco-2 cell cultures in the assessment of intestinal absorption: Effects of some co-administered drugs and natural compounds in biological matrices., *Division of Biopharmaceutics and Pharmacokinetics*, University of Helsinki, Helsinki, 2006.

55. A. Avdeef. Physicochemical profiling (solubility, permeability and charge state). Curr Top Med Chem. 1:277-351 (2001).

56. P.L.S.a.G.W. Ronald T. Borchardt. General Principles in the Characterization and Use of Model Systems for Biopharmaceutical Studies. Models for Assessing Drug Absorption and Metabolism, Vol. 8, Plenum Press, New York, 1999, pp. 1-9.

57. M.L. Chenand L. Yu. The use of drug metabolism for prediction of intestinal permeability (dagger). Mol Pharm. 6:74-81 (2009).

58. G.L. Amidon, H. Lennernas, V.P. Shah, and J.R. Crison. A theoretical basis for a biopharmaceutic drug classification: the correlation of in vitro drug product dissolution and in vivo bioavailability. Pharm Res. 12:413-420 (1995).

59. P.V.B.a.S. Chong. Evaluation of Permeability and P-glycoprotein Interations: Industry Outlook. In R.K.a.L. Yu (ed.), Biopharmaceutics Applications in Drug Development, Springer, 2008, pp. 101-132.

60. K.P. Per Artursson, Kristina Luthman. Caco-2 monolayers in experimental and theoretical predictions of drug transport. Advanced Drug Delivery Reviews. 22:67-84 (1996).

61. P.J. Ho N, Morozowich W and Higuchi W. Physical model approach to the design of drugs with improved intestinal absorption. In R.E. ed (ed.), Design of biopharmaceutical propertiesthrough prodrugs and analogues, APhA/APS, Washington, DC., 1977, pp. 136-277.

62. C.A. Lipinski, F. Lombardo, B.W. Dominy, and P.J. Feeney. Experimental and computational approaches to estimate solubility and permeability in drug discovery and development settings. Adv Drug Deliv Rev. 46:3-26 (2001).

63. P. Arturssonand J. Karlsson. Correlation between oral drug absorption in humans and apparent drug permeability coefficients in human intestinal epithelial (Caco-2) cells. Biochem Biophys Res Commun. 175:880-885 (1991).

64. S. Yee. In vitro permeability across Caco-2 cells (colonic) can predict in vivo (small intestinal) absorption in man--fact or myth. Pharm Res. 14:763-766 (1997).

65. H. Lennernas, Palm, K., Fagerholm, U. and Artursson, P. Correlation between paracellular and transcellular drug permeability in the human jejunum and Caco-2 monolayers. Adv Drug Deliv Rev. 22:67-94 (1996).

66. D. Sun, H. Lennernas, L.S. Welage, J.L. Barnett, C.P. Landowski, D. Foster, D. Fleisher, K.D. Lee, and G.L. Amidon. Comparison of human duodenum and Caco-2 gene expression profiles for 12,000 gene sequences tags and correlation with permeability of 26 drugs. Pharm Res. 19:1400-1416 (2002).

67. B.H. Stewart, O.H. Chan, R.H. Lu, E.L. Reyner, H.L. Schmid, H.W. Hamilton, B.A. Steinbaugh, and M.D. Taylor. Comparison of intestinal permeabilities determined in multiple in vitro and in situ models: relationship to absorption in humans. Pharm Res. 12:693-699 (1995).

68. G. Englund, F. Rorsman, A. Ronnblom, U. Karlbom, L. Lazorova, J. Grasjo, A. Kindmark, and P. Artursson. Regional levels of drug transporters along the human intestinal tract: co-expression of ABC and SLC transporters and comparison with Caco-2 cells. Eur J Pharm Sci. 29:269-277 (2006).

69. A.M. Calcagno, J.A. Ludwig, J.M. Fostel, M.M. Gottesman, and S.V. Ambudkar. Comparison of drug transporter levels in normal colon, colon cancer, and Caco-2 cells: impact on drug disposition and discovery. Mol Pharm. 3:87-93 (2006).

70. P. Arturssonand R.T. Borchardt. Intestinal drug absorption and metabolism in cell cultures: Caco-2 and beyond. Pharm Res. 14:1655-1658 (1997).

71. P.H. Vachonand J.F. Beaulieu. Transient mosaic patterns of morphological and functional differentiation in the Caco-2 cell line. Gastroenterology. 103:414-423 (1992).

72. I. Behrensand T. Kissel. Do cell culture conditions influence the carrier-mediated transport of peptides in Caco-2 cell monolayers? Eur J Pharm Sci. 19:433-442 (2003).

73. T. Bansal, M. Singh, G. Mishra, S. Talegaonkar, R.K. Khar, M. Jaggi, and R. Mukherjee. Concurrent determination of topotecan and model permeability markers (atenolol, antipyrine, propranolol and furosemide) by reversed phase liquid chromatography: utility in Caco-2 intestinal absorption studies. J Chromatogr B Analyt Technol Biomed Life Sci. 859:261-266 (2007).

74. P. Augustijnsand R. Mols. HPLC with programmed wavelength fluorescence detection for the simultaneous determination of marker compounds of integrity and P-gp functionality in the Caco-2 intestinal absorption model. J Pharm Biomed Anal. 34:971-978 (2004).

75. R. Elsby, D.D. Surry, V.N. Smith, and A.J. Gray. Validation and application of Caco-2 assays for the in vitro evaluation of development candidate drugs as substrates or inhibitors of P-glycoprotein to support regulatory submissions. Xenobiotica. 38:1140-1164 (2008).

76. P.V. Balimaneand S. Chong. A combined cell based approach to identify P-glycoprotein substrates and inhibitors in a single assay. Int J Pharm. 301:80-88 (2005).

77. I.J. Hidalgo. Assessing the absorption of new pharmaceuticals. Curr Top Med Chem. 1:385-401 (2001).

78. L.Z. Benet, C.L. Cummins, and C.Y. Wu. Transporter-enzyme interactions: implications for predicting drug-drug interactions from in vitro data. Curr Drug Metab. 4:393-398 (2003).

79. C.L. Cummins, W. Jacobsen, U. Christians, and L.Z. Benet. CYP3A4-transfected Caco-2 cells as a tool for understanding biochemical absorption barriers: studies with sirolimus and midazolam. J Pharmacol Exp Ther. 308:143-155 (2004).

80. M. Koljonen, K. Rousu, J. Cierny, A.M. Kaukonen, and J. Hirvonen. Transport evaluation of salicylic acid and structurally related compounds across Caco-2 cell monolayers and artificial PAMPA membranes. Eur J Pharm Biopharm. 70:531-538 (2008).

81. H. Woehlecke, A. Pohl, N. Alder-Baerens, H. Lage, and A. Herrmann. Enhanced exposure of phosphatidylserine in human gastric carcinoma cells overexpressing the half-size ABC transporter BCRP (ABCG2). Biochem J. 376:489-495 (2003).

82. H. Li, H.E. Jin, W. Kim, Y.H. Han, D.D. Kim, S.J. Chung, and C.K. Shim. Involvement of P-glycoprotein, multidrug resistance protein 2 and breast cancer resistance protein in the transport of belotecan and topotecan in Caco-2 and MDCKII cells. Pharm Res. 25:2601-2612 (2008).

83. K. Lee, C. Ng, K.L. Brouwer, and D.R. Thakker. Secretory transport of ranitidine and famotidine across Caco-2 cell monolayers. J Pharmacol Exp Ther. 303:574-580 (2002).

84. B. Rothen-Rutishauser, S.D. Kramer, A. Braun, M. Gunthert, and H. Wunderli-Allenspach. MDCK cell cultures as an epithelial in vitro model: cytoskeleton and tight junctions as indicators for the definition of age-related stages by confocal microscopy. Pharm Res. 15:964-971 (1998).

85. W.S. Putnam, S. Ramanathan, L. Pan, L.H. Takahashi, and L.Z. Benet. Functional characterization of monocarboxylic acid, large neutral amino acid, bile acid and peptide transporters, and P-glycoprotein in MDCK and Caco-2 cells. J Pharm Sci. 91:2622-2635 (2002).

86. U. Fagerholm, M. Johansson, and H. Lennernas. Comparison between permeability coefficients in rat and human jejunum. Pharm Res. 13:1336-1342 (1996).

87. S. Wu-Pong, V. Livesay, B. Dvorchik, and W.H. Barr. Oligonucleotide transport in rat and human intestine ussing chamber models. Biopharm Drug Dispos. 20:411-416 (1999).

88. M.V. Varma, N. Kapoor, M. Sarkar, and R. Panchagnula. Simultaneous determination of digoxin and permeability markers in rat in situ intestinal perfusion samples by RP-HPLC. J Chromatogr B Analyt Technol Biomed Life Sci. 813:347-352 (2004).

89. S. Berggren, P. Lennernas, M. Ekelund, B. Westrom, J. Hoogstraate, and H. Lennernas. Regional transport and metabolism of ropivacaine and its CYP3A4 metabolite PPX in human intestine. J Pharm Pharmacol. 55:963-972 (2003).

90. H. Lennernas, S. Nylander, and A.L. Ungell. Jejunal permeability: a comparison between the ussing chamber technique and the single-pass perfusion in humans. Pharm Res. 14:667-671 (1997).

91. M. Sugawara, K. Iseki, and K. Miyazaki. H+ coupled transport of orally active cephalosporins lacking an alpha-amino group across brush-border membrane vesicles from rat small intestine. J Pharm Pharmacol. 43:433-435 (1991).

92. H. Saitoh, S. Kawai, K. Iseki, K. Miyazaki, and T. Arita. Binding of organic cations to brush border membrane from rat small intestine. J Pharm Pharmacol. 40:776-780 (1988).

93. Y.L. Eun Ju Jeong, Huimin Lin and Ming Hu. In situ single-pass perfused rat intestinal model for absorption and metabolism. In Z.Y.a.G.W. Caldwell (ed.), Methods in Pharmacology and Toxicology, Humana Press, Inc., Totowa, pp. 65-76.

94. M. Sugawara, H. Saitoh, K. Iseki, K. Miyazaki, and T. Arita. Contribution of passive transport mechanisms to the intestinal absorption of beta-lactam antibiotics. J Pharm Pharmacol. 42:314-318 (1990).

95. M.R. Uhingand R.E. Kimura. The effect of surgical bowel manipulation and anesthesia on intestinal glucose absorption in rats. J Clin Invest. 95:2790-2798 (1995).

96. H. Lennernas. Human intestinal permeability. J Pharm Sci. 87:403-410 (1998).

97. H. Lennernas. Intestinal permeability and its relevance for absorption and elimination. Xenobiotica. 37:1015-1051 (2007).

98. C.L. Cummins, W. Jacobsen, and L.Z. Benet. Unmasking the dynamic interplay between intestinal P-glycoprotein and CYP3A4. J Pharmacol Exp Ther. 300:1036-1045 (2002).

99. Y. Zhangand L.Z. Benet. The gut as a barrier to drug absorption: combined role of cytochrome P450 3A and P-glycoprotein. Clin Pharmacokinet. 40:159-168 (2001).

100. K. Ito, H. Kusuhara, and Y. Sugiyama. Effects of intestinal CYP3A4 and P-glycoprotein on oral drug absorption--theoretical approach. Pharm Res. 16:225-231 (1999).

101. J.H. Hochman, M. Chiba, J. Nishime, M. Yamazaki, and J.H. Lin. Influence of P-glycoprotein on the transport and metabolism of indinavir in Caco-2 cells expressing cytochrome P-450 3A4. J Pharmacol Exp Ther. 292:310-318 (2000).

102. C.L. Cummins, L. Salphati, M.J. Reid, and L.Z. Benet. In vivo modulation of intestinal CYP3A metabolism by P-glycoprotein: studies using the rat single-pass intestinal perfusion model. J Pharmacol Exp Ther. 305:306-314 (2003).

103. C.Y. Wuand L.Z. Benet. Disposition of tacrolimus in isolated perfused rat liver: influence of troleandomycin, cyclosporine, and GG918. Drug Metab Dispos. 31:1292-1295 (2003).

104. Y.Y. Lau, C.Y. Wu, H. Okochi, and L.Z. Benet. Ex situ inhibition of hepatic uptake and efflux significantly changes metabolism: hepatic enzyme-transporter interplay. J Pharmacol Exp Ther. 308:1040-1045 (2004).

105. J.L. Lamand L.Z. Benet. Hepatic microsome studies are insufficient to characterize in vivo hepatic metabolic clearance and metabolic drug-drug interactions: studies of digoxin metabolism in primary rat hepatocytes versus microsomes. Drug Metab Dispos. 32:1311-1316 (2004).

106. W.e.a. Bowen. A Biopharmaceutical Classification System approach to Dissolution: Mechanisms and Strategies. In R.K.a.L. Yu (ed.), Biopharmaceutics Applications in Drug Development, Springer, 2008.

107. FDA. Guidance for Industry: Waiver of In Vivo Bioavailability and Bioequivalence Studies for Immediate-Release Solid Oral Dosage Forms Based on a Biopharmaceutics Classification System.

In F.a.D.A. U.S. Department of Health and Human Services, Center for Drug Evaluation and Research (CDER) (ed.), Rockville, MD., 2000, p. 13.

108. CHMP. Guideline on the Investigation of Bioequivalence. In C.f.M.P.f.H.U.C. European Medicines Agency (ed.), *CPMP/EWP/QWP/1401/98 Rev 1*, 2009.

109. C.Y. Wuand L.Z. Benet. Predicting drug disposition via application of BCS: transport/absorption/ elimination interplay and development of a biopharmaceutics drug disposition classification system. Pharm Res. 22:11-23 (2005).

110. D.A. Smith. Design of drugs through a consideration of drug metabolism and pharmacokinetics. Eur J Drug Metab Pharmacokinet. 19:193-199 (1994).

111. T. Takagi, C. Ramachandran, M. Bermejo, S. Yamashita, L.X. Yu, and G.L. Amidon. A provisional biopharmaceutical classification of the top 200 oral drug products in the United States, Great Britain, Spain, and Japan. Mol Pharm. 3:631-643 (2006).

112. Y.Y. Lau, H. Okochi, Y. Huang, and L.Z. Benet. Multiple transporters affect the disposition of atorvastatin and its two active hydroxy metabolites: application of in vitro and ex situ systems. J Pharmacol Exp Ther. 316:762-771 (2006).

113. L.Z. Benet. The drug transporter-metabolism alliance: uncovering and defining the interplay. Mol Pharm. 6:1631-1643 (2009).

114. J.E. Polli, B.S. Abrahamsson, L.X. Yu, G.L. Amidon, J.M. Baldoni, J.A. Cook, P. Fackler, K. Hartauer, G. Johnston, S.L. Krill, R.A. Lipper, W.A. Malick, V.P. Shah, D. Sun, H.N. Winkle, Y. Wu, and H. Zhang. Summary workshop report: bioequivalence, biopharmaceutics classification system, and beyond. AAPS J. 10:373-379 (2008).

115. L.Z. Benet, G.L. Amidon, D.M. Barends, H. Lennernas, J.E. Polli, V.P. Shah, S.A. Stavchansky, and L.X. Yu. The use of BDDCS in classifying the permeability of marketed drugs. Pharm Res. 25:483-488 (2008).

116. S. Tolle-Sander, J. Rautio, S. Wring, J.W. Polli, and J.E. Polli. Midazolam exhibits characteristics of a highly permeable P-glycoprotein substrate. Pharm Res. 20:757-764 (2003).

117. Y.Y. Lau, Y. Huang, L. Frassetto, and L.Z. Benet. Effect of OATP1B transporter inhibition on the pharmacokinetics of atorvastatin in healthy volunteers. Clin Pharmacol Ther. 81:194-204 (2007).

118. B.N. Singh. Effects of food on clinical pharmacokinetics. Clin Pharmacokinet. 37:213-255 (1999).

119. R.Z. Harris, G.R. Jang, and S. Tsunoda. Dietary effects on drug metabolism and transport. Clin Pharmacokinet. 42:1071-1088 (2003).

120. D. Fleisher, C. Li, Y. Zhou, L.H. Pao, and A. Karim. Drug, meal and formulation interactions influencing drug absorption after oral administration. Clinical implications. Clin Pharmacokinet. 36:233-254 (1999).

Chapter 3

Differential transport of Class 1 and 2 compounds in two well-characterized cell systems: the Caco-2 and MDCK cell lines

DIFFERENTIAL TRANSPORT OF CLASS 1 AND 2 COMPOUNDS IN TWO WELL-CHARACTERIZED CELL SYSTEMS: THE CACO-2 AND MDCK CELL LINES

Margarida Estudante[1,2], Selma Sahin[1,3], Leslie Z. Benet[1]

[1] Pharmacological Sciences Unit, iMed.UL, University of Lisbon, Faculty of Pharmacy, Portugal

[2]Department of Biopharmaceutical sciences, University of California San Francisco

[3]Hacettepe University, Faculty of Pharmacy, 06100-Ankara, Turkey

Abstract

The aim of the current study was to investigate the bidirectional transport of highly soluble and highly permeable drugs verapamil and diltiazem (Class 1) and highly permeable and low solubility drug saquinavir (Class 2) across Caco-2 and MDR1-overexpressing MDCK cells. Caco-2 cells grown as epithelial monolayers on polycarbonate membrane inserts (0.4μm) were used in the transport studies 21-28 days after seeding. Transport studies across MDR1-MDCK cell monolayers were conducted 5 to 7 days postseeding. Cells were incubated with drug solution in the absence or presence of the P-gp inhibitor GG918 (0.5μM). At 1, 2 and 3 hours, 200μL-samples were taken from the apical or basolateral side and then replaced with fresh buffer with or without GG918. The apparent permeability (Papp) values were calculated as the product of permeability rate, initial donor concentration and filter surface area. Net flux ratio was defined as the ratio of basolateral to apical (B to A) over apical to basolateral (A to B) transport. The well-known P-gp substrate digoxin (10 nM and 10 μM) was used as a positive control for P-gp in Caco-2 cells and presented a net flux ratio of 4 which decreased to around 1 by GG918 addition, consistent with a P-gp effect in Caco-2 cells. Net flux ratio for verapamil and diltiazem in control transport buffer was nearly unity as observed by the insignificant B to A over A to B transport of these drugs in Caco-2 cells. The presence of GG918 resulted in no change in net flux ratios. On the other hand, the net flux ratio for 10 nM verapamil in control transport buffer was 13.9 and reduced to 0.86 in the presence of GG918 in MDR1-MDCK cells. This ratio for 10 μM verapamil in control transport buffer and with the addition of GG918 was 4.14 and 0.90 in MDR1-MDCK cells, respectively. For 10 μM diltiazem the flux ratio was 16.5 in MDR1-MDCK cells and decreased to 0.87 with the addition of GG918. Regarding the Class 2 drug, saquinavir, the net flux ratio was higher than 2 in both Caco-2 and MDR1-MDCK cell lines and decreased to near the unity with GG918. These results indicate that P-gp plays a minimal role in transcellular transport of highly soluble and highly permeable drugs verapamil and diltiazem across Caco-2 cells. Conversely these drugs are actively secreted by P-gp in MDR1- MDCK cell

monolayers. Saquinavir is actively secreted by P-gp across Caco-2 cells, confirming that Class 2 drugs are significantly affected by P-gp in the intestine.

Keywords:

Caco-2, MDR1-MDCK, permeability, P-glycoprotein, Saquinavir, Verapamil, Diltiazem, Digoxin

INTRODUCTION

The oral absorption of a drug is fundamentally dependent on that drug's aqueous solubility and gastrointestinal permeability. Extensive research into these fundamental parameters by Amidon *et al* (1) led to the Biopharmaceutics Classification System (BCS) that categorizes drugs into four groups, Class 1 – Class 4. The BCS classifies compounds based on the critical components related to oral absorption. Centrally embracing permeability and solubility, the objective of the BCS is to allow prediction of *in vivo* absorption performance of drug products from *in vitro* measurements of permeability and solubility.

In 2000, the FDA promulgated the BCS as a science based approach to allow waiver of *in vivo* bioavailability and bioequivalence testing for immediate release solid dosage forms for Class 1 compounds, highly soluble and highly permeable drugs, when such drug products also exhibit rapid dissolution (2).

Recognition of the elimination pathway differences for Class 1 and Class 2 drugs versus Class 3 and Class 4 drugs, combined with the inherent difficulty in quantifying the percent of drug absorbed in humans at a level of 90%, prompted Wu and Benet (3) to suggest a revised category scheme entitled the Biopharmaceutics Drug Disposition Classification System (BDDCS). The BDDCS replaces the permeability criteria with the major route of elimination because of the belief that it is easier and less ambiguous to determine the assignment of BDDCS for marketed drugs based on the extent of metabolism than using permeability (i.e. extent of absorption) in BCS assignments thereby eliminating many instances of uncertainly in human permeability leading to differences in class designation by different authors.

Recent work (4, 5), initially based on cellular system studies evaluating transporter-enzyme interplay, has led us to a number of generalizations regarding transporter effect following oral dosing. The gut lumen of the gastrointestinal tract is sufficiently leaky so that small molecular weight, soluble, non-polar compounds (i.e. Class 1 compounds) readily pass through the membrane. Alternatively, the high permeability/ high solubility of Class 1 drugs allows high concentrations in the gut to saturate any

transporter, both efflux and absorptive. That is, Class 1 compounds may be substrates for both uptake and efflux transporters *in vitro* in cellular systems under the right conditions [(for example, midazolam (6) and verapamil (2) are substrates for P-glycoprotein)], but transporter effects will not be important clinically.

For Class 2 drugs, the high permeability will allow ready access into the gut membranes making intestinal uptake transporters generally unimportant due to the rapid permeation of the drug molecule into the enterocytes. That is, absorption of Class 2 compounds is primarily passive and a function of lipophilicity. However, the low solubility of these compounds will limit the concentrations coming into the enterocytes, thereby preventing saturation of the efflux transporters. Consequently, efflux transporters will affect the extent of oral bioavailability and the rate of absorption of Class 2 drugs. Moreover, there will be little opportunity to saturate intestinal enzymes such as CYP3A4 and UDP-glucuronosyltransferases (UGTs) due to the low solubility. Thus, changes in transporter expression, and inhibition or induction of efflux transporters will cause changes in intestinal metabolism of drugs that are substrates for the intestinal enzymes. Many Class 2 compounds are primarily substrates for CYP3A as well as substrates or inhibitors of the efflux transporter P-glycoprotein. This interplay was characterized in the absorption process for the investigational cysteine protease inhibitor K77 (7, 8) and the immunosuppressive sirolimus (9), substrates for CYP3A and P-glycoprotein and for raloxifene (10), a substrate for UGTs and P-glycoprotein. Class 2 compounds may be affected by both uptake and efflux transporters in the liver (11).

For Class 3 compounds, sufficient drug will be available in the gut lumen due to good solubility, but an absorptive transporter will be necessary to overcome the poor permeability characteristics of these compounds. However, intestinal apical efflux transporters may also be important for the absorption of such compounds when sufficient enterocyte penetration is achieved via an uptake transporter. That is, since influx of Class 3 compounds will generally be rate limited by an absorptive transporter, the counter effects of efflux transporters will not be saturated and can also be important. In general, these principles also hold for Class 4 compounds, although Class 4 drugs may achieve sufficient solubility in the natural surfactant containing gut contents so that they act like Class 3 compounds.

Research focused on elucidating the influence of transporters on drug disposition has been ongoing for many years (12). Various *in vitro* technologies exist to investigate transporters, examples being the well characterized Madin-Darby canine kidney (MDCK) cell line and the industry standard, human colonic adenocarcinoma (Caco-2) cell line. Cellular assays assessing the bidirectional transport of compounds across a cell monolayer is a widely accepted approach that accounts for passive and active components of absorption. Another facet of this investigational approach includes introduction, via transfection, of the transporter of interest into an epithelial, adherent cell line such as the MDCK cells. Contrastingly, with the Caco-2 cell model, transporter effects may emerge from endogenously expressed proteins (13, 14). In this study, we focus on the transfected MDR1-MDCK (MM) cell line incorporating the stable expression of the MDR1 gene encoding for the P-glycoprotein (P-gp) efflux transporter (15-17). We compare the MDR1-MDCK cell system to the Caco-2 endogenous cell system and evaluate the utility and adequacy of both systems in assessing the P-gp mediated efflux of Class 1, Class 2 and Class 3 drugs.

We believe that the effects of transporters on the highly soluble, highly permeable and extensively metabolized Class 1 drugs will be minimal and clinically irrelevant, while Class 2 and Class 3 drugs will be significantly affected by efflux transporters in the intestine like P-gp (3). As the Caco-2 cells are derived from the human gastrointestinal (GI) tract as opposed to the canine kidney derived MDCK cells, we believe the assays conducted in the Caco-2 cell system will more closely imitate *in vivo* drug behavior. That is, Class 1 drugs that are shown to be P-gp substrates in the MDR1-MDCK model will not appear as such in the Caco-2 model (18). In the case of Class 2 drugs, both cellular model systems will produce P-gp substrate properties (18). The study designed to investigate our hypothesis includes the Class 1 drugs, verapamil and diltiazem, the Class 2 drug, saquinavir and the Class 3 drug digoxin and the results are presented and discussed herein.

MATERIALS AND METHODS

Materials

MDR1-MDCK (MM) and MDCK cell lines were generously provided by Dr. Ira Pastan (National Cancer Institute, National Institutes of Health, Bethesda, MD). The Caco-2 cell line (HTB-37) was purchased from the American Type Culture Collection (ATCC - Manassas, VA). All components necessary for proper cell culture growth conditions (described below) were purchased from the University of California, San Francisco Cell Culture Facility (San Francisco, CA). D-[1-^{3}H(N)]-Mannitol was purchased from NEN

(Boston, MA). [^{3}H]-Saquinavir and [^{3}H]-Digoxin were purchased from Moravek Biochemicals and Radiochemicals (Brea, CA). [N-methyl-^{3}H]-Verapamil hydrochloride and [^{3}H]-Diltiazem was purchased from Perkin Elmer (Waltham, MA). GG918 (GF120918: N-(7-tetrahydro-6,7-dimethoxy-2-isoquinolinyl)-ethyl]-phenyl)-9,10-dihydro-5-methoxy-9-oxo-4-acridine carboxamine) was a kind gift from GlaxoSmithKline (Research Triangle Park, NC). All other chemicals were of reagent grade and purchased from Sigma-Aldrich (St. Louis, MO).

Six-well tissue culture treated polystyrene plates were obtained from Corning Life Science (Acton, MA). Falcon polyethylene terephthalate cell culture inserts (pore size 0.4 μm, diameter 4.2 cm^2) were obtained from BD Biosciences (Bedford, MA).

Cell cultures

Caco-2 cells were grown in a humidified 5% CO_2 atmosphere at 37°C using minimum essential medium (MEM) Eagle's with Earle's balances salt solution (BSS) containing 1.0 g/L glucose, 0.292 g/L L-glutamine, 2.2 g/L $NaHCO_3$, which was supplemented with 15% heat-inactivated FBS, 1.0 mM sodium pyruvate, 0.1 mM nonessential amino acids, 100 U/mL penicillin and 100 U/mL streptomycin. Cells were grown to 90-100% confluence and harvested using 0.05% trypsin EDTA. Monolayers were prepared by seeding harvested cells onto polyethylene terephthalate cell culture inserts at a density of approximately 60,000 cells/cm^2. Growth medium for the Caco-2 was refreshed 48 hours post-seeding and then twice weekly, including one day prior to the experiment. Caco-2 cell monolayers were used for bidirectional transport experiments 21-28 days postseeding.

MDCK cells were grown in a humidified 5% CO_2 atmosphere at 37°C using Dulbecco's modified Eagle's medium (DMEM) containing 4.5 g/L glucose, 3.7 g/L $NaHCO_3$, 0.584 g/L *l*-glutamine, which was supplemented with 10% heat-inactivated FBS, 100 U/mL penicillin and 100 U/mL streptomycin. MDR1-MDCK cell culture medium was as described above with the addition of 80 ng/mL colchicine as a selective supplement. Cells were grown to 90-100% confluence and harvested using 0.05% trypsin EDTA. Monolayers were prepared by seeding harvested cells onto polyethylene terephthalate cell culture inserts at a density of approximately 1,000,000 cells/insert. Growth medium was refreshed once every two days and one day prior to the experiment, which was performed 5-7 days postseeding for both cell lines.

Bidirectional Transport Experiments

The transport assays were performed following a modified protocol previously described (9, 19). In brief, cell monolayers were preincubated in control transport buffer (Hank's buffered salt solution containing 25 mM HEPES and 1% FBS, pH 7.4) at 37°C for 20 minutes. Transepithelial electrical resistance (TEER) values were then measured by the Millicell electrical resistance system utilizing "chopstick" electrodes (Millipore Corporation, Bedford, MA). On average, the MDR1-MDCK cells possessed values of approximately 7000-8000 $\Omega \cdot cm^2$, while the VECTOR-MDCK cells possessed TEER values of approximately 600-700 $\Omega \cdot cm^2$. On average, the Caco-2 cells system possessed TEER values of approximately 800-1000 $\Omega \cdot cm^2$. All experiments were performed in triplicate and conducted on at least three separate occasions to ensure reproducibility. In the case of the MDR1-MDCK and parental MDCK cells, both these transfected and control cell lines were run on the same day to account for potential between-day variability of radiolabeled counts and TEER values.

The experiment was started by the addition of test compound in control transport buffer to the donor compartment and control transport buffer only to the receiver compartment. For inhibition studies, the inhibitor (GG918) was put into both the donor and receiver compartments. The final volume in each of the chambers was 1.5 mL on the apical side and 2.5 mL on the basolateral side. Experimental samples were isolated from the receiver compartment at 1 hour, 2 hours and 3 hours. At the first two time points, 200 µL samples were removed and then replaced with fresh media to restore initial starting volumes. At the final time point, following collecting of the last 200 µL sample, content of both chambers was removed by suction, each cell culture insert was dipped three times into ice-cold PBS and the cell culture insert membranes were collected. All experiments were run at 37°C with a shaking speed of 25 strokes/minute in the Boekel Shake 'N' Bake Incubator Shaker II (Boekel Scientific, Feasterville, PA).

All samples were added to 5 mL Econo-Safe™ Counting Cocktail (Research Products International Corporation, Mount Prospect, IL) and vortexed. Cells monolayers were solubilized by sonication (in an ultrasonic bath) for 15 minutes. All samples were analyzed using a Beckman LS180 scintillation counter (Beckman Industries, Palo Alto, CA).

The apparent permeability (P_{app}) values were calculated as follows where the rate of transport was measured from the flux of drug across the cells.

Papp = Rate of transport/(surface area x initial donor concentration)

Net flux ratio was defined as the ratio of basolateral to apical (B to A) over apical to basolateral (A to B) transport.

RESULTS

Bidirectional transport studies in MDR1-MDCK (MM) and MDCK cells

Transport profiles of 10 nM and 10 µM verapamil and 10 µM diltiazem across MDR1-MDCK (MM) and parental control MDCK cells in control and inhibitory conditions are depicted in Figures 1 and 2, respectively. The net flux ratio (B to A/ A to B) for 10 nM verapamil in control transport buffer was 13.9 and reduced to 0.86 in the presence of GG918 (0.5 µM) (Figure 1A, Table 1). The net flux ratio of 10 µM verapamil in contol buffer and with the addition of GG918 was 4.14 and 0.90, respectively (Figure 1B, Table 1). The net flux ratio for 10 µM diltiazem in control transport buffer was 16.49 and reduced to 0.87 in the presence of GG918 (Figure 2, Table 2).

On the other hand, bidirectional transport of verapamil (10 nM and 10 µM) and 10 µM diltiazem across MDCK cells was not influenced by GG918 as indicated by comparable Papp A to B and Papp B to A values obtained in control and inhibitory conditions (Figure 1 and 2 and Tables 1 and 2).

Figure 3A depicts the observed decrease in the basolateral to apical (B to A) transport coupled with an increase in apical to basolateral (A to B) transport for saquinavir in MDR1-MDCK cells, in the presence of GG918 (0.5 µM). Addition of this inhibitor resulted in a reduction of the net flux ratio (B to A / A to B) by 98%, from 154 to 1.8 (Table 3).

Fig 1A

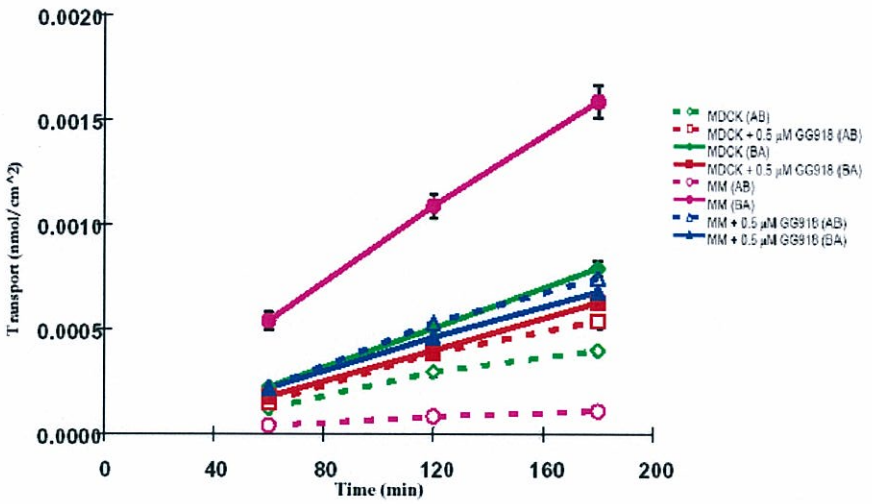

Fig 1B

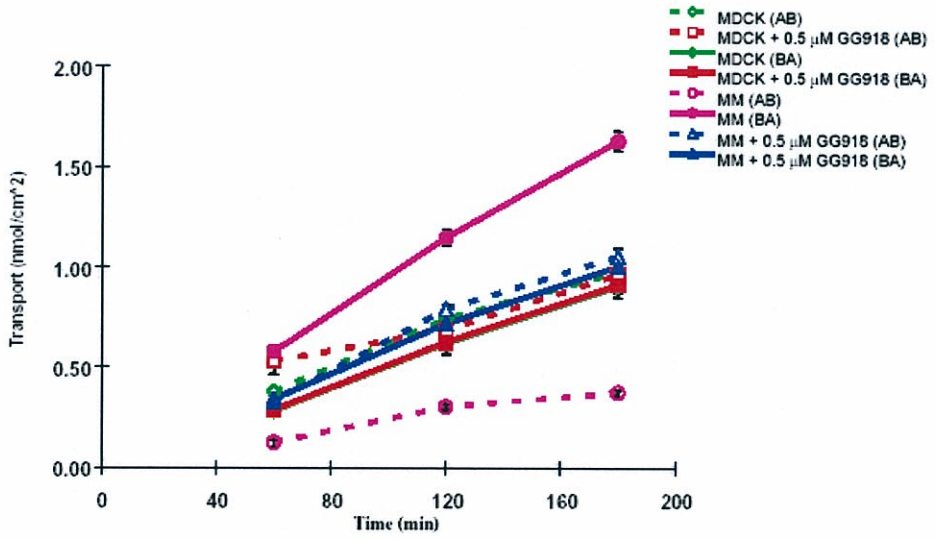

Figure 1. Bidirectional transport of 10 nM (A) and 10 µM (B) verapamil in MDR1-MDCK cells (MM) and parental MDCK cells in the presence or absence of known P-gp inhibitor, GG918 (0.5 µM).

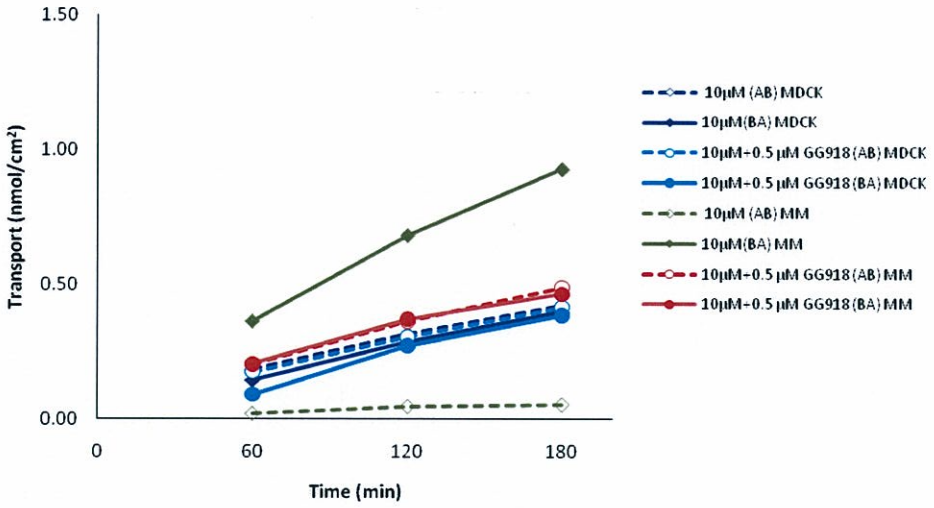

Figure 2 – Bidirectional transport of 10 μM diltiazem in MDCK and MDR1-MDCK (MM) cells in the presence and absence of the known P-gp inhibitor, GG918 (0.5 μM).

Table 1. Apparent permeability values (P_{app} and net flux ratios for verapamil (10 nM and 10 μM) in Caco-2, MDCK and MDR1-MDCK cells. P_{app} values ± sd are listed for the apical to basolateral (A→B) direction and the basolateral to apical (B→A) direction, each with n = 3 transwells.

Cell Line	Verapamil	Condition	Apparent Permeability (P_{app}) Values ($nm \cdot sec^{-1}$)		Net Flux Ratio (B→A/ A→B)
			$P_{app(A→B)}$	$P_{app(B→A)}$	
Caco-2	10 nM	Control	65.2 ± 2.9	71.2 ± 3.6	1.09
		+ GG918 (0.5 μM)	72.4 ± 4.7	73.1 ± 2.0	1.01
	10 μM	Control	93.3 ± 4.1	84.5 ± 2.9	0.90
		+ GG918 (0.5 μM)	91.3 ± 1.2	82.9 ± 2.2	0.91
MDCK	10 nM	Control	33.6 ± 0.4	64.3 ± 3.1	1.91
		+ GG918 (0.5 μM)	45.5 ± 3.1	50.6 ± 2.3	1.1
	10 μM	Control	82.1 ± 1.6	73.0 ± 4.5	0.89
		+ GG918 (0.5 μM)	80.4 ± 0.4	73.5 ± 3.1	0.91
MDR1-MDCK	10 nM	Control	9.1 ± 0.3	127.0 ± 6.1	13.9
		+ GG918 (0.5 μM)	62.6 ± 0.9	54.1 ± 0.5	0.86
	10 μM	Control	31.5 ± 1.3	130.4 ± 3.8	4.14
		+ GG918 (0.5 μM)	89.4 ± 3.5	80.3 ± 3.7	0.90

Table 2 - Permeability (Papp ± sd) values of diltiazem across Caco-2 and MDCK/ MDR1- MDCK cells.

Cell line	**Drug**	**Apparent Permeability (P_{app}) Values ($nm \bullet sec^{-1}$)**		**Net efflux ratio B→A/A→B**
		A→B	**B→A**	
Caco-2	**Diltiazem**			
	10 nM	59.4 ± 5.6	98.6 ± 4.3	1.66
	10 µM	72.8 ± 2.4	64.4 ± 3.6	0.88
	Diltiazem + GG918			
	10 nM	68.0 ± 6.0	105.4 ± 2.5	1.55
	10 µM	68.6 ± 3.8	63.8 ± 1.9	0.93
MDCK	**Diltiazem**			
	10 µM	48.9 ± 0.9	43.7 ± 0.4	0.89
	Diltiazem + GG918			
	10 µM	40.4 ± 1.0	36.2 ± 0.6	0.89
MDR1-MDCK	**Diltiazem**			
	10 µM	5.5 ± 4.8	90.9 ± 2.9	16.49
	Diltiazem + GG918			
	10 µM	46.9 ± 1.6	41.2 ± 2.3	0.87

Fig 3A

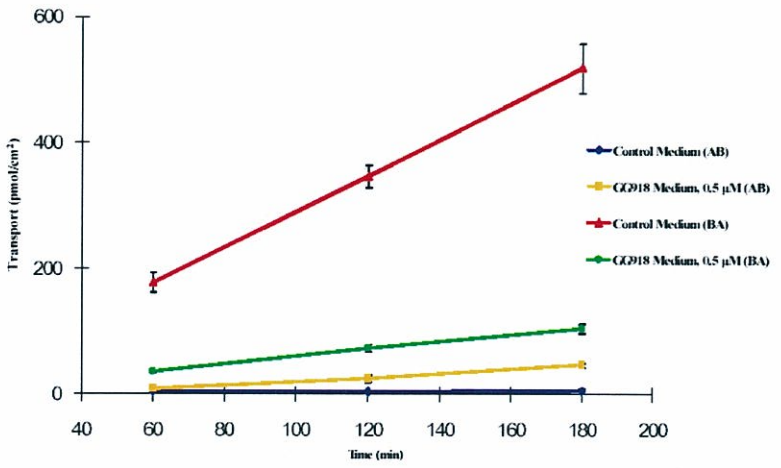

Fig 3B

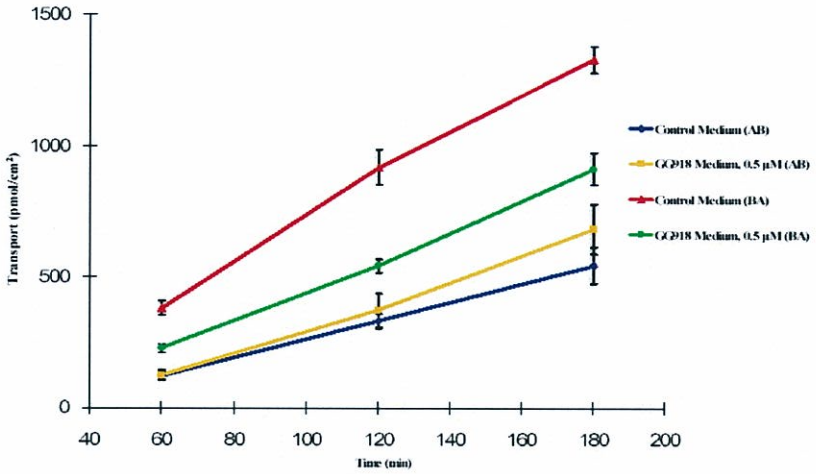

Figure 3. Bidirectional transport of saquinavir in MDR1-MDCK (A) and Caco-2 (B) cells in the presence or absence of known P-gp inhibitor, GG918 (0.5 µM).

Table 3 - Apparent permeability values (P_{app}) and net flux ratios (B to A / A to B) for saquinavir (20 µM) in Caco-2, MDCK and MDR1-MDCK cells. P_{app} values ± sd are listed for the apical to basolateral (A→B) direction and the basolateral to apical (B→A) direction, each with n = 3 transwells.

Cell Line	**Saquinavir (20 µM)**	**Apparent Permeability (P_{app}) Values (nm•sec^{-1})**		**Net Flux Ratio** (B→A/ A→B)
		$P_{app(A→B)}$	$P_{app(B→A)}$	
Caco-2	Control	29.2 ± 2.7	65.8 ± 3.2	2.3
	+GG918 (0.5µM)	38.8 ± 4.1	47.5 ± 2.3	1.2
MDR1-MDCK	Control	1.54 ± 0.3	237 ± 14.7	154
	+ GG918 (0.5µM)	26.4 ± 3.7	47.0 ± 4.2	1.8

Bidirectional transport studies in Caco-2 cells

Figure 4 and 5 depicts the overlapping transport profiles in control and inhibitory conditions for 10 nM (Figure 4A) and 10 µM (Figure 4B) verapamil and for 10 nM (Figure 5A) and 10 µM (Figure 5B) diltiazem in Caco-2 cells. The net flux ratio (B to A / A to B) in control transport buffer was nearly unity as observed by the insignificant difference in B to A and A to B transport. The presence of GG918 (0.5 µM) resulted in no change in net flux ratios (Tables 1 and 2).

Fig 4A

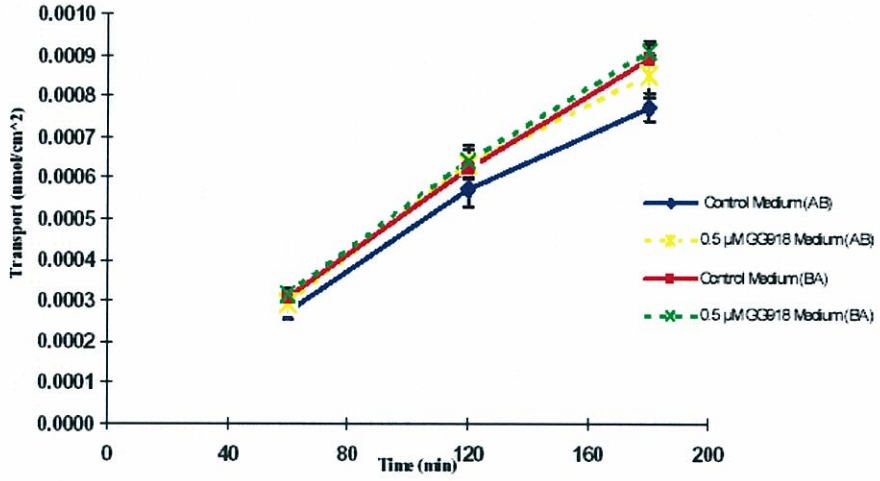

Fig 4B

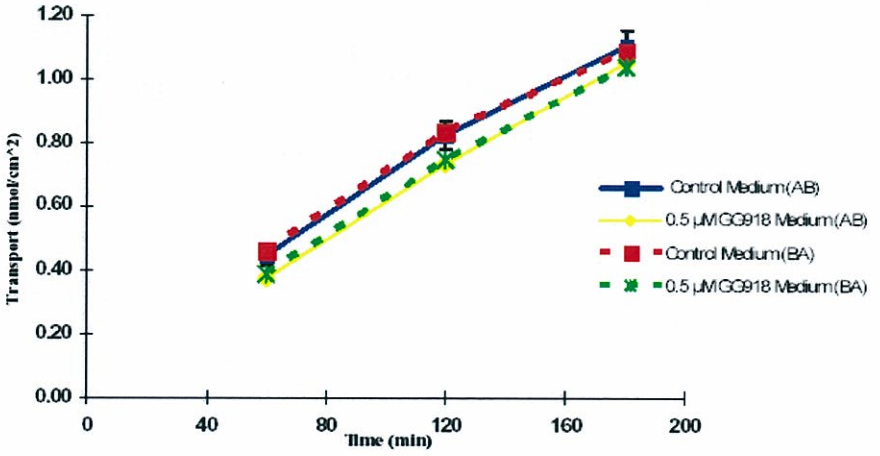

Figure 4. Bidirectional transport of 10 nM (A) and 10 µM (B) verapamil in Caco-2 cells in the presence or absence of known P-gp inhibitor, GG918 (0.5 µM).

Figure 3B and Figure 6 illustrate the transport profiles of saquinavir and digoxin, respectively, across Caco-2 cells in control and inhibitory conditions. With the addition of GG918, basolateral to apical (B to A) transport decreased and apical to basolateral (A to B) increased. The net flux ratio (B to A / A to B) in control transport buffer was 2.3 for saquinavir and 4.5 for digoxin 10 nM and 10µM. The presence of GG918 (0.5 µM) resulted in a reduction of the net flux ratio to 1.2 for saquinavir and 1.4 for digoxin, a decrease of 46% and 68%, respectively (Tables 3 and 4).

Fig 5A

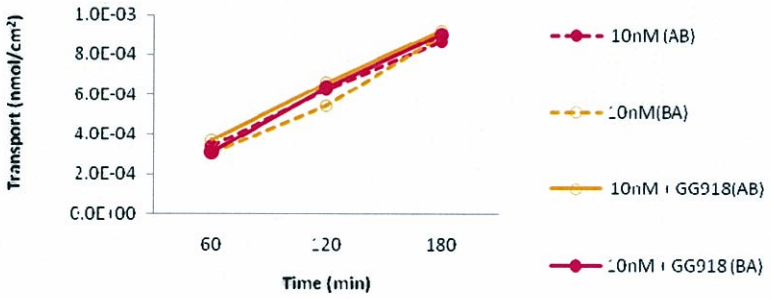

Fig 5B

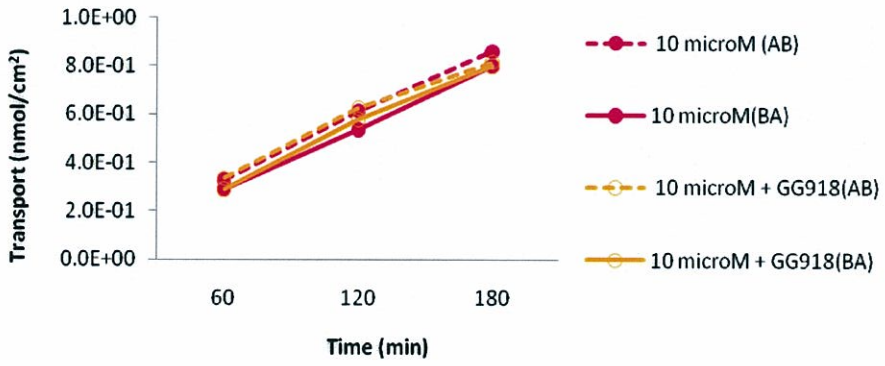

Figure 5. Bidirectional transport of 10 nM (A) and 10 µM (B) diltiazem in Caco-2 cells in the presence or absence of known P-gp inhibitor, GG918 (0.5 µM).

Fig 6A

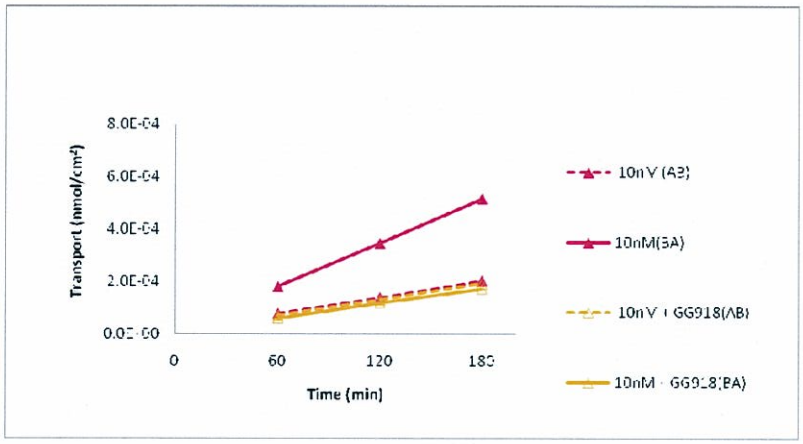

Fig 6B

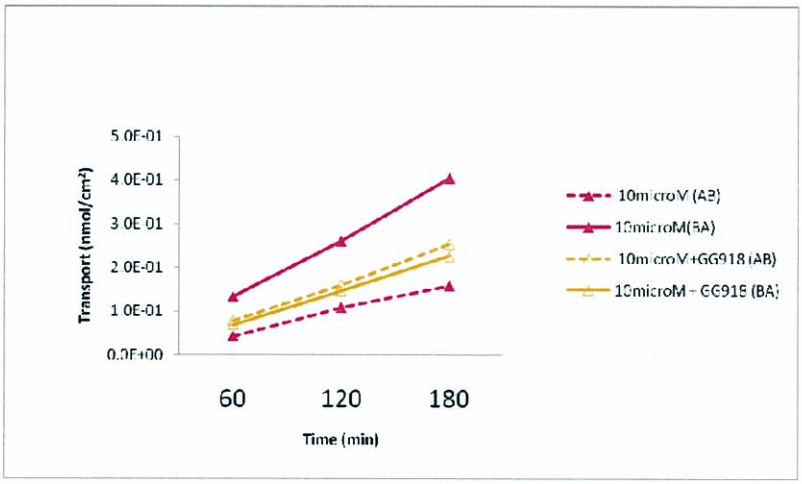

Figure 6. Bidirectional transport of 10 nM (A) and 10 µM (B) digoxin in Caco-2 cells in the presence or absence of known P-gp inhibitor, GG918 (0.5 µM).

Table 4 - Apparent permeability values (P_{app}) and net flux ratios ((B to A / A to B) for digoxin 10 nM and 10 μM in Caco-2 cells. P_{app} values ± sd are listed for the apical to basolateral (A→B) direction and the basolateral to apical (B→A) direction, each with n = 3 transwells.

Cell line	**Drug**	**Apparent Permeability (P_{app}) Values ($nm \bullet sec^{-1}$)**		**Net efflux ratio** B→A/A→B
		A→B	B→A	
Caco-2	**Digoxin**			
	10 nM	14.7± 2.2	59.7 ± 3.1	4.05
	10 μM	13.5 ± 3.1	54.7 ± 2.1	4.05
	Digoxin + GG918			
	10 nM	20.9 ± 0.6	29.3 ± 2.1	1.40
	10 μM	21.8 ± 2.4	30.6 ± 1.3	1.40

DISCUSSION

Comprehensive data resulting from years of *in vitro* cellular assays and *in vivo* animal studies has lead to our presumption that almost all drugs are substrates for some transporter. However, this is not to say that transporter effects will always be clinically relevant. In other words, an *in vitro* net flux ratio (B to A / A to B) of 4 for a given drug, which according to the Food and Drug Administration (FDA) is indicative of a transporter substrate (20), may translate *in vivo* to a negligible contribution of the transporter to that same drug's disposition.

In this study, we selected the anti-hypertensive drugs verapamil (Calan® and Isoptin®) and diltiazem (Herbesser® and Balcor®) as our BCS and BDDCS Class 1 compounds. We also selected the antiretroviral drug, saquinavir (Invirase® and Fortovase®) as our BCS and BDDCS Class 2 compound. Both drugs are highly permeable and extensively metabolized by the CYP3A4 enzyme. Moreover, both are known substrates of the efflux transporter, P-gp. In fact, verapamil is considered by the FDA to be a model P-gp substrate and probe (2). We also selected the digitalic drug digoxin (Lanoxin®), a Class 3 drug, as a positive control for P-gp activity in Caco-2 cells as it is a well known P-gp substrate. The results obtained with digoxin revealed a P-gp effect, therefore validating our Caco-2 model regarding P-gp function.

We performed scores of bidirectional transport studies with each drug in the MDR1-MDCK, MDCK, and Caco-2 cell systems in the presence or absence of the known P-gp inhibitor, GG918. In general, a compound is considered a P-gp substrate if it exhibits a net flux ratio *in vitro* of 2-3 or greater (20). But the question remains, what cell line is the appropriate model system for determining these net flux ratios?

Following experimentation with verapamil, diltiazem, saquinavir and digoxin we have reached the answer to that question and the answer is two-fold. First, the MDR1-MDCK cell system may be the appropriate model to utilize for determination of a P-gp substrate. Second, the Caco-2 cell system may be the appropriate model system to utilize to determine whether a P-gp effect may play a significant role in absorption and disposition.

As stated earlier, verapamil, diltiazem, saquinavir and digoxin are known P-gp substrate. Our data in the MDR1-MDCK cells confirm this. Figures 1 and 2 depict the bidirectional transport profile verapamil and diltiazem, respectively. Figure 3A depicts the profile of saquinavir. In each case the basolateral to apical (B to A) flux is markedly greater than the apical to basolateral (A to B) flux. This results in significant net flux ratios representative of a P-gp substrate. For verapamil the net flux ratio is 13.9 (10 nM) and 4.1 (10 μM) (Table 1), for diltiazem 10 μM the flux ratio is 16.49 (Table 2) and for saquinavir (20 μM) the ratio is 154 (Table 3). In each case, removing the P-gp mediated transport by addition of GG918 results in net flux ratios of nearly 1 (Tables 1-3).

Our data from Caco-2 cells, however, do not confirm that both drugs are P-gp substrates by definition. Only the Class 2 saquinavir and the Class 3 digoxin results in data indicative of a P-gp substrate with transport in the B to A direction greater than A to B direction (Figure 3B and Figure 6) and net flux ratio of 2.3 and 4.05 (Tables 3-4). The bidirectional transport of the Class 1 verapamil and diltiazem results in overlapping B to A and A to B profiles (Figures 4 and 5) and net flux ratios close to 1 (Table 1 and 2), which indicate passive permeability as the driving force and no influence of P-gp. It follows, that saquinavir and digoxin transport, and not verapamil or diltiazem, is affected by addition of GG918, which results in returning the net flux ratio to unity (Tables 3 and 4).

The apparent permeability (P_{app}) values for verapamil (10 μM) in the MDR1-MDCK cells in control conditions demonstrate the strong influence of P-gp mediated transport with a permeability more than 4 times faster in the B to A direction than in the A to B direction, 130.4 ± 3.8 nm•sec^{-1} versus 31.5 + 1.3 nm•sec^{-1} (Table 1). In the Caco-2 cells, however, the P_{app} values are nearly the same in both directions,

93.3 ± 4.1 nm•sec^{-1} (A to B) compared to 84.5 + 2.9 nm•sec^{-1} (B to A). These P_{app} values are unaffected by addition of the P-gp inhibitor GG918 and the net flux ratio remains unchanged, suggesting that verapamil absorption is controlled by its passive diffusion and not P-gp (Table 1). Moreover, inhibiting the active P-gp mediated mechanism with GG918 in the MDR1-MDCK cells results in P_{app} values of 89.4 ± 3.5 nm•sec^{-1} (A to B) and 80.3 + 3.7 nm•sec^{-1} (A to B) for verapamil. These P_{app} values are representative of the passive permeability observed in the values calculated for Caco-2 cells (Table 1). Similar results were observed for diltiazem (Table 2), with P_{app} values of 90.9±2.9 (B to A) and P_{app} values of 5.5.9±4.8 (A to B). In the presence of GG918 the values changed to 41.2±2.3 and 46.9±1.6, respectively.

The apparent permeability (P_{app}) values for saquinavir (20 μM) in control conditions for both the Caco-2 and the MDR1-MDCK cell systems show the significant influence of P-gp mediated transport resulting in B to A permeabilities greater than A to B permeabilities (Table 3). The P-gp effect is markedly greater in the MDR1-MDCK cells than in the Caco-2 cells. The MDR1-MDCK P_{app} values of 237 ± 14.7 nm•sec^{-1} (B to A) and 1.54 + 0.3 nm•sec^{-1} (A to B) demonstrate the role of P-gp in the transport of saquinavir, which results in a BA/AB ratio of 154 as seen in Table 3 and confirms the ratio calculated by Polli and colleagues (16) in their work describing saquinavir as an "unambiguous substrate." Furthermore, in both the MDR1-MDCK and the Caco-2 cell system, the P-gp inhibitor GG918 is capable of blocking the active transport mechanism, which results in faster A to B P_{app} values and slower B to A P_{app} values upon addition of GG918 (Table 3). Clearly, these data show that efflux is important for the Class 2 drug saquinavir.

One major criteria that leads researchers to employ the MDR1-MDCK cell line is its superior TEER values. This exceedingly tight cell system allows for increased sensitivity in identifying P-gp substrates. However, a transporter effect observed in the MDR1-MDCK cell system may not necessarily be observed in the Caco-2 cell system (18). The lower TEER values of the Caco-2 cells makes for a leakier system that we believe is far more representative of the human intestine. Verapamil, as well as drugs like midazolam and diazepam, are often used as model substrates (2, 20). However, each are Class 1 compounds thereby bringing that methodology into question because our data demonstrate that we can ignore the transporter effects for Class 1 compounds. Consequently, for certain drugs considered to be "model" P-gp substrates it may be difficult to predict their transporter interactions in the intestine.

REFERENCES

1. G.L. Amidon, H. Lennernas, V.P. Shah, and J.R. Crison. A theoretical basis for a biopharmaceutic drug classification: the correlation of in vitro drug product dissolution and in vivo bioavailability. Pharm Res. 12:413-420 (1995).

2. FDA. Guidance for Industry: Waiver of In Vivo Bioavailability and Bioequivalence Studies for Immediate-Release Solid Oral Dosage Forms Based on a Biopharmaceutics Classification System. In F.a.D.A. U.S. Department of Health and Human Services, Center for Drug Evaluation and Research (CDER) (ed.), Rockville, MD.p. 13. (2000)

3. C.Y. Wuand L.Z. Benet. Predicting drug disposition via application of BCS: transport/absorption/ elimination interplay and development of a biopharmaceutics drug disposition classification system. Pharm Res. 22:11-23 (2005).

4. L.Z. Benet. The drug transporter-metabolism alliance: uncovering and defining the interplay. Mol Pharm. 6:1631-1643 (2009).

5. L.Z. Benet, C.L. Cummins, and C.Y. Wu. Transporter-enzyme interactions: implications for predicting drug-drug interactions from in vitro data. Curr Drug Metab. 4:393-398 (2003).

6. S. Tolle-Sander, J. Rautio, S. Wring, J.W. Polli, and J.E. Polli. Midazolam exhibits characteristics of a highly permeable P-glycoprotein substrate. Pharm Res. 20:757-764 (2003).

7. C.L. Cummins, W. Jacobsen, and L.Z. Benet. Unmasking the dynamic interplay between intestinal P-glycoprotein and CYP3A4. J Pharmacol Exp Ther. 300:1036-1045 (2002).

8. C.L. Cummins, L. Salphati, M.J. Reid, and L.Z. Benet. In vivo modulation of intestinal CYP3A metabolism by P-glycoprotein: studies using the rat single-pass intestinal perfusion model. J Pharmacol Exp Ther. 305:306-314 (2003).

9. C.L. Cummins, W. Jacobsen, U. Christians, and L.Z. Benet. CYP3A4-transfected Caco-2 cells as a tool for understanding biochemical absorption barriers: studies with sirolimus and midazolam. J Pharmacol Exp Ther. 308:143-155 (2004).

10. J.H. Changand L.Z. Benet. Glucuronidation and the transport of the glucuronide metabolites in LLC-PK1 cells. Mol Pharm. 2:428-434 (2005).

11. Y.Y. Lau, Y. Huang, L. Frassetto, and L.Z. Benet. Effect of OATP1B transporter inhibition on the pharmacokinetics of atorvastatin in healthy volunteers. Clin Pharmacol Ther. 81:194-204 (2007).

12. K. Ito, H. Suzuki, T. Horie, and Y. Sugiyama. Apical/basolateral surface expression of drug transporters and its role in vectorial drug transport. Pharm Res. 22:1559-1577 (2005).

13. C. Hilgendorf, G. Ahlin, A. Seithel, P. Artursson, A.L. Ungell, and J. Karlsson. Expression of thirty-six drug transporter genes in human intestine, liver, kidney, and organotypic cell lines. Drug Metab Dispos. 35:1333-1340 (2007).

14. D. Sun, H. Lennernas, L.S. Welage, J.L. Barnett, C.P. Landowski, D. Foster, D. Fleisher, K.D. Lee, and G.L. Amidon. Comparison of human duodenum and Caco-2 gene expression profiles for 12,000 gene sequences tags and correlation with permeability of 26 drugs. Pharm Res. 19:1400-1416 (2002).

15. R.B. Kim, M.F. Fromm, C. Wandel, B. Leake, A.J. Wood, D.M. Roden, and G.R. Wilkinson. The drug transporter P-glycoprotein limits oral absorption and brain entry of HIV-1 protease inhibitors. J Clin Invest. 101:289-294 (1998).

16. J.W. Polli, S.A. Wring, J.E. Humphreys, L. Huang, J.B. Morgan, L.O. Webster, and C.S. Serabjit-Singh. Rational use of in vitro P-glycoprotein assays in drug discovery. J Pharmacol Exp Ther. 299:620-628 (2001).

17. M.E. Taub, L. Kristensen, and S. Frokjaer. Optimized conditions for MDCK permeability and turbidimetric solubility studies using compounds representative of BCS classes I-IV. Eur J Pharm Sci. 15:331-340 (2002).

18. J.M. Custodio, C.Y. Wu, and L.Z. Benet. Predicting drug disposition, absorption/elimination/transporter interplay and the role of food on drug absorption. Adv Drug Deliv Rev. 60:717-733 (2008).

19. Y.Y. Lau, H. Okochi, Y. Huang, and L.Z. Benet. Multiple transporters affect the disposition of atorvastatin and its two active hydroxy metabolites: application of in vitro and ex situ systems. J Pharmacol Exp Ther. 316:762-771 (2006).

20. FDA. Drug interaction studies. Department of Health and Human Services, Center for Drug Evaluation and Research (CDER) (ed), Rockville, MD, (2006).

Chapter 4

Effect of P-gp on the rat intestinal permeability and metabolism of the BDDCS Class 1 drug verapamil

EFFECT OF P-GP ON THE RAT INTESTINAL PERMEABILITY AND METABOLISM OF THE BDDCS CLASS 1 DRUG VERAPAMIL

Margarida Estudante[a,b], Manuela Maya[a], José G. Morais[a], Graca Soveral[c,d], Leslie Z. Benet[b]

[a]*Pharmacological Sciences Unit, iMed.UL, University of Lisbon, Faculty of Pharmacy, Portugal;* [b]*Department of Bioengineering and Therapeutic Sciences, University of California, San Francisco, USA;* [c] *REQUIMTE, Dep. Química, FCT-UNL, 2829-516 Caparica, PortugaL;* [d] *Dep. Bioquímica e Biologia Humana, Faculdade de Farmácia, Universidade de Lisboa, 1649-003 Lisboa, Portugal*

Purpose: The Biopharmaceutics Drug Disposition Classification System (BDDCS) predicts intestinal transporter effects to be clinically insignificant following oral dosing for highly soluble and permeable/ metabolized drugs (Class 1 drugs). We investigated the effect of inhibiting P-glycoprotein (P-gp) on the *in vitro* rat intestinal permeability (Papp) and metabolism of the Class 1 drug verapamil.

Methods: Jejunal segments from Sprague-Dawley rats fasted overnight were mounted in Ussing chambers filled with 10 ml Krebs-Ringer buffer (KRB). For P-gp inhibition studies, GG918 0.5 μM was added to the KBR solution. The experiment started by the addition of verapamil (1 or 10 μM) to either apical or basolateral sides. Samples from verapamil donor and receiver compartments were collected at 30 seconds, 0.166, 0.5, 1, 1.83 and 3 hours after the start of the experiment. Analysis of verapamil and its major metabolite, norverapamil, in the samples and intracellularly at 3hr was performed by HPLC. The same experiment was repeated with norverapamil 10 μM (verapamil metabolite), digoxin 100 nM (positive control for P-gp activity) and atorvastatin 1 and 10 μM (example of a Class 2 drug).

Results: For 1 μM verapamil, net flux ratio (B to A Papp /A to B Papp) was 4.6 and changed by GG918 (net flux ratio = 1.1). For 10 μM verapamil net flux ratio was 3.3 (control) *vs.* 1.4 (GG918), comparable to the change seen for digoxin 100 nM with a net flux ratio of 3.6 (control) *vs.* 1.6 (with GG918) and atorvastatin (net flux ratio of 5.2 and 3 for atorvastatin 1 and 10 μM, respectively, changed to 1 and 0.7 with GG918). However, clearly the changes observed in the norverapamil 10 μM experiment were significant. Net flux ratio of norverapamil decreased from 13.5 (control) to 1.5 (GG918). The Extraction Ratio (ER) of verapamil to norverapamil decreased from 0.25 after an apical dose to 0.092 after a basolateral dose, but was unafected by the incubation with GG918.

Conclusion: The results suggest that P-gp inhibition may have an effect on Class 1 drug verapamil and Class 2 drug atorvastatin Papp in the rat intestine, but that the effect on the more polar norverapamil metabolite Papp is higher. The effect of GG918 on the ER of verapamil suggests that P-gp does not have a prominent role in the metabolism of Class 1 substrates.

Introduction

The extent of drug absorption and bioavailability (BA) are some of the central questions for pharmaceutical scientists during the course of drug discovery and development (1, 2). Amidon et al. (3) recognized that the fundamental parameters controlling the rate and extent of drug absorption were the drug's aqueous solubility and gastrointestinal permeability. They devised a Biopharmaceutics Classification System (BCS) that categorizes drugs into four classes based on their solubility (S) and permeability (Papp).

When the BCS was first developed there was little understanding of the importance of drug transporters to bioavailability. Now it is recognized that both uptake and efflux transporters in the intestine and liver are important in determining oral drug absorption and biovailability (1). Over the past 15-20 years a number of drug uptake and efflux transporters have been identified that are expressed at the apical (A) or basolateral (B) side of epithelial cells in various tissues (4). The most investigated examples are the ABC family of ATP-dependent efflux transporters P-glycoprotein (P-gp), multidrug resistance –associated protein 2 (MRP 2) and breast cancer resistance protein (BCRP), expressed in organs of excretion including gut, liver and kidney. ABC transporters are highly abundant at the apical (luminal) membrane of enterocytes thereby limiting the intestinal absorption of many clinically important and frequently prescribed drugs such as statins, antibiotics, HIV protease inhibitors, immunosuppressants, anticancer and cardiac drugs (5). Human oral bioavailability studies with cyclosporine (6) were the first to point out the possible interplay between intestinal metabolism and efflux in the gut as the cause for the limited absorption of this immunosuppressive agent, followed by similar studies with sirolimus and tacrolimus. The synergistic action of CYP3A and P-glycoprotein in limiting oral drug delivery is further suggested by their joint presence in the small intestine, the significant overlap in their substrate specificities and the poor oral bioavailability of joint substrates (7). This may control the access of drug molecules to the

enzymes and changes in transporter function can modulate intestinal metabolism without changes of enzyme activity (7-15).

In 2005, Wu and Benet (16) recognized that the overwhelming majority of Classes 1 and 2 (high P drugs) were extensively metabolized while for the great majority of Classes 3 and 4 (low P drugs) compounds elimination was predominantly via biliary and/or renal excretion of unchanged drug. They suggested that changing the permeability component to a route of elimination component in a Biopharmaceutics Drug Disposition Classification System (BDDCS) may be useful in predicting overall drug disposition, including routes of drug elimination, potential for drug-drug interactions and the effects of efflux and absorptive transporters on oral drug-absorption. BDDCS aims to characterize the factors affecting BA taking into account the new set of knowledge regarding transporters and transporter-enzyme interplay, which are key determinants for drug absorption.

Our previous studies suggest that for Class 2, 3 and 4 compounds intestinal transporters effects will be significant following oral dosing, while for Class 1 compounds, following oral dosing, intestinal transporters will generally be unimportant (16). The gut lumen of the GI tract is sufficiently leaky so that low molecular weight, soluble, non-polar compounds (i.e. Class 1 compounds) readily pass through the membrane. Alternatively, the high permeability/high solubility of Class 1 drugs allows high concentrations in the gut to saturate any transporter, both efflux and absorptive. That is, Class 1 compounds may be substrates for both uptake and efflux transporters *in vitro* in cellular systems under the right conditions, but transporter effects in the gut and the liver will not be important clinically. Sahin *et al.* showed that verapamil and quinidine (17) (BCS and BDDCS Class 1 drugs) are substrates for P-gp in MDCK P-gp transfected cell line, but not in parenteral MDCK or Caco-2 cell monolayer.

Verapamil is a calcium channel blocker widely used to control hypertension, chest pain and arrhythmia. It is classified as a BCS and BDDCS Class 1 drug and has been identified as both a P-glycoprotein substrate and inhibitor (1, 18, 19). Verapamil is also a CYP3A substrate in both human (20) and rat (21) and undergoes extensive hepatic and intestinal first pass metabolism by N-demethylation (norverapamil, the major metabolite in plasma) and N-dealkation (D-617) (20). It has been suggested that some verapamil metabolites might be actively transported by P-gp (22).

Studies with selective P-glycoprotein and CYP3A inhibitors are required to elucidate and separate the effects of efflux and metabolism on verapamil permeability *in vitro* and *in situ* in an attempt to understand the relationship that may exist between these two processes *in vivo* (21).

In the present study we investigated the interplay between P-glycoprotein and Cyp3a in the intestine, through measurement of parent drug (verapamil, 1 μM and 10 μM dose) and primary metabolite (norverapamil) levels across segments of rat jejunum in the absence and presence of the specific P-glycoprotein inhibitor GG918 (0.5 μM). This work allowed us to evaluate the predictability of the recently proposed BDDCS on the role of intestinal transporters and transporter-enzyme interplay for the Class 1 drug verapamil.

We repeated the experiment for a BCS/BDDCS Class 2 drug, atorvastatin (1 μM and 10 μM dose), in order to compare the permeability values and net flux ratios (B to A Papp/ A to B Papp) between Class 1 and Class 2 drugs.

Materials and Methods

Materials

Verapamil hydrochloride, norverapamil, the internal standards propranolol and fluvastatin, digoxin and sodium fluorecein were supplied by Sigma-Aldrich (Sintra, Portugal), GG918 was kindly provided by Glaxo SmithKline (Research Triangle Park, North Carolina), atorvastatin was kindly provided by Pfizer (New York City, United States) and the anesthetic agent (Pentobarbital sodium; Eutasil) was supplied by Sanofi Veterinária (Miraflores, Algés, Portugal). All other reagents were analytical grade, all solvents were HPLC grade and water was obtained from a Millipore Direct-Q water purification system.

Study Protocol

Sprague-Dawley rats (250–400 g) fasted overnight until anaesthetized i.p. with pentobarbital. A 20 cm intestinal segment was removed from the junction between the duodenum and jejunum. Jejunal segments of about 3 cm in length were mounted in Ussing chambers (23). Each chamber compartment

was filled with 10ml Krebs-Ringer buffer (KBR; pH 6.5 at the apical compartment (A) and pH 7.4 at the basolateral compartment (B)), and 5% CO_2 in O_2 bubbled continuously. For P-gp inhibition studies, GG918 0.5 µM was added to the KBR solution 20 minutes before the start of the experiment. Independent experiments were conducted for each study drug, verapamil (1 and 10 µM) (n = 6), norverapamil (10 µM)(n = 3), atorvastatin (1 and 10 µM)(n = 3) or digoxin (100 nM)(n = 3) by addition to either A or B sides and the temperature was kept at 37 ^{0}C. Samples from drug donor and receiver compartments were collected at 30 seconds, 0.166, 0.5, 1, 1.83 and 3 hours after the start of the experiment. Analysis of verapamil and its major metabolite, norverapamil, in the samples and intracellularly at 3hr was performed by HPLC. Atorvastatin in the samples was quantified by LC/MS/MS. Digoxin appearance in the receiver compartment was analyzed by immunoassay (Siemens Medical Solutions). Membrane integrity was confirmed by measuring sodium fluorescein 0.001% (w/v) permeation across the rat intestinal segments (24).

The permeability assessment of each drug was performed under sink conditions.

Verapamil and Norverapamil Assays

All verapamil and norverapamil metabolite samples were analyzed by HPLC under isocratic conditions on a reverse phase LiChroCART/ LiChrospher 60 RP-select B C18 column (4 x 250 mm, particle size 5 µm) (Merck KGaA, Darmstadt, Germany) and a C18 guard column. The HPLC system consisted of an integrated solvent and sample management platform (Waters e2695 Separations Module, Waters Corporation) with a Waters 2475 Fluorescence Detector and Empower system control software. The mobile phase was a mixture of 10 mM ammonium acetate buffer pH=3.0 with 0.01% diethylamine, acetonitrile and tetrahydrofuran (15:73:12) pumped at 1 ml/min. Verapamil, norverapamil and the internal standard, propranolol, were monitored fluorometrically at an excitation wavelength of 275 nm and emission wavelength of 315 nm, with retention times of 10.7, 12.1 and 8.5 minutes, respectively.

Procedures for sample analysis were modified based on previously published methods (25-27) and validated adequately. Briefly, samples were alkalinized by addition of NaOH 2 N, extracted by methyl *t*-butyl ether and evaporated to dryness in a stream of nitrogen. The dry extract was reconstituted in 100 µl of mobile phase before injection.

Atorvastatin Assay

The LC/MS-MS method for analyzing atorvastatin was modified based on a previously method described by Lau et al. Briefly, a MicroMass® Quattro micro instrument (Waters Corporation) with electrospray-positive ionization was used, connected to an HPLC Waters® Alliance 2695. The multiple reaction monitor was set at 559.6 to 440.8 m/z for ATV and 412.3 to 265.9 m/z for the internal standard, fluvastatine. The cone voltage and collision energy were set at 35 V and 21 eV, respectively. The analytical column was a Sunfire RP, C18 (4.6x50 mm, 5 µm particle size). The mobile phase consisted of acetonitrile and acetic acid 0.05%. The flow rate was set at 0.3 ml/min. The quantification limit for atorvastatin was 2.5 ng/ml. The samples were prepared in SPE (solid phase extraction) columns (Sec Pak Vac C18, Waters), previously activated and then eluted in 100% methanol.

Data Analysis

Apparent permeability coefficients (Papp) were calculated from drug appearance in the receptor chamber using eq. 1:

$$Papp\ (nm/s) = (dX/dt)_{initial}/(A.C_o) \qquad \text{eq. 1}$$

Where dX/dt is the initial rate of change of amount of drug transported into the receptor chamber with respect to time (i.e., the flux, $nmol.min^{-1}$), C_o is the initial concentration in the donor chamber and A is the surface area available for diffusion (1.78 cm^2).

Net flux ratio was defined as the ratio of basolateral to apical (B to A) over apical to basolateral (A to B) transport. Net flux ratio was calculated as the mean of the net flux ratios obtained for each individual rat.

The Extraction ratio (ER) of verapamil 10 µM across the tissue was determined at t = 180 min by eq. 2 (8), where the subscripts *d*, *r* and *t* represent the total amount (nmol) of metabolite or parent compound in the donor, receptor, and tissue compartments, respectively.

$$ER = (\Sigma\ METABOLITE_{d,r,t})/(\Sigma\ METABOLITE_{d,r,t} + \Sigma\ PARENT_{r,t}) \qquad \text{eq. 2}$$

Statistical Analysis

Statistical analysis of drug and metabolite intracellular levels under the different tested conditions as well as Extraction ratios was performed using ANOVA. A probability of $p < 0.05$ was considered to be statistically significant.

Results

Effect of P-gp on Verapamil Transport and Intracellular Levels

Figure 1 shows the results of a typical Ussing Chamber experiment where the time course of verapamil appearance at either the apical (B-A) or basolateral compartment (A-B) is depicted with and without inhibitor (Fig. 1A = 1 µM verapamil; Fig. 1B = 10 µM verapamil).

The appearance permeability of verapamil was determined (eq. 1) when dosed either at the apical (Papp A-B) or basolateral (Papp B-A) side of the intestinal sheet at 1 µM and 10 µM. P-glycoprotein effect on verapamil permeation was addressed in inhibition studies using the selective P-glycoprotein inhibitor GG918 (0.5 µM). The results are presented in Table I.

For 1 µM verapamil, there was an increase in permeability when it was dosed at the basolateral side *vs.* the apical side. Verapamil permeability value in the basolateral to apical direction (B to A = efflux) was 346 nm/s *vs.* 100 nm/s for verapamil permeability in the absorptive direction (A to B). Net flux ratio, a measure of efflux given by B to A Papp /A to B Papp, was 4.6 and decreased by the addition of GG918 (net flux ratio = 1.1) a potent Pg-p inhibitor (Table I). For 10 µM verapamil, permeability value in the basolateral to apical direction (B to A) was 284 nm/s versus 94 nm/s for verapamil permeability in the absorptive direction (A to B). By addition of GG918, efflux permeability (B to A) decreased to 205 nm/s while absorptive permeability (A-B) increased to 194 nm/s. Net flux ratio for verapamil 10 µM was 3.3 (control) *vs.* 1.4 in the presence of GG918 (Table I).

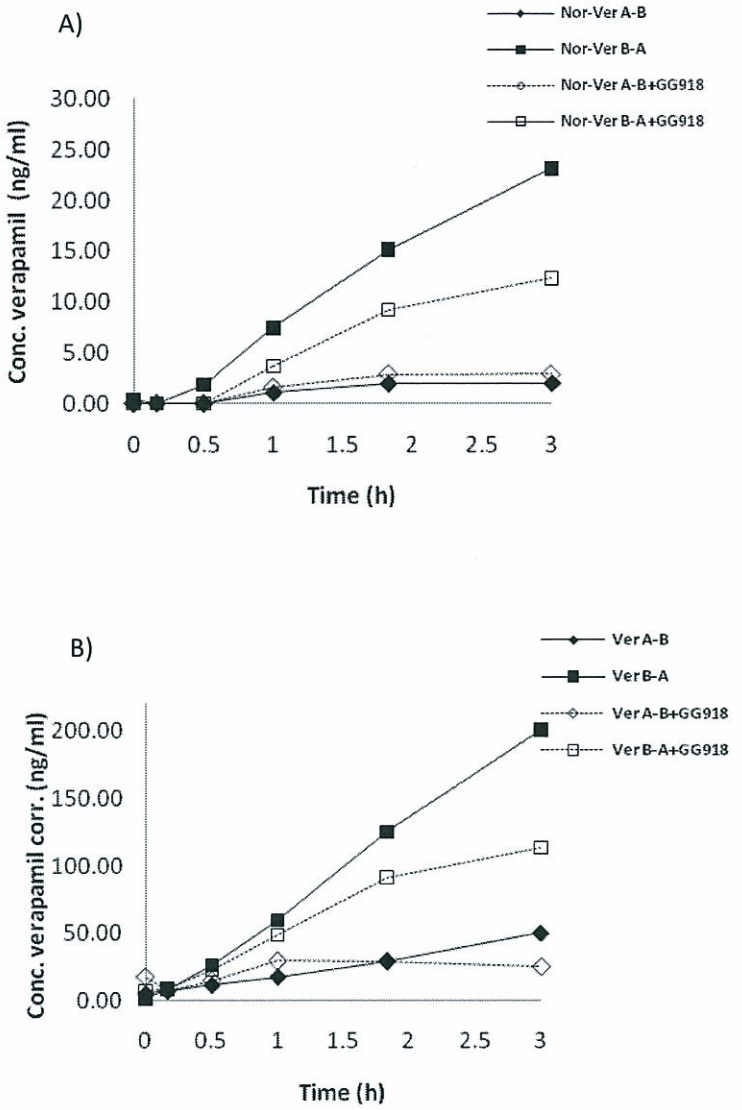

Figure 1 –Appearance of verapamil 1 µM (A) and 10 µM (B) at the basolateral compartment when added to the apical side (A-B) and appearance at the apical compartment when added to the basolateral side (B-A) with (+GG918) and without inhibitor. Control experiments are represented with solid lines and solid symbols while inhibitor experiments are represented with dashed line and open symbols. One representative set of data.

Table I – Permeability (Papp A- B and Papp B- A) and net flux ratios values of verapamil 1 μM and 10 μM and norverapamil 10 μM across segments of rat jejunum in absence and presence of the P-gp inhibitor GG918 (0.5 μM) (mean ± sd)(n = 6 for verapamil experiments; n = 3 for norverapamil experiments).

	Papp (nm/s)		**Net flux ratio**
	A to B	**B to A**	**B to A/ A to B**
Drug			
Verapamil 1 μM	100±10	346±86	4.6±0.6
Verapamil 10 μM	94±77	284±120	3.3±0.8
Norverapamil 10 μM	25±5	357±215	13.5±8
with GG918			
Verapamil 1 μM	173±8	166±85	1.1±0.7
Verapamil 10 μM	194±169	205±100	1.4±0.3
Norverapamil 10 μM	162±20	221±130	1.5±1.2

For verapamil 1 μM intracellular concentration was larger from a basolateral dose compared with an apical dose (2.5 fold for control and 2.2 fold for GG918 incubation) (Figure 2A). For verapamil 10 μM the intracellular levels are very similar for A-B and B-A dose, although P-gp inhibition caused intracellular verapamil values to slightly increase from both directions (Figure 2B). Nevertheless, the effect of P-gp inhibitor on verapamil intracellular concentration was not statistically significant ($p>0.05$).

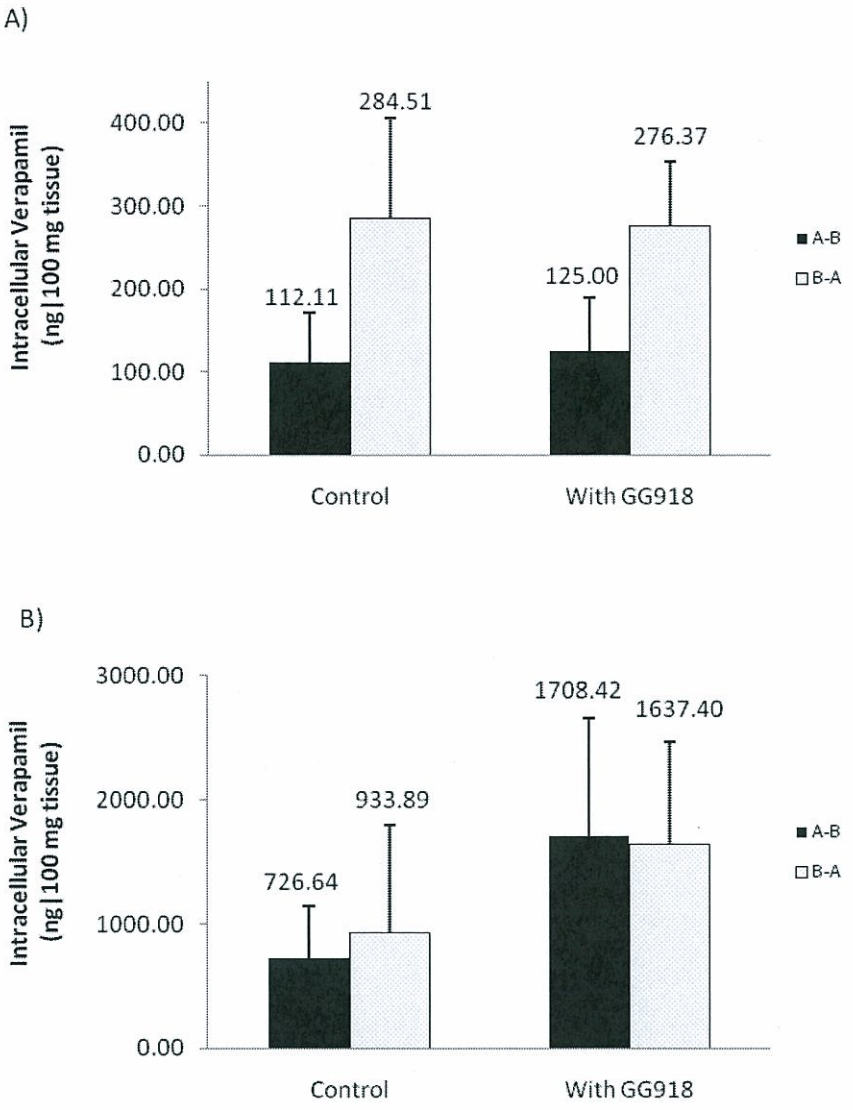

Figure 2 – Intracellular verapamil at the end of the experiment, when verapamil 1 µM (A) or 10 µM (B) was added to the apical (A-B) or basolateral (B-A) side with (+GG918) (n=6) and without inhibitor (control) (n=6).

Effect of P-gp on the *in situ* generated Norverapamil

A primary verapamil metabolite, norverapamil, was measured after incubation of verapamil with rat intestinal sheets. As Cyp3a is located inside the cells, metabolites are formed intracellularly; therefore,

samples were obtained from both the apical and basolateral compartments at experiment sampling times to determine the excretion patterns of norverapamil from the cells. The intracellular level of metabolites was determined at the last time point.

After a verapamil apical dose, norverapamil was preferentially excreted toward the apical side. The addition of GG918 to the incubation media caused a 45% decrease (1 μM verapamil experiment; Figure 3A) and a 79% decrease (10 μM verapamil experiment; Figure 3B) in appearance of norverapamil at the apical side, suggesting that P-gp is involved in the apical excretion of this metabolite. These experiments suggested that the norverapamil changes for the verapamil 10 μM experiment were significant.

Norverapamil concentrations at the basolateral (receiver side) following the verapamil apical dose and at both donor and receiver sides following a verapamil basolateral dose were below the Limit of quantification (LOQ). For verapamil 1 μM and 10 μM there was no significant difference in the norverapamil intracellular levels from either dosing direction and, as observed for the 10 μM verapamil dose, P-gp inhibition seemed to slightly increase the intracellular levels of metabolite (data not shown). As concluded for the parent drug, all of the norverapamil intracellular changes were apparent but not statistically different ($p>0.05$).

Effect of P-gp on Norverapamil Transport and Intracellular Levels

In order to confirm our hypothesis that norverapamil is a good P-gp substrate in the rat intestine, we repeated the same experiment using norverapamil as the donor drug. We chose the higher concentration of 10 μM. There was a significant increase in permeability when norverapamil was dosed at the basolateral side versus the apical side. Norverapamil permeability value in the basolateral to apical direction (B to A = efflux) was 357 nm/s versus 25 nm/s for verapamil permeability in the absorptive direction (A to B). These Papp values led to a net flux ratio of 13.5 that decreased close to the unity (1.5) in the P-gp inhibition experiments (Table I; Figure 4). B-A Papp of norverapamil decreased to 221 nm/s (1.6-fold decrease) and A B Papp increased to 162 (6-fold increase) with GG918. These results confirm that norverapamil is a good P-gp substrate in the rat intestine.

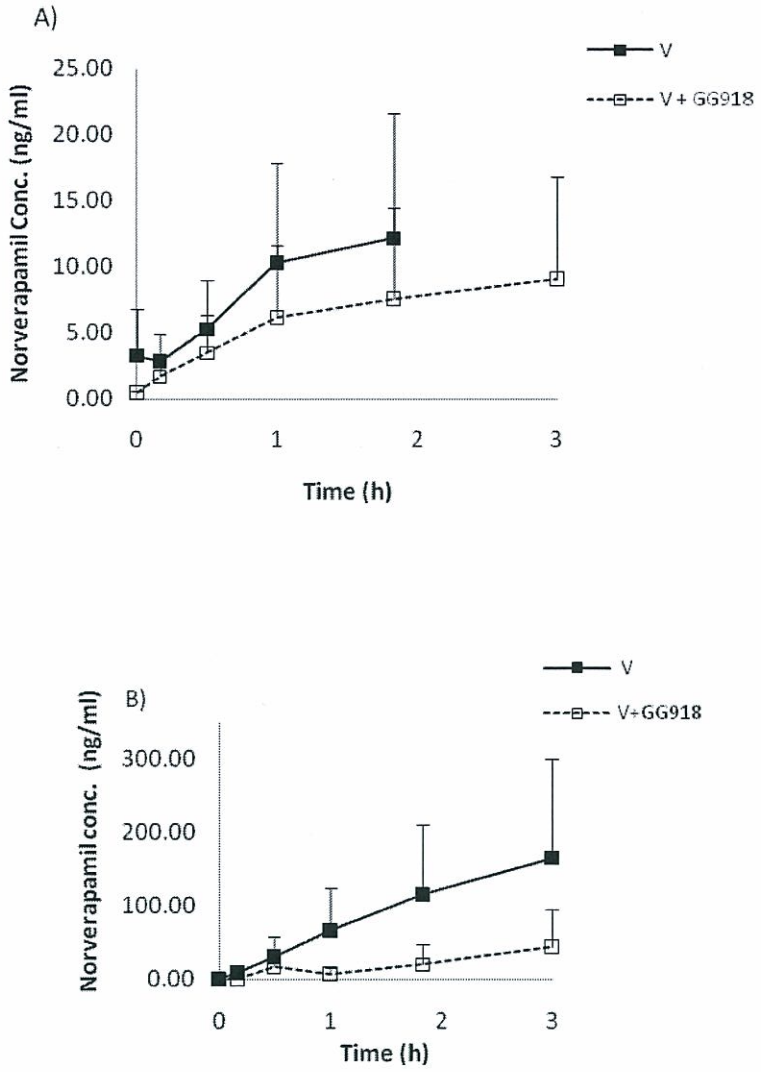

Figure 3 – Norverapamil apical exit profiles after a 1 µM (A) or a 10 µM (B) verapamil apical dose. Verapamil was dosed alone (V) or in combination with the inhibitor 0.5 µM GG918 (V+GG918). Control experiments are represented with solid line and solid symbol while inhibitor experiments are represented with dashed line and open symbol.

Nevertheless, intracellular norverapamil concentrations at the end of the experiment (Figure 5) were somehow similar to the ones seen in the verapamil experiment. Although the net flux ratio is 4 times higher for norverapamil than for verapamil the norverapamil intracellular concentrations remain

unchanged by the addition of the P-gp inhibitor GG918, as observed for the parent drug. B-A intracellular norverapamil concentrations seem to be higher (although not statistically significant) than A-B, but again, not affected by GG918.

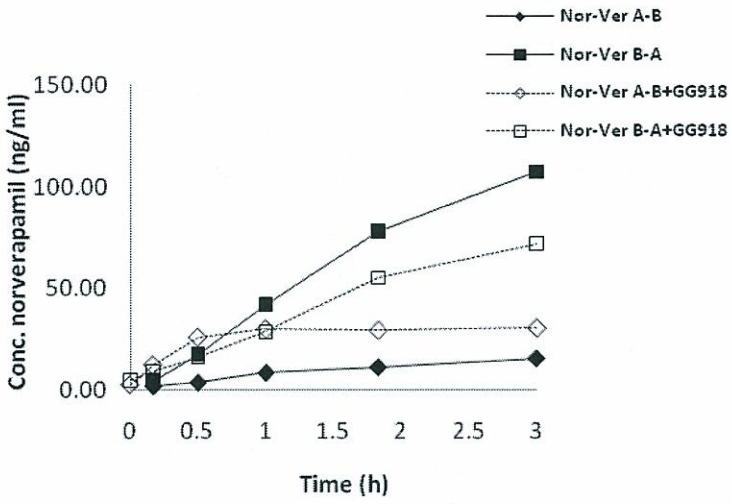

Figure 4 – Appearance of norverapamil 10 µM at the basolateral compartment when added to the apical side (A-B) and appearance at the apical compartment when added to the basolateral side (B-A) with (+GG918) and without inhibitor. Control experiments are represented with solid lines and solid symbols while inhibitor experiments are represented with dashed line and open symbols. One representative set of data.

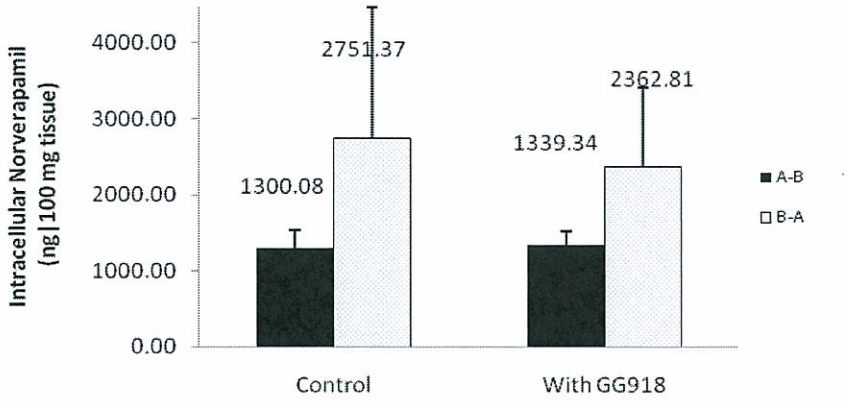

Figure 5 – Intracellular norverapamil at the end of the experiment, when norverapamil 10 µM was added to the apical (A-B) or basolateral (B-A) side with (+GG918) and without inhibitor (control) (n=3).

Effect of P-gp on the Class 2 drug Atorvastatin

The cholesterol-lowering agent atorvastatin (1 µM and 10 µM) was used as a model of a BCS/BDDCS Class 2 drug that is a dual CYP3A and P-gp substrate. Both atorvastatin concentrations led to net flux ratios higher or equal to 3 (5.24 and 3.00 for atorvastatin 1 µM and atorvastatin 10 µM, respectively) as the permeability values were higher on the B-A (57 nm/s and 235 nm/s for atorvastation 1 and 10 µM, respectively) than on the A-B (13 nm/s and 87 nm/s for atorvastation 1 and 10 µM, respectively) directions. The addition of the P-gp inhibitor GG918 brought the permeability values to become very similar in both directions (70 nm/s *vs.* 76.7 nm/s for A to B *vs.* B-A for atorvastatin 1 µM and 156 nm/s *vs.* 105 nm/s for atorvastation 10 µM) and net flux ratios approached the unity (Table II). These results are the ones expected for a model P-gp substrate in the rat intestine.

Table II – Permeability (Papp A- B and Papp B- A) and net flux ratios values of atorvastatin 1 μM and 10 μM and digoxin 100 nM across segments of rat jejunum in absence and presence of the P-gp inhibitor GG918 (0.5 μM) (mean±sd)(n=3).

	Papp (nm/s)(± sd)		Net flux ratio(± sd)
	A to B	**B to A**	**B to A/ A to B**
Drug			
Atorvastatin 1 μM	13±3.6	57±25	5.24±4
Atorvastatin 10 μM	87±69	235±214	3.00±1.2
Digoxin 100 nM	64±19	223±46	3.60±0.5
with GG918			
Atorvastatin 1 μM	70±21	76.7±46	1.04±0.3
Atorvastatin 10 μM	156±61	105±81	0.65±0.3
Digoxin 100 nM	145±65	194±40	1.57±0.8

Effect of Rat Intestinal P-gp on Digoxin Bidirectional Transport

The digoxin 100 nM net flux ratio value was 3.6 (control), decreasing to 1.6 by addition of GG918. A to B and B to A permeability results for digoxin are presented in Table II. The present results are comparable with those obtained with digoxin 10 nM and 10 μM in Caco-2 cells, where net flux ratio decreased from 4.05 (control) to 1.4 with P-gp inhibition (Chapter 3).

Role of P-gp in Influencing CYP3A4-Mediated Verapamil Metabolism: Extraction Ratio Calculations

Table III depicts the Extraction ratios obtained for verapamil calculated using equation 2 (page 97). The extraction ratio yields a measure of the extent of metabolism obtained relative to the amount of drug that was accessible to the metabolizing enzyme (i.e., drug that crossed the intestinal sheet, drug inside the cell and drug that was metabolized). A 25 % Extraction ratio for verapamil (considering the norverapamil metabolite) was obtained after an apical dose versus 9 % from a basolateral 10 μM dose (Table II). That is, relative to the amount of drug that entered or crossed the cell, metabolism is about 3

times higher from an apical dose, although this difference is not statistically significant ($p>0.05$). Consistent with verapamil not being a P-gp substrate, the presence of GG918 did not alter the Extraction ratio in either direction.

Table III – Extraction ratios of verapamil 10 μM after an apical (A-B) or basolateral (B-A) dose without and with (+GG918) inhibitor (n = 6).

	Extraction ratios (Verapamil 10 μM)	
	Drug alone (control)	Drug + GG918
A-B	0.25 ± 0.015	0.17 ± 0.17
B-A	0.092 ± 0.12	0.076± 0.076

For the verapamil 1 μM and atorvastatin 1 μM and 10 μM doses the extraction ratios were not calculated as metabolite concentration was most of the time below the LOQ.

Discussion

Drug transporters have become increasingly important in furthering our understanding of the pharmacokinetic properties (including absorption, distribution and excretion). BDDCS aims to predict bioavailability taking in account the new set of knowledge regarding transporters and transporter-enzyme interplay. Several studies were carried out to investigate the interplay between P-glycoprotein and CYP3A4 in CYP3A4-transfected Caco-2 cells (8, 28) in the rat intestinal perfusion model (9) and *in vivo* in humans (7, 29). We realized that intestinal metabolism could be changed as a function of P-glycoprotein activity without either inhibiting or inducing CYP3A enzymes (7). That is, if efflux by P-glycoprotein is inhibited, the drug molecule passes through the intestine in a single pass and intestinal metabolism will decrease since there is less access of the drug to the enzymes. We tested this hypothesis by carrying out studies with a substance that had negligible effects on CYP3A but which we

knew could affect P-glycoprotein (GG918). For compounds that were substrates of both CYP3A4 and P-glycoprotein, inhibition of intestinal P-glycoprotein would not only increase absorption by blocking efflux but decrease total metabolism as well resulting in a significantly enhanced intestinal bioavailability (7). For the compounds tested at that time we predict P-glycoprotein-CYP3A4 interplay to be relevant at the intestinal and hepatic levels. Nevertheless, for Class 1 compounds (highly permeable/highly soluble) we predicted that both uptake and efflux transporters effects will not be important *in vivo* as the gut lumen of the GI tract is sufficiently leaky so that low molecular weight, soluble, non-polar compounds readily pass through the membrane by a diffusion process. Alternatively, the high concentrations obtained in the gut will saturate any transporter, both efflux and absorptive. To test this hypothesis we used verapamil as a model of Class 1 drug that is a substrate for intestinal CYP3A4 in humans and in rats and that is a well-known substrate for P-glycoprotein in certain cellular systems (MDR1-MDCK, MCF-7/ADR cells) (17) (20, 22), at the blood brain barrier (30, 31) and in certain tumors (18, 30).

However, as the levels of transporters and membrane characteristics in these systems are different from the intestine, the significance of P-glycoprotein in modulating verapamil overall intestinal permeability *in vivo* is still an area of controversia (32) that has been addressed by several authors (17, 18, 21, 30, 31 33, 34, 35).

Previous verapamil permeability studies across rat jejunal tissue (18, 21, 33, 34) and human intestinal segments (33) mounted in side-by-side diffusion chambers suggest a preferential permeation of verapamil in the basolateral to apical direction, consistent with the involvement of an efflux transporter. On the other hand, studies using the rat intestinal perfusion model (35), mdr1a/1b$^{-/-}$ rats (36), Caco-2 cell lines (17, 31) and the human intestinal perfusion model (30) conclude that verapamil intestinal absorption is unaffected by P-glycoprotein mediated efflux. In vivo studies in rats (27) and humans (20) suggest an interaction between verapamil and statins at the intestinal levels, but the mechanism behind this interaction (efflux transporter or metabolism) is not clarified.

In some of the above studies (17, 18, 30, 31, 34) the results are confounded by the use of dual P-glycoprotein and metabolism inhibitors as well as by the use of high concentrations where verapamil is already inhibiting the efflux pump.

In the present study we examined the *in vitro* intestinal permeability and metabolism of the Class 1 drug verapamil dosed at two concentrations (1 μM and 10 μM) on the apical or basolateral side of excised rat jejunum tissue mounted in Ussing chambers. We investigated the possible impact of P-glycoprotein efflux on verapamil bidirectional permeability and intestinal extraction ratio by incubation with the selective P-glycoprotein inhibitor GG918 (0.5 μM). The concentrations used are below the Km for both P-glycoprotein mediated transport and CYP3A4 mediated metabolism and it is therefore assumed that neither process was saturated during this study (33, 37).

Our results demonstrate that verapamil has a preferential transport in the basolateral to the apical direction, which was more visible at the 1 μM dose (Table I). With P-glycoprotein inhibition the basolateral permeability drecreased 2-fold for verapamil 1 μM and apical permeability increased 2-fold for verapamil 10 μM, resulting in net flux ratios to approach one (Table I). The changes observed in verapamil permeability suggest that P-gp can have an effect on rat jejunum permeability, as control net flux ratios were higher than 3, the cut off value to consider P-glycoprotein effect. A net flux ratio decrease to around 1 following P-gp inhibition confirms the involvement of P-gp on the permeability of verapamil. The results obtained for verapamil 10 μM are consistent with net flux ratios previously reported for verapamil in the rat intestine (21, 33), although the net effux with verapamil 1 μM is higher.

The metabolites formed after incubation of verapamil with CYP3A4 have been extensively studied (37). Verapamil is metabolized by P450s 3A4 and 1A2 to two initial metabolites, norverapamil and D-617, and these two metabolites are subject to further breakdown to form at least three additional metabolites. Enterocyte-based CYP3A metabolim has been shown to reduce the intestinal bioavailability of a number of drugs, including verapamil (34) ,tacrolimus and cyclosporine (7).

The norverapamil metabolite exit profiles were monitored over time in both chamber compartments and intracellularly at the last time point. A preferential efflux of norverapamil toward the apical side was observed when the parent drug was dosed at the same side which does not guarantee that the metabolite itself is a substrate for efflux transport (8, 28). The polarized secretion of metabolites toward the apical side has been noted previously for a number of CYP3A4 metabolites in Caco-2 cells (8, 28) which was not affected in the P-gp inhibition studies. There seems to be a bias at the apical membrane that facilitates the exit of metabolites toward the apical side, probably due to CYP3A4 being closer to the apical side as well as the greater surface area of the apical membrane. In the current study the

apical appearance of norverpamil was decreased by 45% and 79% (1 μM vs. 10 μM dose; Figure 3A and 3B) in inhibition studies which is consistent with P-glycoprotein effect. Additionally, a net flux ratio of 13.5 for norverapamil was significant (Table I). The decrease in net flux ratio in presence of GG918 (Table I) reinforces the role of the efflux transporter on the permeability of the more polar verapamil metabolite. This suggests intestinal P-glycoprotein effect to be more relevant as passive diffusion of substrates tends to be less prominent.

Digoxin is a well-established Pg-p substrate (38, 39) and was used as a P-gp positive control for the validation of the Ussing chamber experimental model. The net flux ratio of 3.6 obtained for digoxin is consistent with the occurrence of digoxin efflux in the rat intestinal segments. The decrease of digoxin net flux ratio to 1.4 following GG918 addition, a specific P-gp inhibitor, confirms that digoxin efflux was mainly mediated by the P-gp pump. Therefore, the current Ussing chamber model proved to be suitable for the study of P-gp effects on the permeability of substrates across rat jejunum.

Atorvastatin was used as an example of a Class 2 drug. In clinical studies, significant interactions between atorvastatin and cytochrome P450 3A (CYP3A) inhibitors such as itraconazole and erythromycin were observed (14). Various cell-based studies have suggested that multiple transporters (both uptake and efflux) located in the intestine and liver have the potential to affect the disposition of atorvastatin *in vivo*. It has been demonstrated that atorvastatin undergoes Oatp-mediated hepatic uptake in a rat liver perfusion model (14). In bidirectional Caco-2 studies polarized permeation of atorvastatin was observed with the basolateral to apical (B-A) permeability being 7-fold greater than A-B permeability. The secretion of atorvastatin was inhibited by P-gp inhibitors like verapamil (100 μM), cyclosporine A (10 μM) and a P-glycoprotein specific monoclonal antibody, UIC2 (10 μM) (40).

In our studies both atorvastatin 1 μM and 10 μM concentrations led to net flux ratios higher or equal to 3 (5.2 and 3 for atorvastatin 1 μM *vs.* atorvastatin 10 μM) but smaller than the ones obtained in the Caco-2 model. The values became close to the unity in inhibition studies, consistent with atorvastatin being a P-gp substrate (Table II).

Extraction ratios of 10 μM verapamil following an apical dose doubled the ones obtained with a basolateral dose (Table III). Although this difference is not statistically significant, the preferential apical metabolism is consistent with results obtained for the P-glycoprotein substrates K77 and sirolimus in

CYP3A4-Transfected Caco-2 cells (8, 28), as P-gp at the apical membrane slows absorption through the cell. Nevertheless, for assuming a P-gp effect on verapamil metabolism, Extraction ratio from A to B should decrease and from B to A should increase in the presence of GG918. In this case, we do not have any statistically significant difference in the extraction ratios during inhibition experiments, which shows the apparent directional dependence of extraction ratios for verapamil 10 μM cannot be attributed to P-gp. A similar result was obtained with midazolam extraction ratios across CYP3A4-transfected Caco-2 cells, where the preferential apical extraction ratio was unaffected by P-gp inhibition (28). We assume that at the end of the 3 hours experiment the intracellular compartment reached equilibrium.

Based on published data we assume the experiments were performed at the linear range for verapamil (37) and atorvastatin. Working in the linearity metabolism range is important to rule out enzyme saturation as a possible mechanism for a decresead Extraction ratio.

Conclusion

Prediction of the extent of oral drug absorption is a key issue in the early drug discovery process. BDDCS is a recently proposed tool for predicting overall drug disposition, including potential for drug-drug interactions and the effects of efflux and absorptive transporters on oral drug absorption.

In this study we investigated the effect of inhibiting P-glycoprotein on the *in vitro* rat intestinal permeability and metabolism of the Class 1 drug verapamil. The results suggest that P-glycoprotein inhibition have an effect on verapamil permeability in the rat intestine, but the effect on the more polar norverapamil metabolite is more relevant. These results are in accordance with previous work that points out for an *in vivo* role of P-glycoprotein in the rat intestine. On the other hand, the lack of effect of P-glycoprotein on the Extraction ratio of verapamil shows that the differences on permeability are not affecting verapamil metabolism after the 3 hours experiment.

The results suggest that P-gp inhibition has an effect on both Class 1 verapamil and Class 2 atorvastatin drugs Papp in the rat intestine, but that the effect on the more polar norverapamil metabolite is more significant.

Acknowledgments

This work was supported by FCT grant SFRH/BD/31025/2006.

Research Institute for Medicines and Pharmacological Sciences (iMed.UL) acknowledges Fundação para a Ciência e Tecnologia (FCT) for the project REDE/1518/REM/2005 and Professor Rui Moreira for the LC-MS/MS experiments at LCLEM, Faculdade de Farmácia da Universidade de Lisboa, Portugal.

REFERENCES

1. S. Shugartsand L.Z. Benet. The role of transporters in the pharmacokinetics of orally administered drugs. Pharm Res. 26:2039-2054 (2009).
2. T. Hou, J. Wang, W. Zhang, and X. Xu. ADME evaluation in drug discovery. 7. Prediction of oral absorption by correlation and classification. J Chem Inf Model. 47:208-218 (2007).
3. G.L. Amidon, H. Lennernas, V.P. Shah, and J.R. Crison. A theoretical basis for a biopharmaceutic drug classification: the correlation of in vitro drug product dissolution and in vivo bioavailability. Pharm Res. 12:413-420 (1995).
4. H.X. Zhangand L.S. Wang. [Effect of genetic polymorphism on the activity of drug transporters and its clinical significance]. Zhong Nan Da Xue Xue Bao Yi Xue Ban. 33:765-769 (2008).
5. S. Oswald, M. Grube, W. Siegmund, and H.K. Kroemer. Transporter-mediated uptake into cellular compartments. Xenobiotica. 37:1171-1195 (2007).
6. M.F. Hebert, J.P. Roberts, T. Prueksaritanont, and L.Z. Benet. Bioavailability of cyclosporine with concomitant rifampin administration is markedly less than predicted by hepatic enzyme induction. Clin Pharmacol Ther. 52:453-457 (1992).
7. L.Z. Benet. The drug transporter-metabolism alliance: uncovering and defining the interplay. Mol Pharm. 6:1631-1643 (2009).
8. C.L. Cummins, W. Jacobsen, and L.Z. Benet. Unmasking the dynamic interplay between intestinal P-glycoprotein and CYP3A4. J Pharmacol Exp Ther. 300:1036-1045 (2002).

9. C.L. Cummins, L. Salphati, M.J. Reid, and L.Z. Benet. In vivo modulation of intestinal CYP3A metabolism by P-glycoprotein: studies using the rat single-pass intestinal perfusion model. J Pharmacol Exp Ther. 305:306-314 (2003).

10. L.Z. Benet, C.L. Cummins, and C.Y. Wu. Transporter-enzyme interactions: implications for predicting drug-drug interactions from in vitro data. Curr Drug Metab. 4:393-398 (2003).

11. C.Y. Wuand L.Z. Benet. Disposition of tacrolimus in isolated perfused rat liver: influence of troleandomycin, cyclosporine, and GG918. Drug Metab Dispos. 31:1292-1295 (2003).

12. J.L. Lamand L.Z. Benet. Hepatic microsome studies are insufficient to characterize in vivo hepatic metabolic clearance and metabolic drug-drug interactions: studies of digoxin metabolism in primary rat hepatocytes versus microsomes. Drug Metab Dispos. 32:1311-1316 (2004).

13. Y.Y. Lau, C.Y. Wu, H. Okochi, and L.Z. Benet. Ex situ inhibition of hepatic uptake and efflux significantly changes metabolism: hepatic enzyme-transporter interplay. J Pharmacol Exp Ther. 308:1040-1045 (2004).

14. Y.Y. Lau, H. Okochi, Y. Huang, and L.Z. Benet. Multiple transporters affect the disposition of atorvastatin and its two active hydroxy metabolites: application of in vitro and ex situ systems. J Pharmacol Exp Ther. 316:762-771 (2006).

15. J.E. Polli, B.S. Abrahamsson, L.X. Yu, G.L. Amidon, J.M. Baldoni, J.A. Cook, P. Fackler, K. Hartauer, G. Johnston, S.L. Krill, R.A. Lipper, W.A. Malick, V.P. Shah, D. Sun, H.N. Winkle, Y. Wu, and H. Zhang. Summary workshop report: bioequivalence, biopharmaceutics classification system, and beyond. AAPS J. 10:373-379 (2008).

16. C.Y. Wu and L.Z. Benet. Predicting drug disposition via application of BCS: transport/absorption/ elimination interplay and development of a biopharmaceutics drug disposition classification system. Pharm Res. 22:11-23 (2005).

17. J.M. Custodio, C.Y. Wu, and L.Z. Benet. Predicting drug disposition, absorption/elimination/transporter interplay and the role of food on drug absorption. Adv Drug Deliv Rev. 60:717-733 (2008).

18. H. Saitoh and B.J. Aungst. Possible involvement of multiple P-glycoprotein-mediated efflux systems in the transport of verapamil and other organic cations across rat intestine. Pharm Res. 12:1304-1310 (1995).

19. P.E. Golstein, A. Boom, J. van Geffel, P. Jacobs, B. Masereel, and R. Beauwens. P-glycoprotein inhibition by glibenclamide and related compounds. Pflugers Arch. 437:652-660 (1999).

20. D.H. Choi, J.H. Chung, and J.S. Choi. Pharmacokinetic interaction between oral lovastatin and verapamil in healthy subjects: role of P-glycoprotein inhibition by lovastatin. Eur J Clin Pharmacol. 66:285-290 (2010).

21. B.M. Johnson, W.N. Charman, and C.J. Porter. The impact of P-glycoprotein efflux on enterocyte residence time and enterocyte-based metabolism of verapamil. J Pharm Pharmacol. 53:1611-1619 (2001).

22. C. Pauli-Magnus, O. von Richter, O. Burk, A. Ziegler, T. Mettang, M. Eichelbaum, and M.F. Fromm. Characterization of the major metabolites of verapamil as substrates and inhibitors of P-glycoprotein. J Pharmacol Exp Ther. 293:376-382 (2000).

23. G.M. Grassand S.A. Sweetana. In vitro measurement of gastrointestinal tissue permeability using a new diffusion cell. Pharm Res. 5:372-376 (1988).

24. D. Guggiand A. Bernkop-Schnurch. Improved paracellular uptake by the combination of different types of permeation enhancers. Int J Pharm. 288:141-150 (2005).

25. J.R. Kunta, S.H. Lee, B.A. Perry, Y.H. Lee, and P.J. Sinko. Differentiation of gut and hepatic first-pass loss of verapamil in intestinal and vascular access-ported (IVAP) rabbits. Drug Metab Dispos. 32:1293-1298 (2004).

26. M.A. Campanero, M. Escolar, M.A. Arangoa, B. Sadaba, and J.R. Azanza. Development of a chromatographic method for the determination of saquinavir in plasma samples of HIV patients. Biomed Chromatogr. 16:7-12 (2002).

27. D.H. Choi, K.S. Chang, S.P. Hong, J.S. Choi, and H.K. Han. Effect of atorvastatin on the intravenous and oral pharmacokinetics of verapamil in rats. Biopharm Drug Dispos. 29:45-50 (2008).

28. C.L. Cummins, W. Jacobsen, U. Christians, and L.Z. Benet. CYP3A4-transfected Caco-2 cells as a tool for understanding biochemical absorption barriers: studies with sirolimus and midazolam. J Pharmacol Exp Ther. 308:143-155 (2004).

29. Y.Y. Lau, Y. Huang, L. Frassetto, and L.Z. Benet. Effect of OATP1B transporter inhibition on the pharmacokinetics of atorvastatin in healthy volunteers. Clin Pharmacol Ther. 81:194-204 (2007).

30. R. Sandstrom, A. Karlsson, L. Knutson, and H. Lennernas. Jejunal absorption and metabolism of R/S-verapamil in humans. Pharm Res. 15:856-862 (1998).

31. S. Doppenschmitt, H. Spahn-Langguth, C.G. Regardh, and P. Langguth. Role of P-glycoprotein-mediated secretion in absorptive drug permeability: An approach using passive membrane permeability and affinity to P-glycoprotein. J Pharm Sci. 88:1067-1072 (1999).

32. Y. Shirasaka, Y. Masaoka, M. Kataoka, S. Sakuma, and S. Yamashita. Scaling of in vitro membrane permeability to predict P-glycoprotein-mediated drug absorption in vivo. Drug Metab Dispos. 36:916-922 (2008).

33. V.D. Makhey, A. Guo, D.A. Norris, P. Hu, J. Yan, and P.J. Sinko. Characterization of the regional intestinal kinetics of drug efflux in rat and human intestine and in Caco-2 cells. Pharm Res. 15:1160-1167 (1998).

34. B.M. Johnson, W.N. Charman, and C.J. Porter. Application of compartmental modeling to an examination of in vitro intestinal permeability data: assessing the impact of tissue uptake, P-glycoprotein, and CYP3A. Drug Metab Dispos. 31:1151-1160 (2003).

35. X. Cao, L.X. Yu, C. Barbaciru, C.P. Landowski, H.C. Shin, S. Gibbs, H.A. Miller, G.L. Amidon, and D. Sun. Permeability dominates in vivo intestinal absorption of P-gp substrate with high solubility and high permeability. Mol Pharm. 2:329-340 (2005).

36. T. Ogihara, M. Kamiya, M. Ozawa, T. Fujita, A. Yamamoto, S. Yamashita, S. Ohnishi, and Y. Isomura. What kinds of substrates show P-glycoprotein-dependent intestinal absorption? Comparison of verapamil with vinblastine. Drug Metab Pharmacokinet. 21:238-244 (2006).

37. T.S. Tracy, K.R. Korzekwa, F.J. Gonzalez, and I.W. Wainer. Cytochrome P450 isoforms involved in metabolism of the enantiomers of verapamil and norverapamil. Br J Clin Pharmacol. 47:545-552 (1999).

38. O. Lacombe, J. Woodley, C. Solleux, J.M. Delbos, C. Boursier-Neyret, and G. Houin. Localisation of drug permeability along the rat small intestine, using markers of the paracellular, transcellular and some transporter routes. Eur J Pharm Sci. 23:385-391 (2004).

39. R.H. Stephens, C.A. O'Neill, A. Warhurst, G.L. Carlson, M. Rowland, and G. Warhurst. Kinetic profiling of P-glycoprotein-mediated drug efflux in rat and human intestinal epithelia. J Pharmacol Exp Ther. 296:584-591 (2001).

40. X. Wu, L.R. Whitfield, and B.H. Stewart. Atorvastatin transport in the Caco-2 cell model: contributions of P-glycoprotein and the proton-monocarboxylic acid co-transporter. Pharm Res. 17:209-215 (2000).

Chapter 5

Involvement of carrier-mediated uptake transport in the absorption of Biopharmaceutics Drug disposition Classification System (BDDCS) Class 3, but not Class 1 drugs: *in vitro* studies with digoxin and verapamil.

INVOLVEMENT OF CARRIER-MEDIATED UPTAKE TRANSPORT IN THE ABSORPTION OF BIOPHARMACEUTICS DRUG DISPOSITION CLASSIFICATION SYSTEM (BDDCS) CLASS 3, BUT NOT CLASS 1 DRUGS: *IN VITRO* STUDIES WITH DIGOXIN AND VERAPAMIL

Margarida Estudante[a,b], José G. Morais[a], Graca Soveral[c,d], Leslie Z. Benet[b]

[a]Pharmacological Sciences Unit, iMed.UL, University of Lisbon, Faculty of Pharmacy, Portugal; [b]Department of Bioengineering and Therapeutic Sciences, University of California, San Francisco, USA; [c] REQUIMTE, Dep. Química, FCT-UNL, 2829-516 Caparica, Portugal; [d] Dep. Bioquímica e Biologia Humana, Faculdade de Farmácia, Universidade de Lisboa, 1649-003 Lisboa, Portugal

Purpose: The Biopharmaceutics Drug Disposition Classification System (BDDCS) predicts intestinal transporter effects to be clinically insignificant following oral dosing for highly soluble and permeable/metabolized drugs (Class 1 drugs) while for low soluble and highly permeable/metabolized compounds (Class 2 drugs), transporter effects can occur in the gut. In this study the role of gut uptake transporters in the absorption of verapamil (Class 1 drug) and digoxin (Class 3 drug) was investigated.

Methods: Verapamil and digoxin uptake in Caco-2 cells was assessed in the absence or presence of several uptake transporters inhibitors: tetraethylammonium, quinidine, rifampicin and verapamil.

Results: Initial uptake rates of verapamil by Caco-2 cells exhibited a linear profile. In contrast, initial uptake rates of digoxin showed saturation, with a Km and Vmax of 530 nM and 312 nM/ug prot/ min, respectively. In the presence of inhibitors, an apparent decrease in the uptake of digoxin was observed .

Conclusion: The present results support the BDDCS prediction that transporter effects can be relevant in intestinal absorption of a Class 3 drug but not a Class 1 drug. Although digoxin uptake is a saturable process, none of the classical uptake inhibitors significant decreased digoxin uptake, consistent with the lack of identification of the transporter involved.

Introduction

Over the past 15-20 years a number of drug uptake and efflux transporters that are expressed at the apical (A) or basolateral (B) side of epithelial cells in various tissues (1) have been identified. The investigation of the effects of drug transporters on drug disposition have been addressed by many authors (2-4). In particular, more than 400 membrane transporters in two major superfamilies- ATP-binding cassette (ABC; efflux transporters) and solute carrier (SLC; uptake transporters) have been annotated in the human genome (5). The most prominent and thoroughly investigated examples are the efflux transporters P-glycoprotein (P-gp), multidrug resistance-associated protein 2 (MRP2), and breast cancer resistance protein (BCRP). The later proteins are mainly expressed in organs of excretion including gut, liver and kidney to facilitate directed drug efflux and thus counteracting systemic accumulation of potentially toxic compounds (6). To date, much less is known about uptake transporters and recent research focus on the role of uptake transporters in the liver and the kidney (6). For example, the organic anion transporting polypeptide (OATP) family on the basolateral membrane and MRP2 on the apical bile canalicular membrane of hepatocytes take up and excrete organic anionic compounds from blood to bile (2) . Although it is widely recognized that uptake proteins expressed at the enterocyte membrane are involved in the uptake of endogenous compounds and drugs ((3, 4, 7), the need for further research addressing the relevance of drug uptake transporters in the intestinal mucosa has been reinforced by several authors (3, 6, 8).

Wu and Benet (9) proposed a Biopharmaceutics Drug Disposition Classification System (BDDCS) that classifies drugs in 4 classes according to their solubility (S) and metabolism (M) (Figure 1). The extent of metabolism replaces the Biopharmaceutics Classification System (BCS) permeability (P) criteria, because it is believed that since a drug gets metabolized, it must be absorbed. The BDDCS allows for some general predictions regarding the role of transporters in oral drug disposition based upon drug's classification (Figure 2)(4): for Class 1 drugs transporter effects are minimal, for Class 2 drugs efflux transporter effects predominate in the gut, while uptake and efflux transporter effect can occur in the liver. For Class 3 and Class 4 drugs both absorptive and efflux transporter effects can be important.

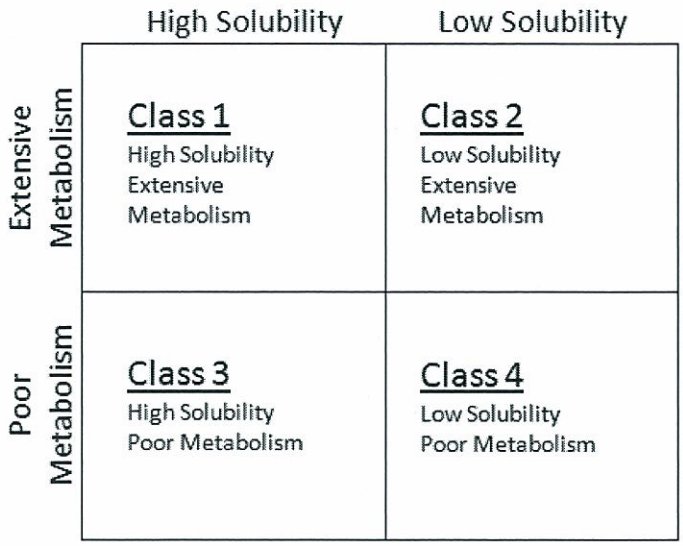

Figure 1 – The Biopharmaceutics Drug Disposition Classification System (BDDCS) after Wu and Benet.

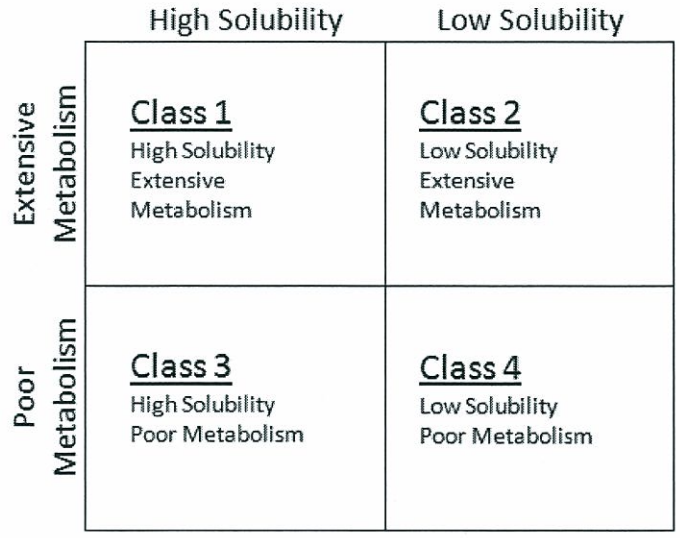

Figure 2 – Efflux and uptake transporter effects on oral drug absorption by BDDCS class.

Some drugs may be 90% absorbed (high P criteria) because of the activity of uptake transporters in the intestine, rather than just due to high lipid passive P. D-glucose, levodopa, L-leucine and phenylalanine are classified as "high P" based on the BCS criteria, although these hydrophilic compounds are known to be absorbed via the endogenous carrier-mediated mechanism (10). Thus some drugs listed as highly

permeable according to BCS may show marked changes in BA when intestinal uptake transporters are inhibited.

In order to evaluate the role of intestinal uptake transporters and to evaluate the predictability of BDDCS regarding transporter effects, Caco-2 cells uptake experiments were performed with verapamil (Class 1 drug) and digoxin (Class 3 drug). Caco-2 cells have been widely used as an *in vitro* model of small intestinal epithelia and are known to express intrinsically the physiological relevant transporters P-gp (11, 12), BCRP, MRP2 (12), peptide transporters (PEPT), organic cation transporter (OCT), organic anion transporter (OAT), large neutral amino acids transporter, bile acids transporter, cobalamin and dipeptides transport systems (13, 14).

A wide range of verapamil and digoxin concentrations was used, beginning with low (nM), non-saturating concentrations, to elucidate whether saturation is a limiting step of absorption. The role of uptake transporters was further elucidated by uptake studies in the presence and absence of known uptake transporters inhibitors such as OCT transporters inhibitors tetraethylammonium (TEA), quinidine (QUI) and verapamil (VER) (15) and OATP transporters inhibitor rifampicin (RIF) (16) to determine the relevance of uptake inhibition to overall permeability (3).

Materials and Methods

Materials

H^3-verapamil and H^3-digoxin were supplied by American Radiochemicals. Tetraethylammonium, quinidine, rifampicin and verapamil were supplied by Sigma-Aldrich (Sintra, Portugal). Caco-2 cells were provided by Prof. Leslie Benet, UCSF. All other reagents were analytical grade, all solvents were HPLC grade and water was obtained from a Millipore Direct-Q water purification system.

Study Protocol

Caco-2 cells were routinely maintained in modified Eagle's medium (MEM) with Earle's BSS containing 10% fetal bovine serum (FBS), 1% nonessential aminoacids, 1% sodium pyruvate and 1% penicillin-streptomycin in a humidified incubator at 37°C and 5% CO_2. Caco-2 cells at passage number 22 were plated at 10^4 cells/cm^2 density in 12-well plates and the experiment was performed 1 week after. In the

second day post-seeding 2 ml of complete media were added to each well. 2 min buffer incubation was performed with H^3-verapamil and H^3-digoxin, with a range of concentrations from 10 nM to 2 mM. Buffer composition was Hanks B with 2% Hepes and 1% fetal bovine serum (FBS), with pH of 6.5. Incubation of 1 µM H^3-verapamil and 1 µM H^3-digoxin was studied in the absence and in the presence of several uptake transporters inhibitors: tetraethylammonium, (100 µM and 1 mM) quinidine (100 µM and 1 mM), rifampicin (100 µM and 1 mM), and verapamil (100 µM and 1 mM). Drug uptake was stopped by the addition of 500 µl of water. The cells were scraped and an aliquot saved for protein determination. Drug concentration in the samples was determined by liquid scintillation counting.
Data points for each treatment were based on 3 replicates per plate; the transport assays were repeated in 3 separate experiments (n = 3). Protein content was determined using the Bradford technique (REF) with bovine albumin as standard (17). Kinetic parameters were estimated using the slopes of linear regression fits or fits to the Michaelis –Menton equation using Prism (GraphPad Software Inc., San Diego, CA).

Statistical Analysis

Statistical analysis was performed with Student's *t* test, taking $p<0.05$ as the criteria of significance.

Results and Discussion

Kinetic analysis of [H^3]-verapamil and [H^3]-digoxin uptake by Caco-2 cells.

Digoxin is a well-known P-gp substrate (18, 19) and verapamil is well known as both P-gp substrate and inhibitor (4, 20, 21) but the potential role of intestinal uptake transporters in the absorption of these drugs has not been characterized. In this study the role of uptake transporters in gastrointestinal absorption of the BDDCS Class 1 drug verapamil and BDDCS Class 3 drug digoxin was investigated using an *in vitro* model of the human intestine, the Caco-2 cell line.

Initial uptake rates of [H^3]-verapamil by Caco-2 cells at concentrations from 10 nM to 2 mM exhibited a linear profile. On the contrary, initial uptake rates of [H^3]-digoxin by Caco-2 cells at concentrations from 10 nM to 2 mM exhibited saturation with a Km and Vmax of 530 nM and 312 nM/ug prot/ min, respectively (Figure 3).

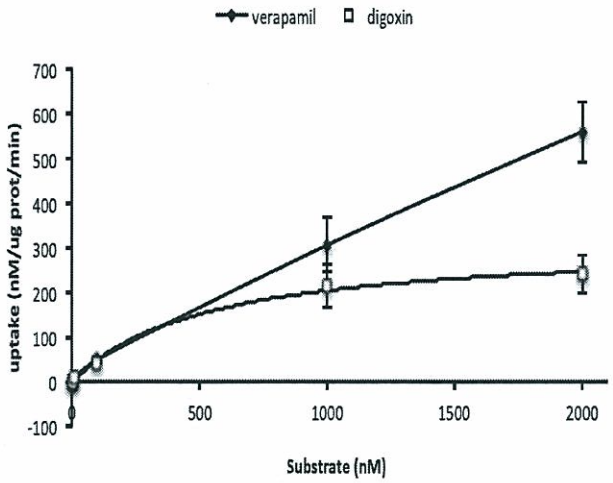

Figure 3- Uptake of [H^3]-verapamil and [H^3]-digoxin at various concentrations by Caco-2 cells.

These results suggest that the transepithelial transport of digoxin includes a carrier-mediated mechanism, while verapamil absorption occurs mainly by passive diffusion. The digoxin results are consistent with a study from Yao et al (22), suggesting the involvement of a carrier-mediated uptake mechanism, possibly OATP, in digoxin absorption in the rat intestine. Although the cationic drug verapamil was identified as a hOCTN2 substrate in hOCTN2 transfected human embryonic kidney (HEK) 293 cells (14), no uptake transporter effect was observed in the present Caco-2 studies, which is in accordance with the BDDCS criteria that for highly soluble and highly permeable drugs, uptake transporter effects should be minimally.

Inhibitory effect of various compounds on the uptake of [H^3]-verapamil and [H^3]-digoxin.

To evaluate the role of transporters on the uptake of verapamil and digoxin by Caco-2 cells, the inhibitory effects of various compounds were examined (Figure 4). We used several known OCT uptake transporters inhibitors such as tetraethylammonium, quinidine and verapamil (15) as well as the OATP transporter inhibitor rifampicin (16). In the presence of these compounds, an apparent decrease in the uptake of digoxin by Caco-2 cells was observed, although not statistically significant for any of the tested inhibitors ($p>0.05$). TEA inhibition of digoxin uptake was more relevant for the 1 mM concentration (33% inhibition) than for the 100 µM concentration (4.8% inhibition), which may suggest an inhibitory role of TEA. The higher inhibition was obtained with QUI 100 µM (55.7% inhibition) but the result obtained with

QUI 1 mM show an increase in digoxin uptake of 40.9%. Both RIF and VER inhibitors caused an apparent decrease in digoxin uptake (28.4% *vs*. 35.4% for RIF 100 µM *vs*. RIF 1 mM and 35.6% *vs*. 36.6% for VER 100 µM *vs*. VER 1 mM).

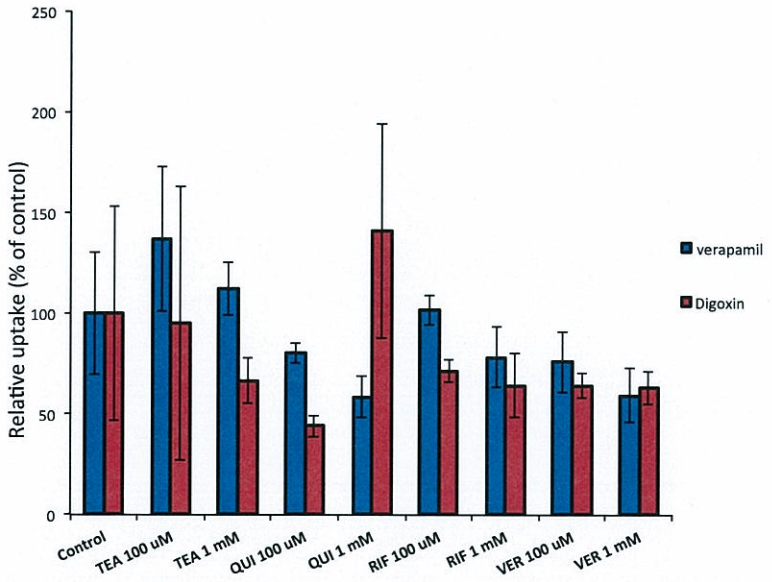

Figure 4 – Effects of several inhibitors on the uptake of [H^3]-verapamil and [H^3]-digoxin by Caco-2 cells. TEA- tetraethylammonium, QUI- quinidine, RIF- rifampicin, VER- verapamil.

TEA caused an increase of verapamil uptake of 37.1% (TEA 100 µM) and 12.6% (TEA 1 mM). QUI 100 µM inhibited verapamil uptake by 19.7% while QUI 1 mM induced 41.2% inhibition. Verapamil uptake was unaffected by RIF 100 µM and was inhibited by 21.4% with RIF 1 mM. VER caused an apparent decrease on its own uptake (23.6% for VER 100 µM and 40.3% for VER 1 mM). As for digoxin, all the verapamil results were apparent but not statistically significant ($p>0.05$).

Conclusions

The present results support the BDDCS prediction that transporter effects can be relevant in intestinal absorption of a Class 3 drug but not a Class 1 drug. The results suggest that, although digoxin (Class 3 drug) uptake is a saturable process, none of the classical uptake inhibitors yield a significant decrease,

consistent with the lack of identification of the transporter responsible for digoxin uptake. Regarding verapamil (Class 1 drug) uptake none of the tested uptake inhibitors caused a significant change, reinforcing the BDDCS prediction that uptake transporter effects are not relevant for Class 1 drugs. Future work will be required in order to identify the transporter responsible for digoxin uptake in the gut.

Acknowledgments

This work was supported by FCT grant SFRH/BD/31025/2006.

REFERENCES

1. H.X. Zhangand L.S. Wang. [Effect of genetic polymorphism on the activity of drug transporters and its clinical significance]. Zhong Nan Da Xue Xue Bao Yi Xue Ban. 33:765-769 (2008).
2. K. Ito, H. Suzuki, T. Horie, and Y. Sugiyama. Apical/basolateral surface expression of drug transporters and its role in vectorial drug transport. Pharm Res. 22:1559-1577 (2005).
3. J.R. Kuntaand P.J. Sinko. Intestinal drug transporters: in vivo function and clinical importance. Curr Drug Metab. 5:109-124 (2004).
4. S. Shugartsand L.Z. Benet. The role of transporters in the pharmacokinetics of orally administered drugs. Pharm Res. 26:2039-2054 (2009).
5. K.M. Giacomini, S.M. Huang, D.J. Tweedie, L.Z. Benet, K.L. Brouwer, X. Chu, A. Dahlin, R. Evers, V. Fischer, K.M. Hillgren, K.A. Hoffmaster, T. Ishikawa, D. Keppler, R.B. Kim, C.A. Lee, M. Niemi, J.W. Polli, Y. Sugiyama, P.W. Swaan, J.A. Ware, S.H. Wright, S.W. Yee, M.J. Zamek-Gliszczynski, and L. Zhang. Membrane transporters in drug development. Nat Rev Drug Discov. 9:215-236.
6. S. Oswald, M. Grube, W. Siegmund, and H.K. Kroemer. Transporter-mediated uptake into cellular compartments. Xenobiotica. 37:1171-1195 (2007).

7. H. Glaeser, D.G. Bailey, G.K. Dresser, J.C. Gregor, U.I. Schwarz, J.S. McGrath, E. Jolicoeur, W. Lee, B.F. Leake, R.G. Tirona, and R.B. Kim. Intestinal drug transporter expression and the impact of grapefruit juice in humans. Clin Pharmacol Ther. 81:362-370 (2007).

8. J.E. Polli, L.X. Yu, J.A. Cook, G.L. Amidon, R.T. Borchardt, B.A. Burnside, P.S. Burton, M.L. Chen, D.P. Conner, P.J. Faustino, A.A. Hawi, A.S. Hussain, H.N. Joshi, G. Kwei, V.H. Lee, L.J. Lesko, R.A. Lipper, A.E. Loper, S.G. Nerurkar, J.W. Polli, D.R. Sanvordeker, R. Taneja, R.S. Uppoor, C.S. Vattikonda, I. Wilding, and G. Zhang. Summary workshop report: biopharmaceutics classification system--implementation challenges and extension opportunities. J Pharm Sci. 93:1375-1381 (2004).

9. C.Y. Wuand L.Z. Benet. Predicting drug disposition via application of BCS: transport/absorption/ elimination interplay and development of a biopharmaceutics drug disposition classification system. Pharm Res. 22:11-23 (2005).

10. M.L. Chenand L. Yu. The use of drug metabolism for prediction of intestinal permeability (dagger). Mol Pharm. 6:74-81 (2009).

11. J. Hunter, M.A. Jepson, T. Tsuruo, N.L. Simmons, and B.H. Hirst. Functional expression of P-glycoprotein in apical membranes of human intestinal Caco-2 cells. Kinetics of vinblastine secretion and interaction with modulators. J Biol Chem. 268:14991-14997 (1993).

12. G. Englund, F. Rorsman, A. Ronnblom, U. Karlbom, L. Lazorova, J. Grasjo, A. Kindmark, and P. Artursson. Regional levels of drug transporters along the human intestinal tract: co-expression of ABC and SLC transporters and comparison with Caco-2 cells. Eur J Pharm Sci. 29:269-277 (2006).

13. P. Arturssonand J. Karlsson. Correlation between oral drug absorption in humans and apparent drug permeability coefficients in human intestinal epithelial (Caco-2) cells. Biochem Biophys Res Commun. 175:880-885 (1991).

14. K. Watanabe, T. Sawano, K. Terada, T. Endo, M. Sakata, and J. Sato. Studies on intestinal absorption of sulpiride (1): carrier-mediated uptake of sulpiride in the human intestinal cell line Caco-2. Biol Pharm Bull. 25:885-890 (2002).

15. R. Ohashi, I. Tamai, H. Yabuuchi, J.I. Nezu, A. Oku, Y. Sai, M. Shimane, and A. Tsuji. Na(+)-dependent carnitine transport by organic cation transporter (OCTN2): its pharmacological and toxicological relevance. J Pharmacol Exp Ther. 291:778-784 (1999).

16. J.L. Lamand L.Z. Benet. Hepatic microsome studies are insufficient to characterize in vivo hepatic metabolic clearance and metabolic drug-drug interactions: studies of digoxin metabolism in primary rat hepatocytes versus microsomes. Drug Metab Dispos. 32:1311-1316 (2004).

17. M.M. Bradford. A rapid and sensitive method for the quantitation of microgram quantities of protein utilizing the principle of protein-dye binding. Anal Biochem. 72:248-254 (1976).

18. O. Lacombe, J. Woodley, C. Solleux, J.M. Delbos, C. Boursier-Neyret, and G. Houin. Localisation of drug permeability along the rat small intestine, using markers of the paracellular, transcellular and some transporter routes. Eur J Pharm Sci. 23:385-391 (2004).

19. R.H. Stephens, C.A. O'Neill, A. Warhurst, G.L. Carlson, M. Rowland, and G. Warhurst. Kinetic profiling of P-glycoprotein-mediated drug efflux in rat and human intestinal epithelia. J Pharmacol Exp Ther. 296:584-591 (2001).

20. H. Saitohand B.J. Aungst. Possible involvement of multiple P-glycoprotein-mediated efflux systems in the transport of verapamil and other organic cations across rat intestine. Pharm Res. 12:1304-1310 (1995).

21. P.E. Golstein, A. Boom, J. van Geffel, P. Jacobs, B. Masereel, and R. Beauwens. P-glycoprotein inhibition by glibenclamide and related compounds. Pflugers Arch. 437:652-660 (1999).

22. H.M. Yaoand W.L. Chiou. The complexity of intestinal absorption and exsorption of digoxin in rats. Int J Pharm. 322:79-86 (2006).

Chapter 6

General discussion and future perspectives

General discussion

Biopharmaceutics Drug Disposition Classification System (BDDCS) predicts transporter effects to be clinically irrelevant for Class 1 drugs (highly P and highly S), intestinal efflux transporter effects and efflux transporter-metabolizing enzyme interplay to be relevant for Class 2 drugs (highly P and low S) while uptake and efflux transporter effects can occur in the liver, uptake transporter effects to be most relevant for Class 3 drugs (low P and high S) and both uptake and efflux transporters to be relevant to the absorption of Class 4 drugs (low P and low S) (1).

These predictions are based on transporter data gathered over the years by Wu and Benet but its applicability still lacks confirmation. The current work was designed in order to evaluate the predictive role of BDDCS in efflux and absorptive transporters effects on oral drug-absorption.

The present studies evidenced the need to be cautious when interpreting and extrapolating results from *in vitro* experiments. In Madin-Darby canine kidney (MDCK) cells transfected with the P-glycoprotein (P-gp) gene MDR1 (MDR1-MDCK cells), all the studied drugs presented results consistent with being P-gp substrates. Nevertheless, when the same experiment was repeated on the human colon carcinoma cell line (Caco-2), only Class 2 (saquinavir) and Class 3 (digoxin) drugs behaved as P-gp substrates. In this cell line, class 1 drugs verapamil and diltiazem permeabilities showed not to be influenced by the efflux transporter P-gp. Bidirectional studies using both cell models are currently used to study drug intestinal absorption, namely P-gp effect on bioavailability. Caco-2 cell line is more representative of the human intestine, although the levels of transporters have been showed to vary between different laboratories and different cell culture conditions (2, 3). MDR1-MDCK cell line is characterized by extremely high TEER values (5000 to 6000 ohm.cm^2) when compared to the human small intestine (25-45 ohm.cm^2) and contains high levels of the efflux transporter. This cell line is therefore a very sensitive model to identify P-gp substrates, but is not ideal to predict P-gp effects on the gut. Caco-2 results are in accordance with BDDCS prediction that for Class 1 (highly P and highly S) drug transporter effects are not relevant, while for Class 2 (highly P and low S) efflux transporters effect may occur.

The synergistic action of CYP3A and P-glycoprotein in limiting oral drug delivery has been described and BDDCS predicts that for Class 2 drugs efflux transporter-metabolizing enzyme interplay is relevant in the gut (1). Caco-2 cell line expresses some drug metabolizing enzymes such as hydrolases and esterases (2) but they do not express adequate quantities of CYP3A4, the main CYP presented in human epithelial

cells. Therefore, Caco-2 cell line is not an adequate system to study transporter-enzyme interplay. We used segments of rat jejunum mounted in Ussing Chambers as the rat intestine presents physiological levels of both enzymes and transporters. Besides being a P-gp substrate, verapamil is also a CYP3A4 substrate so we studied the efflux transporter-enzyme interplay for verapamil in the rat jejunum. The extraction ratio for the norverapamil metabolite in the absence and presence of the P-gp inhibitor GG918 did not significantly change, consistent with no observable efflux transporter-enzyme interplay. If efflux transporter-enzyme interplay was present, extraction ratio following P-gp inhibition should decrease. This result is in accordance with BDDCS prediction that transporter-metabolizing enzyme interplay is relevant for Class 2 drugs (highly P and low S), but not for the Class 1 drug verapamil.

Interestingly, in the rat jejunum, verapamil showed a net flux ratio higher than 3 that was reduced with GG918. These results are consistent with a P-gp effect in the rat intestine. As shown in Caco-2 cells, a human colon carcinoma cell line, P-gp effect does not occur for verapamil which may be due to species differences.

The Class 2 drug atorvastatin also presented a net flux ratio higher than 3 that was reduced with GG918, showing that it is a P-gp substrate in the rat intestine. Digoxin was used as a positive control for P-gp activity. We also measured *in situ* formed levels of verapamil and atorvastatin metabolites. Norverapamil, the verapamil metabolite, appeared consistently augmented in the apical side, which suggested that it could be a P-gp substrate. 2-OH-atorvastatin, the atorvastatin metabolite, presented levels below the limit of quantification, and therefore we could not conclude regarding P-gp effect on this metabolite or efflux transporter enzyme interplay for atorvastatin, as initially planned.

Ussing chamber experiments were performed using norverapamil and confirmed that this metabolite is a P-gp substrate in the rat intestine.

BDDCS predicts gut uptake transporter effects to be most relevant for Class 3 drugs (low P and high S) and not for Class 2 or Class 1 drugs. We measured the uptake of the Class 3 drug digoxin and Class 1 drug verapamil by Caco-2 cells, resulting in saturation kinetics for digoxin, consistent with an uptake transporter effect. Verapamil presented a linear kinetics. The present results support the BDDCS prediction that transporter effects can be relevant in intestinal absorption of Class 3 drug but not a Class 1 drug. Although digoxin uptake is a saturable process, none of the classical uptake inhibitors yield a

significant decrease, consistent with the lack of identification of the transporter responsible for digoxin uptake. Further studies are required to completely characterize digoxin intestinal absorption.

Future perspectives

The overall results presented in this thesis provide an increased understanding of the role of transporters on the intestinal absorption of the studied drugs and the predictive role of the BDDCS regarding intestinal transporter effects.

The role of hepatic transporters in drug bioavailability is still one major question that requires confirmation. Further studies using the isolated perfused rat liver (IPRL) and rat/ human hepatocytes should be conducted with Class 1 and Class 2 drugs to elucidate the role of hepatic uptake and efflux transporters on the bioavailability and disposition of these drugs. Studies comparing the effects of transporter inhibitors on orally *versus* intravenous dosed rats would allow to assess the effects of combined intestinal and hepatic transporters and intestinal and hepatic enzymes *in vivo versus* hepatic transporters and hepatic enzymes effects, respectively.

Some new questions were raised from the work presented in the previous chapters, and a brief overview will be presented.

The results obtained for the Pg-p effect on the Class 1 drug verapamil in the rat intestine point to a different behavior regarding intestinal permeability among species. Therefore the use of human jejunum was planned in order to uncover potential species differences in the role of transporters on overall drug permeability and transporter-enzyme interplay in the gut. Intestinal tissues will be obtained from surgery patients undergoing duodenal pancreatectomy and each mucosa will be carefully mounted in the Ussing diffusion chambers according to the rat intestine protocol described in this thesis.

Appropriate studies should be conducted in order to try to identify the transporter responsible for digoxin uptake in Caco-2 cells.

The fact that Class 2 drugs are affected by uptake transporters in the liver but may not be by those in the intestine suggests that there are differences in the passive permeability of compounds between the plasma membranes of enterocytes and hepatocytes. The passive permeabilities of highly metabolized CYP3A substrate drugs are higher in the intestine than in the liver so we hypothesize that drugs are not affected by uptake transporter-enzyme interplay in the intestine but are in the liver. Uptake transporter-

enzyme interplay has only begun to be understood in the liver and has not been completely evaluated for the intestine.

Further research is needed to advance the understanding of membrane transport differences between the intestine and liver. This research will provide novel information on the differences in the passive permeabilities and carrier-mediated transport of compounds between the membranes of enterocytes and hepatocytes that has not been studied before.

REFERENCES

1. C.Y. Wu and L.Z. Benet. Predicting drug disposition via application of BCS: transport/absorption/ elimination interplay and development of a biopharmaceutics drug disposition classification system. Pharm Res. 22:11-23 (2005).

2. P.V. Balimane and S. Chong. Cell culture-based models for intestinal permeability: a critique. Drug Discov Today. 10:335-343 (2005).

3. P. Artursson and R.T. Borchardt. Intestinal drug absorption and metabolism in cell cultures: Caco-2 and beyond. Pharm Res. 14:1655-1658 (1997).

Annex 1

Analytical methods

Table of contents

1. ANALYTICAL DRUG ASSAYS

1. Analytical drug assays

1.1. HPLC measurement of verapamil and norverapamil

1.1.1. Drug Standards

Verapamil

Molecular formula=$C_{27}H_{38}N_2O_4$

Molecular weight= 454.60

pKa= 9.04

A

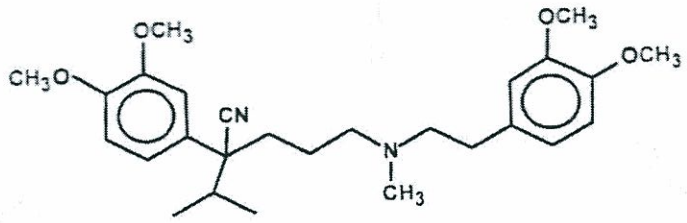

Norverapamil

Molecular formula=$C_{26}H_{36}N_2O_4$

Molecular weight=438.00

B

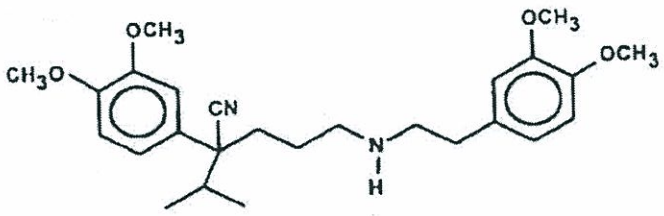

Propranolol

(Internal Standard; IS)

Molecular formula=$C_{16}H_{21}NO_2$

Molecular weight = 259.34

pKa= 9.5

C

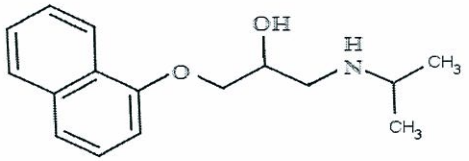

Figure 1- Chemical structure of verapamil (A), norverapamil (B) and the IS propranolol (C).

1.1.2. Chromatographic conditions

All verapamil and norverapamil metabolite samples were analyzed by HPLC under isocratic conditions on a reverse phase LiChroCART/ LiChrospher 60 RP-select B C18 column (4 x 250 mm, particle size 5 um) (Merck KGaA, Darmstadt, Germany) and a C18 guard column. The HPLC system consisted of an integrated solvent and sample management platform (Waters e2695 Separations Module, Waters Corporation) with a Waters 2475 Fluorescence Detector and Empower system control software (all Waters technologies). The mobile phase was a mixture of 10 mM ammonium acetate buffer pH=3.0 with 0.01% diethylamine, acetonitrile and tetrahidrufuran (15:73:12) pumped at 1 ml/min. Verapamil, norverapamil and the internal standard, propranolol, were monitored fluorometrically at an excitation wavelength of 275 nm and emission wavelength of 315 nm, with retention times of 10.7, 12.1 and 8.5 minutes, respectively.

1.1.3. Sample preparation

Procedures for sample analysis were modified based on previously published methods (1) (2) (3). Buffer samples from verapamil and norverapamil Ussing Chamber experiments were kept at -70^{0}C until analysis. After thawing, 30 µl of propranolol 0.5µg/ml (PI) was added to 450 µl of each receiver side sample followed by 100 ul NaOH 2N. Before PI and NaOH addition, donor side samples were split into two aliquots of 350 µl and 100 µl each, and the latest was diluted to 1 ml (1 µM dose) or 10 ml (10 µM dose) with Krebs in order to bring verapamil (and norverapamil in the case of the norverapamil 10 µM experiment) concentration to the calibration curve range (2.5 to 200 ng/ml). In the verapamil experiment 450 µl of diluted sample was used for verapamil analysis and 350 µl of undiluted sample for norverapamil quantification. In the norverapamil 10 µM experiment 450 µl of diluted sample was used for norverapamil quantification. All samples were then vortexed and 6 ml of extraction solvent, methyl *t*-butyl ether, were added. The samples were vortexed for 1 min and centrifuged at 3000 rpm for 10 min. 5 ml of the ether layer was then removed to a clean 15 ml PP tube and evaporated to dryness in a stream of nitrogen. The dry extract was reconstituted in 100 µl of mobile phase and briefly centrifuged before injection (70 µl). Intestinal tissue segments were washed twice with ice cold Krebs immediately after the end of the experiment. The segments were gently dried before being weighted and stored in

Thawing

⇩

Addition of 30 µl propranolol 0.5 µg/ml (IS) to 450 µl sample

⇩

Addition of 100 µl NAOH 2N

⇩

Vortex mix for 30 seconds

⇩

Addition of 6 ml methyl *t*-butyl ether

⇩

Vortex mix for 60 seconds and mechanical shake for 10 minutes

⇩

Centrifuge at 3000 rpm for 10 min

⇩

Remove 5 ml of supernatant to a new tube and dry in a stream of nitrogen

⇩

Dissolve the organic residue in 100 µl of mobile phase

⇩

Vortex mix for 60 seconds and transfer to microinsert

⇩

Inject 70 µl to HPLC

Scheme 1 - Buffer Samples Extraction Scheme.

liquid nitrogen. After thawing, tissue samples were homogenized with a hand homogenizer with 1 ml Krebs/100 mg intestinal tissue. The samples were then centrifuged and 100 µl of supernatant diluted to 1 ml (1 µM dose) or 10 ml (10 µM dose) with Krebs. 450 µl of dilution were transferred to new tubes with 30 µl of PI and 100 µl NaOH 2N were added followed by 70 µl of perchloric acid 20% to induce protein precipitation. Samples were then vortexed for 1 minute and centrifuged at 3000 rpm for 10 minutes. NaOH 2 N (100 µl) is added to the supernatant and drug extraction and analysis is completed as described above.

1.1.4. Method Validation

1.1.4.1. Selectivity

The developed method was able to differentiate the analyte(s) of interest and IS from endogenous components in the Krebs incubation media or other components in the sample (Figure 2). Selectivity was proved by using 6 sources of the blank matrix (Krebs incubation media), each following incubation of individual rat intestines from 6 different rats. Absence of interference was proven for all blanks, including the ones containing GG918 (P-gp inhibitor used during the inhibition experiments) and fluorescein (paracellular marker used during the permeability experiments)(Figure 3).

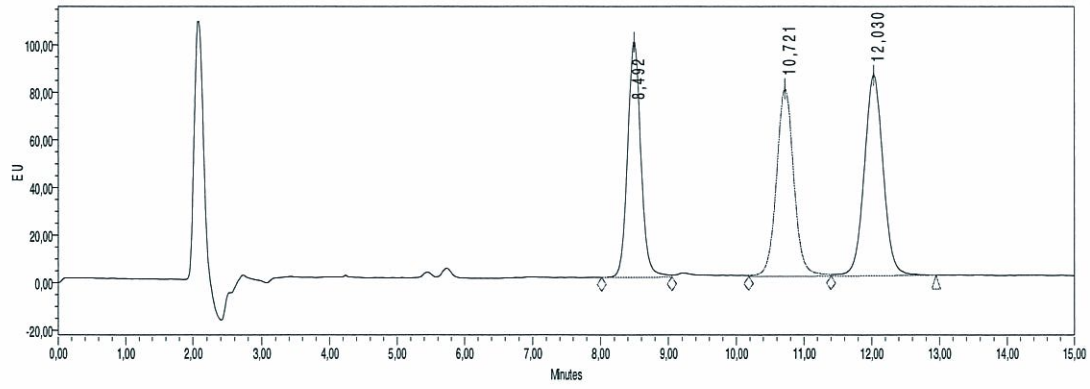

Figure 2 – Chromatogram of verapamil (10.121 min), norverapamil (12.030 min) and propranolol (8.182 min) (IS).

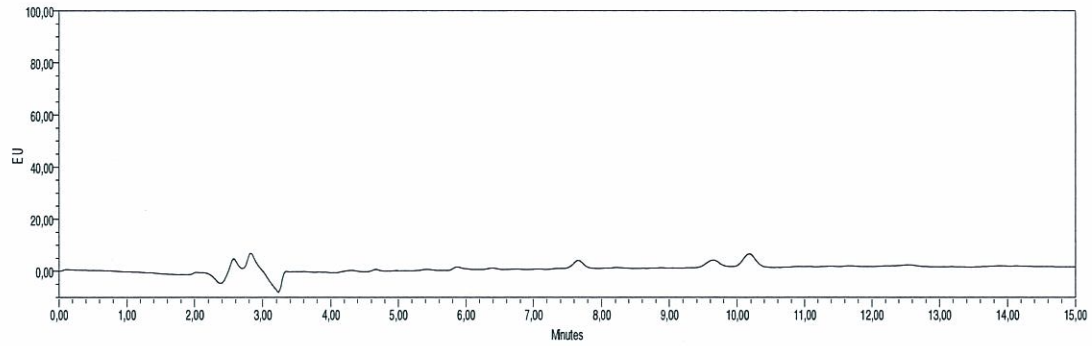

Figure 3 – Chromatogram of Krebs matrix (blank).

1.1.4.2. Carry-over

Carry over was not observed after injection of blank samples following a high concentration sample or a calibration standard. As a preventive measure, one blank injection was performed after injection of higher concentration samples or standard.

1.1.4.3. Lower Limit of Quantification (LLOQ)

Accuracy ((Mean/Nominal Concentration-1)*100) for the LLOQ should be within 20% of the nominal value and precision (Standard Deviation (sd)/ Mean*100) (CV%) should not exceed 20% (4). LLOQ for verapamil was 2.5 ng/ml (Table 1) and for norverapamil was 5 ng/ml (Table 2).

Table 1 – LLOQ for verapamil.

Verapamil Concentration (ng/ml)	
Nominal	Calculated
2.5	2.45
2.5	2.36
2.5	2.08
2.5	1.99
2.5	1.84
Mean	2.14
s.d.	0.23
Accuracy (%)	-14.28
CV (%)	10.81

Table 2 – LLOQ for norverapamil.

Norverapamil Concentration (ng/ml)	
Nominal	Calculated
5	5.14
5	5.90
5	4.98
5	6.10
5	5.20
Mean	5.46
s.d.	0.45
Accuracy (%)	9.28
CV (%)	8.20

1.1.4.4. Calibration curve

The expected verapamil and norverapamil sample concentrations (including the diluted samples) ranged from 2,5 ng/ml (LLOQ) until 200 ng/ml. To investigate calibration curve linearity 3 curves were injected for verapamil and nor-verapamil in 3 different days (Table 3) (Figures 4 and 5). The concentrations to be analysed (calibration standards) were prepared in the same matrix of the intended study samples (Krebs following 3 hours rat intestine incubation) by spiking the blank matrix with known concentrations of the analyte (and IS). Each curve point was prepared in duplicate, including six calibration concentration levels for verapamil (Table 3.1) , five concentration levels for norverapamil (Table 3.2) and a blank and a zero sample (processed matrix with the IS) for each curve

Table 3 – Calibration curves for verapamil and norverapamil, processed in 3 different days.

	Calibration curves	
	Verapamil	Norverapamil
A	$y = 0.0235x + 0.0231$ $R^2 = 0.9988$	$y = 0.026x - 0.2044$ $R^2 = 0.9539$
B	$y = 0.0312x - 0.065$ $R^2 = 0.9972$	$y = 0.0253x - 0.0192$ $R^2 = 0.9983$
C	$y = 0.0266x - 0.1519$ $R^2 = 0.9481$	$y = 0.0208x - 0.0012$ $R^2 = 0.9994$

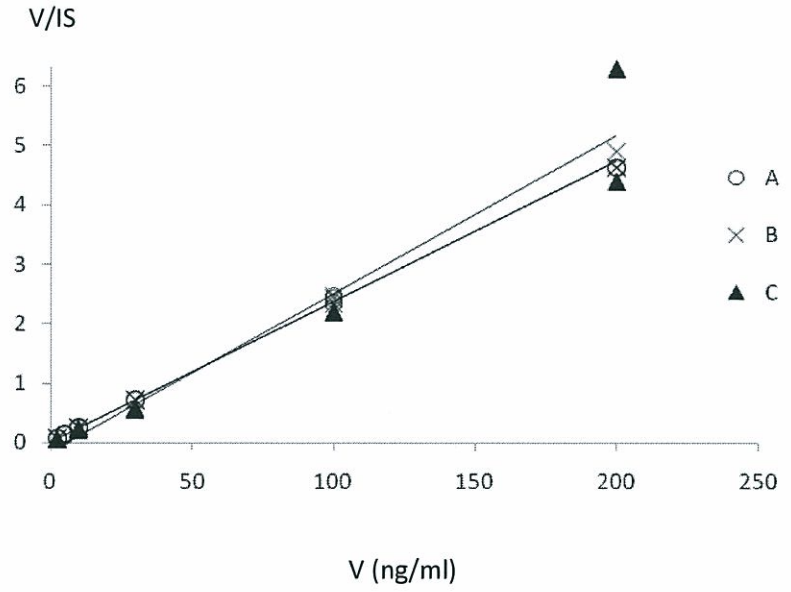

Figure 4– Calibration curves for verapamil (V)(A, B, C), processed in 3 different days.

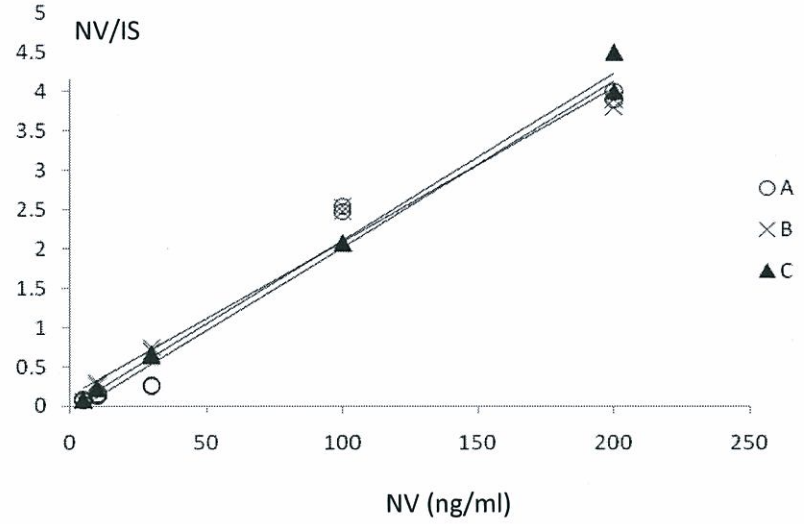

Figure 5– Calibration curves for norverapamil (NV)(A, B, C), processed in 3 different days.

Table 3.1- Calibration curves for verapamil (2.5 to 200 ng/ml), including the back calculation concentrations of the calibration standards and accuracy values.

	Nominal Verapamil concentration (ng/ml)					
	2.5	**5**	**10**	**30**	**100**	**200**
	Calculated concentration (ng/ml) (mean of 2 determinations)					
A	2.63	5.59	10.89	30.14	101.56	196.90
B	2.54	5.46	11.00	28.21	97.30	210.36
C	2.30	4.67	9.75	27.00	111.23	215.00
	Calculated accuracy (%)					
A	5.20	11.80	8.90	0.47	1.56	-1.55
B	1.60	9.20	10.00	-5.97	-2.70	5.18
C	-8.00	-6.60	-2.50	-10.00	11.23	7.50

Back calculation concentrations of the calibration standards and accuracy values for calibration curve of verapamil (Table 3.1) and norverapamil (Table 3.2) are presented below. All the calibration points from the 6 calibration curves evaluated (3 for verapamil and 3 for norverapamil) were within 15% of the nominal value, the cut-off percentage for accuracy criterion (4).

Table 3.2- Calibration curves for norverapamil (5 to 200 ng/ml), including the back calculation concentrations of the calibration standards and accuracy values.

Nominal Norverapamil concentration (ng/ml)					
	5	**10**	**30**	**100**	**200**
Calculated concentration (ng/ml) (mean of 2 determinations)					
A	5.50	11.30	32.90	105.80	207.00
B	4.50	11.78	28.90	103.20	196.45
C	4.32	10.60	29.21	109.00	181.34
	Calculated accuracy (%)				
A	10.00	13.00	9.67	5.80	3.50
B	-10.00	17.80	-3.67	3.20	-1.78
C	-13.60	6.00	-2.63	9.00	-9.33

Accuracy values for calibration curve of verapamil (Table 3.1) and norverapamil (Table 3.2) are presented. All the calibration points from the 6 calibration curves evaluated (3 for verapamil and 3 for norverapamil) were within 15% of the nominal value, the cut-off percentage for accuracy criterion (4).

1.1.4.5. Within-day Accuracy and Precision

The within-day accuracy and precision was calculated based on 5 determinations from 4 concentration levels covering the calibration curve range: the LLOQ, low quality control sample (QC), medium QC and upper QC. QC samples were prepared and extracted in the same day, and the calculated accuracy and precision values are presented at Table 4.

Table 4- Verapamil within-day accuracy and precision.

	Nominal Verapamil concentrations (ng/ml)			
	2.5	30	100	150
Replicates	Calculated concentration (ng/ml)			
1	2.45	30.20	111.00	130.00
2	2.36	34.89	98.56	135.21
3	2.08	29.60	95.10	140.45
4	1.99	35.51	123.56	154.00
5	1.84	34.60	105.02	140.02
Average	2.14	32.96	106.65	139.94
s.d.	0.23	2.52	10.06	7.99
CV (%)	10.81	7.65	9.44	5.71
Accuracy (%)	-14.28	9.87	6.65	-6.71

The accuracy values were within 15% of the nominal values and precision does not exceed 15% for the QC samples, which are the acceptance criteria requirements (4).

The accuracy values were within 15% of the nominal values and precision does not exceed 15% for the QC samples, which are the requirements of the acceptance criteria (4).

1.1.4.6. Between-day Accuracy and Precision

For the validation of between-day accuracy and precision concentrations from 6 different days were used. Each day a low, a medium and a high QC concentration was prepared and analyzed.

The accuracy values were within 15% of the nominal values and precision does not exceed 15% for the QC samples, which are the acceptance criteria requirements (4).

Table 5- Norverapamil within-day accuracy and precision.

	Nominal Norverapamil concentrations (ng/ml)			
	5	30	100	150
Replicates	Calculated concentration (ng/ml)			
1	5.14	31.00	112.00	140.00
2	5.90	28.90	122.35	154.32
3	4.98	30.50	110.00	136.00
4	6.10	29.00	99.85	157.76
5	5.20	27.90	105.00	160.00
Average	5.46	29.46	109.84	149.62
s.d.	0.45	1.13	7.54	9.74
CV (%)	8.20	3.84	6.87	6.51
Accuracy (%)	9.28	-1.80	9.84	-0.26

Table 6 - Between-day accuracy and precision for verapamil.

	Nominal verapamil concentration (ng/ml)		
	5	100	150
Days	Calculated concentration (ng/ml)		
1	5.53	102.00	140.00
2	3.67	97.50	154.65
3	5.43	97.10	168.40
4	5.53	110.00	137.98
5	5.21	107.53	160.51
6	4.36	119.00	158.01
Average	4.96	105.52	153.26
s.d.	0.77	8.41	11.96
CV(%)	15.52	7.97	7.81
Accuracy (%)	-0.90	5.52	2.17

Table 7 - Between-day accuracy and precision for norverapamil.

	Nominal norverapamil concentration (ng/ml)		
	10	100	150
Days	Calculated concentration (ng/ml)		
1	9.00	88.45	145.00
2	12.14	110.32	163.17
3	11.98	96.59	156.78
4	8.97	95.02	140.80
5	11.56	112.00	137.90
6	10.70	120.34	146.75
Average	10.73	103.79	148.40
s.d.	1.44	12.23	9.70
CV(%)	13.40	11.78	6.54
Accuracy (%)	7.25	3.79	-1.07

The accuracy values were within 15% of the nominal values and precision does not exceed 15% for the QC samples, which are the acceptance criteria requirements (4).

1.1.4.7. Dilution integrity

Dilution of samples was studied in order to demonstrate that they do not interfere with the accuracy and precision. Blank Krebs matrix was spiked with the analyte concentration above the upper limit of quantification (ULOQ) and diluted in the same way of the samples. Accuracy and precision of diluted samples were within the set criteria, i.e., within 15%.

1.1.4.8. Stability

As the present analytical method is based on previous, already validated methodology, stability validation was not undertaken (1-4).

1.2. LC/MS-MS measurement of atorvastatin.

1.2.1. Drug Standards

Atorvastatin

A

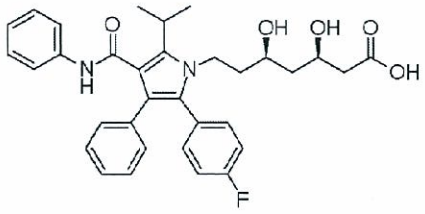

Molecular formula= $C_{33}H_{35}FN_2O_5$

Molecular weight= 558.64

pKa= 4.5

Fluvastatin

B

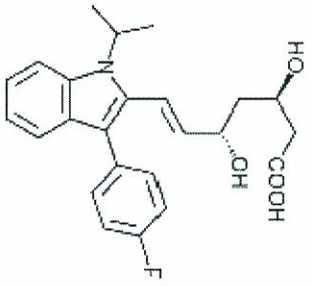

Molecular formula= $C_{24}H_{26}FNO_4$

Molecular weight= 411.466

pKa= 5.5

Figure 6- Chemical structure of atorvastatin (A), and the IS fluvastatin (B).

1.2.2. Chromatographic conditions

The LC/MS-MS method for analyzing atorvastatin was modified based on a previously method described by Lau et al. (5) Briefly, a MicroMass® Quattro micro instrument (Waters Corporation) with electrospray-positive ionization was used, connected to an HPLC Waters® Alliance 2695. The multiple reaction monitor was set at 559.6 to 440.8 m/z for ATV and 412.3 to 265.9 m/z for the internal standard, fluvastatin. The cone voltage and collision energy were set at 35 V and 21 eV, respectively. The analytical column was a Sunfire RP, C18 (4.6x50 mm, 5 µm particle size).The mobile phase consisted of acetonitrile

and acetic acid 0.05%. The flow rate was set at 0.3 ml/min. The quantification limit for atorvastatin was 2.5 ng/ml.

Table 8- Mass parameters.

Intrumental parameters	
Ionization mode	ES+ (Electrospray positive)
Capilar potential	3,50 kV
Cone potential	35,0 V
Source temperature	100°C
Desolvation temperature	350°C

Table 9- Cromatographic conditions.

Eluent A	Acetic acid 0,05%	
Eluent B	ACN	
Flux	0,300 ml/min	
Column temperature	24,0°C (± 5.0°C)	
Sample temperature	4,0°C	
Gradient	0,0-2,0 min	A 52,0% : B 48,0%
	8,0-8,1 min	A 20,0%: B 80,0%
	8,1-13,0 min	A 52.0% : B 48,0%

Table 10- Mass detector conditions (m/z):

Compound	Type	Quantification transition	Collision energy	Retention time
Fluvastatin	Internal standard	412.3 > 265.9	21 V	5.70 min (± 0.5 min)
Atorvastatin (ATV)	Analyte	559.6 > 440.8	21 V	6.00 min (± 0.5 min)

Peak detection was performed in MRM (Multiple Reaction Monitoring) mode for the above mentioned conditions.

1.2.3. Sample preparation

500 µl samples from the *in vitro* intestinal permeability experiments were kept at -70°C until analyses. After thawing, 50 µl of fluvastatin 20 µg/ml (PI) and 500µl water were added to each sample and homogenized. The 1 ml dilution was delivered into SPE (solid phase extraction) columns (Sec Pak Vac C18, Waters), previously activated with 1 ml methanol (MeOH) and 1 ml of water. After the sample, the column was washed with 1 ml of water and then eluted with 1 ml MeOH. The eluted fraction was then evaporated in a rotary evaporator. The residue was reconstituted in 100 µl mobile phase (acetonitrile:water) (70:30) (Scheme 2).

1.2.4. Method Validation

1.2.4.1. Selectivity

The developed method was able to differentiate atorvastatin and the IS fluvastatin from endogenous components in the Krebs incubation media or other components in the sample (Figure 7).

Thawing

⇩

Addition of 50 µl fluvastatin 20 µg/ml (IS) to sample

⇩

Addition of 500 µl H_2O to sample

⇩

Vortex mix for 10 seconds

⇩

Deliver sample to pre-activated SPE column

⇩

Wash column with 10 ml H_2O

⇩

Elute sample with 1 ml MeOH

⇩

Evaporate in rotary evaporator

⇩

Reconstitute with 100 µl mobile phase and transfer to microinsert

⇩

Inject to LC/MS-MS

Scheme 2 - Buffer Samples Extraction Scheme.

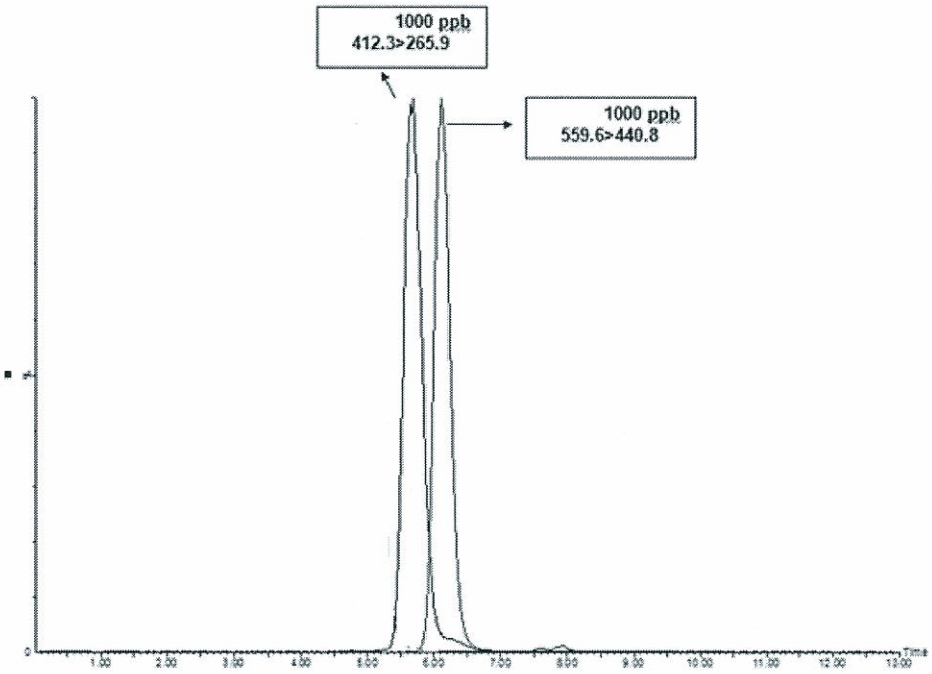

Figure 7– Chromatogram of atorvastatin and fluvastatin (IS) standards.

Selectivity was proven by using 6 sources of the blank matrix (Krebs incubation media), each following incubation of individual rat intestines from 6 different rats. Absence of interference was proven for all blanks, including the ones containing GG918 (P-gp inhibitor used during the inhibition experiments) (Figure 8) and fluorescein (paracellular marker used during the permeability experiments).

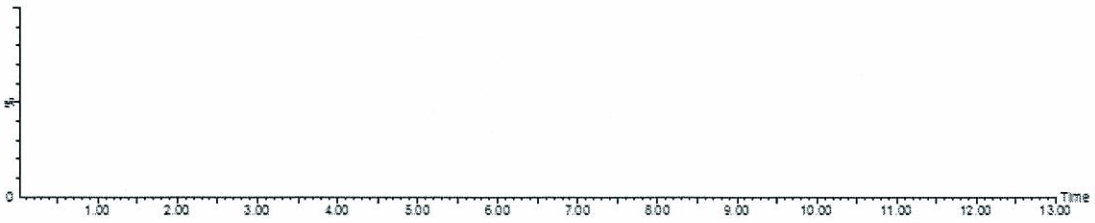

Figure 8 – Chromatogram of Krebs matrix (blank) with GG918.

1.2.4.2. Carry-over

Carry over was observed after injection of blank samples following a high concentration sample or a high calibration standard. To overcome this issue, two blank injections were performed after injection of higher concentration samples or standards.

1.2.4.3. Lower Limit of Quantification (LLOQ)

Accuracy ((Mean/Nominal Concentration-1)*100) for the LLOQ should be within 20% of the nominal value and precision (Standard Deviation (SD)/ Mean*100) (CV%) should not exceed 20% (4). LLOQ for atorvastatin was 2.5 ng/ml (Table 11).

Table 11- LLOQ for atorvastatin.

Atorvastatin Concentration(ng/ml)	
Nominal	Calculated
2,5	3.01
2,5	2.56
2,5	2.96
2,5	2.54
2,5	2.73
Mean	2.76
SD	0.22
Accuracy (%)	7.97
CV (%)	10.35

1.2.4.4. Calibration curve

Calibration curve range was selected based on the expected atorvastatin concentrations in the Ussing chamber experiments. As we expected low concentrations (from 0 to 100 ng/ml) in the receptor chambers and high concentrations in the donor chamber (about 5600 ng/ml for the atorvastatin 10 µM experiment) we divided the calibration curve into three concentration levels to investigate linearity:

- 2.5 to 100 ng/ml,
- 100 to 1000 ng/ml
- 1000 to 10000 ng/ml

3 curves per day were injected for atorvastatin in 3 different days (total of 9 curves; Tables 15, 16, 17; Figure 9).

Table 15 – Calibration curves for atorvastatin: a) 2.5 to 100 ng/ml b) 100 to 1000 ng/ml and c) 1000 to 10000 ng/ml, processed in 3 different days.

a)

Curves	Equation	Correlation coefficient
A	Y=0,0022x-0,0038	R^2=0,9969
B	Y=0,0023x-0,004	R^2=0,9971
C	Y=0,0029x-0,0056	R^2=0,9957

b)

Curves	Equation	Correlation coefficient
D	Y= 0,0051x-0,4368	R^2=0,9956
E	Y=0,0046x-0,216	R^2=0,9953
F	Y=0,0056x-0,221	R^2=0,9992

c)

Curves	Equation	Correlation coefficient
G	Y=0,0047x-0,45	R^2=0,9958
H	Y=0,0034+2,3598	R^2=0,9842
I	Y=0,0034x+2,46	R^2=0,9832

Each curve point was prepared in duplicate, including 13 calibration concentration levels divided by the three different curves (Table 16; Figure 9).

(1)

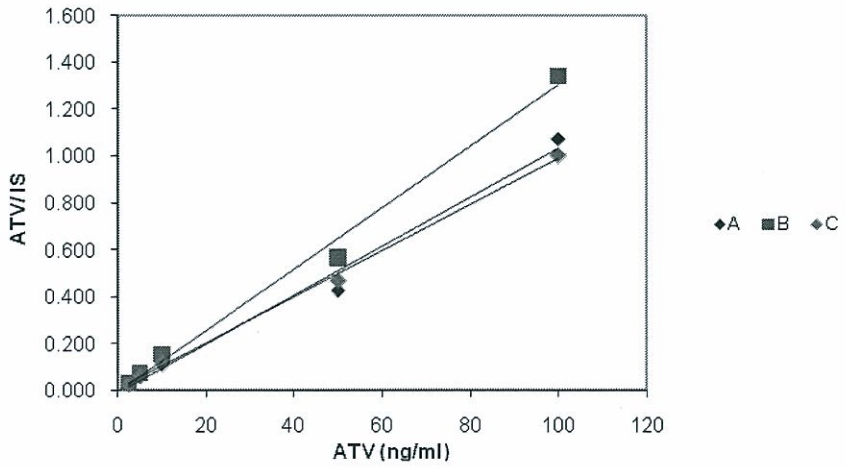

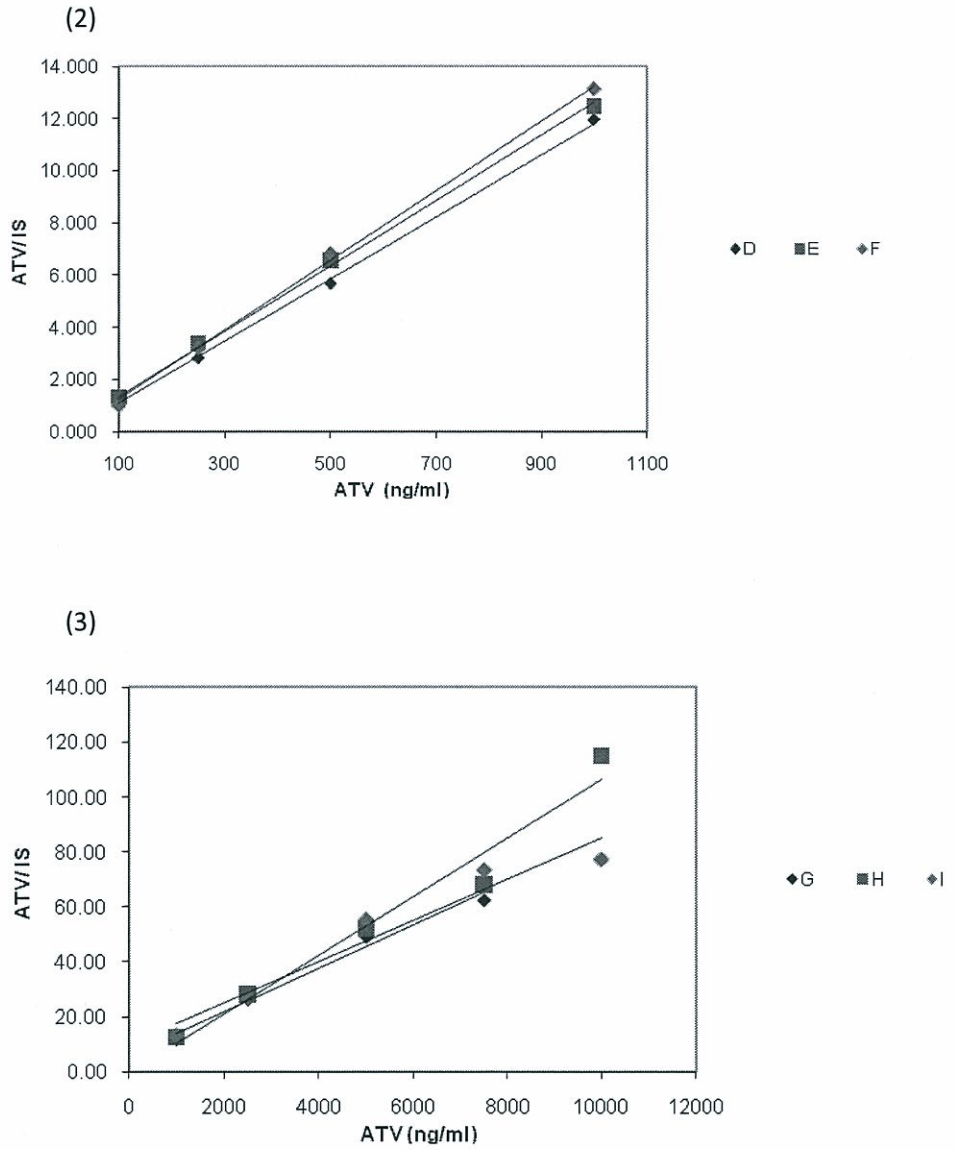

Figure 9 – Calibration curves for atorvastatin (ATV) 2.5 ng/ml to 100 ng/ml (1), 100 ng/ml to 1000 ng/ml (2) and 1000 ng/ml to 10000 ng/ml (3), processed in 3 different days.

Table 16 - Calibration curves for atorvastatin: a) 2.5 to 100 ng/ml b) 100 to 1000 ng/ml and c) 1000 to 10000 ng/ml, including the back calculation concentrations of the calibration standards and accuracy values.

a)

Nominal atorvastatin concentration (ng/ml)					
	2.5	**5**	**20**	**50**	**100**
Calculated concentration (ng/ml) (mean of 2 determinations)					
A	2.30	5.20	21.70	51.00	115.00
B	2.00	5.52	19.00	49.67	98.70
C	2.60	4.90	20.65	48.00	104.00
	Calculated accuracy (%)				
A	-8.00	4.00	8.50	2.00	15.00
B	-20.00	10.40	-5.00	-0.66	-1.30
C	4.00	-2.00	3.25	-4.00	4.00

b)

Nominal atorvastatin concentration (ng/ml)					
	100	**250**	**500**	**750**	**1000**
Calculated concentration (ng/ml) (mean of 2 determinations)					
D	115.00	245.10	487.60	760.00	1100.00
E	98.70	254.80	538.40	749.21	989.00
F	104.00	252.30	575.10	786.90	975.00
	Calculated accuracy (%)				
D	15.00	-1.96	-2.48	1.33	10.00
E	-1.30	1.92	7.68	-0.11	-1.10
F	4.00	0.92	15.02	4.92	-2.50

c)

Nominal atorvastatin concentration (ng/ml)					
	1000	**2500**	**5000**	**7500**	**10000**
Calculated concentration (ng/ml) (mean of 2 determinations)					
G	1100	2470	5660	7540	9600
H	989	2399	4899	7889	10673
I	975	2680	5847	7450	9540
	Calculated accuracy (%)				
G	10.00	-1.20	13.20	0.53	-4.00
H	-1.10	-4.04	-2.02	5.19	6.73
I	-2.50	7.20	16.94	-0.67	-4.60

Accuracy values for calibration curves of atorvastatin (Table 16) are presented. All the calibration points evaluated were within 15% of the nominal value, the cut-off percentage for accuracy fulfill criterion (4). Only one case of atorvastatin 2.5 standard, injected at 24/07/2010, had an accuracy of 20%. Nevertheless, for the LLOQ, the acceptance criteria is 20% of the nominal value (4), so this value was accepted.

1.2.4.5. Within-day Accuracy and Precision

The within-day accuracy and precision was calculated based on 5 replicates from QC samples: LLOQ, ULOQ and a QC from the intermediate level of the curves. Samples were prepared and extracted in the same day, and the calculated accuracy and precision values are presented at Table 17.

The obtained values are within the 15% acceptance criteria.

1.2.4.6. Between-day Accuracy and Precision

For the validation of between-day accuracy and precision concentrations from 6 different days were used. Each day LLOQ, ULOQ and a QC from the intermediate level of the curve were prepared (Table 18).

The obtained values are within the 15% acceptance criteria.

1.2.4.7. Stability

As the present analytical method is based on previous, already validated methodology, stability validation was not undertaken (4, 5).

Table 17 – Within-day accuracy and precision for atorvastatin.

	Nominal concentration (ng/ml)		
Nº Replicates	2,5	500	10000
	Calculated concentration (ng/ml)		
1	3,01	483	11 386
2	2,56	505	10 858
3	2,96	512	10 944
4	2,54	473	11 512
5	2,73	490	10 358
Average	2,76	493	11012
s.d.	0,22	18,3	322
CV (%)	7,93	3,71	2,92
Accuracy (%)	10,4	-1,35	10,1

Table 18 - Between-day accuracy and precision for atorvastatin.

Days	Nominal concentration (ng/ml)		
	2,5	250	10000
	Calculated concentration (ng/ml)		
1	2,79	225	9 927
2	3,55	233	9 815
3	3,64	254	9 636
4	2,85	237	9 873
5	2,75	276	9 957
6	2,46	270	9 982
Average	2,96	249	9 865
s.d.	0,45	20,8	127
CV (%)	18,5	8,36	1,29
Accuracy (%)	15,3	0,333	-1,35

1.3 Conclusion

The presented chromatographic methodology proved to have adequate sensibility, selectivity, accuracy and precision for the quantification of verapamil, norverapamil and atorvastatin in the study samples obtained from Ussing chamber experiments.

REFERENCES

1. J.R. Kunta, S.H. Lee, B.A. Perry, Y.H. Lee, and P.J. Sinko. Differentiation of gut and hepatic first-pass loss of verapamil in intestinal and vascular access-ported (IVAP) rabbits. Drug Metab Dispos. 32:1293-1298 (2004).

2. M.A. Campanero, M. Escolar, M.A. Arangoa, B. Sadaba, and J.R. Azanza. Development of a chromatographic method for the determination of saquinavir in plasma samples of HIV patients. Biomed Chromatogr. 16:7-12 (2002).

3. D.H. Choi, K.S. Chang, S.P. Hong, J.S. Choi, and H.K. Han. Effect of atorvastatin on the intravenous and oral pharmacokinetics of verapamil in rats. Biopharm Drug Dispos. 29:45-50 (2008).

4. CHMP. Guideline on validation of Bioanalytical Methods. In EMA (ed.), 2010.

5. Y.Y. Lau, H. Okochi, Y. Huang, and L.Z. Benet. Multiple transporters affect the disposition of atorvastatin and its two active hydroxy metabolites: application of in vitro and ex situ systems. J Pharmacol Exp Ther. 316:762-771 (2006).